

A new radial lip seal design approach

Citation for published version (APA):

Kuiken, J. (1996). *A new radial lip seal design approach*. [Phd Thesis 1 (Research TU/e / Graduation TU/e), Mechanical Engineering]. Technische Universiteit Eindhoven. <https://doi.org/10.6100/IR466873>

DOI:

[10.6100/IR466873](https://doi.org/10.6100/IR466873)

Document status and date:

Published: 01/01/1996

Document Version:

Publisher's PDF, also known as Version of Record (includes final page, issue and volume numbers)

Please check the document version of this publication:

- A submitted manuscript is the version of the article upon submission and before peer-review. There can be important differences between the submitted version and the official published version of record. People interested in the research are advised to contact the author for the final version of the publication, or visit the DOI to the publisher's website.
- The final author version and the galley proof are versions of the publication after peer review.
- The final published version features the final layout of the paper including the volume, issue and page numbers.

[Link to publication](#)

General rights

Copyright and moral rights for the publications made accessible in the public portal are retained by the authors and/or other copyright owners and it is a condition of accessing publications that users recognise and abide by the legal requirements associated with these rights.

- Users may download and print one copy of any publication from the public portal for the purpose of private study or research.
- You may not further distribute the material or use it for any profit-making activity or commercial gain
- You may freely distribute the URL identifying the publication in the public portal.

If the publication is distributed under the terms of Article 25fa of the Dutch Copyright Act, indicated by the "Taverne" license above, please follow below link for the End User Agreement:

www.tue.nl/taverne

Take down policy

If you believe that this document breaches copyright please contact us at:

openaccess@tue.nl

providing details and we will investigate your claim.

A New Radial Lip Seal Design Approach

PROEFONTWERP

ter verkrijging van de graad van doctor aan de Technische
Universiteit Eindhoven,
op gezag van de Rector Magnificus, prof.dr. M. Rem,
voor een commissie aangewezen door het College van
Dekanen in het openbaar te verdedigen op
dinsdag 1 oktober 1996 om 16.00 uur

door

JAN KUIKEN

geboren te Emmeloord

Dit proefschrift is goedgekeurd door de promotoren:

Prof.dr.ir. M.J.W. Schouten

Prof.dr.ing. M. Vötter

Cover: Cross section of a shock absorber and a new shock absorber seal.

This research was supported and funded by PL Automotive, Kerkrade, The Netherlands.

Druk: Universiteitsdrukkerij TU Eindhoven

SUMMARY	VII
SAMENVATTING	IX
NOMENCLATURE	XI
ABBREVIATIONS	XIV
1. DESCRIPTION OF THE DESIGN TASK	1
1.1 Introduction	1
1.2 Sealing theory	3
1.2.1 Static contact situation	3
1.2.2 Sealing mechanism	5
1.2.2.1 Static sealing	5
1.2.2.2 Dynamic sealing	5
1.2.3 Basic principles of hydrodynamic lubrication	6
1.3 PL Automotive	8
1.4 Shock absorber	8
1.5 Design task	10
1.5.1 Prevention of leakage	10
1.5.1.1 Static leakage	10
1.5.1.2 Dynamic leakage	11
1.5.2 Prevention of oil contamination	11
1.5.3 Seal service life	11
1.6 Design morphology and methodology	11
1.7 Literature review	14
1.7.1 Seal design in general	14
1.7.2 Seal performance of reciprocating rod seals	16
1.8 Strategy for seal design optimization	17
1.9 New design approach	18
2. NEW SEAL DESIGN APPROACH	21
2.1 Introduction	21
2.2 Seal design process	21
2.2.1 Design in general	22
2.2.2 Seal design for reciprocating shafts	22
2.2.3 Demands on state of the art seal design	24
2.3 Implementation of the new seal design procedure	26
2.3.1 Design task	26
2.3.2 Feasibility analysis stage (FA-stage)	27
2.3.3 Initial design stage (ID-stage)	29
2.3.3.1 Temperature profile	29
	III

2.3.3.2 Pressure profile	29
2.3.3.3 Shaft velocity profile	30
2.3.3.4 Determination of the initial seal geometry	30
2.3.3.5 Determination of the seal material	31
2.3.3.6 Determination of the garter spring	32
2.3.4 Seal evaluation stage (SE-stage)	33
2.3.4.1 Material characterization	33
2.3.4.2 Determination of the SC1401A spring behavior	35
2.3.4.3 Determination of the SC1401A CPD	35
2.3.4.4 Determination of leakage and friction	35
2.3.5 Seal optimization stage (SO-stage)	36
2.3.5.1 Design parameters	37
2.3.5.2 Objective function	37
2.3.5.2.1 Optimal shape of the CPD	38
2.3.5.2.2 Definition of the objective function O	40
2.3.5.3 Solution process	41
2.3.5.4 Design optimization based upon existing seal designs	43
2.3.5.5 Design optimization based upon the Taguchi method	45
2.3.5.5.1 Definition of quality	46
2.3.5.5.2 Design quality evaluation	46
2.3.5.5.3 Control and noise factors	47
2.3.5.5.4 Results and conclusions	48
2.3.6 Prototyping	50
2.3.7 Experimental verification stage (EV-stage)	51
2.4 Summary	51
3. EXPERIMENTAL METHODS TO SUPPORT SEAL DESIGN	53
3.1 Introduction	53
3.2 Experimental testing of the new SC1401 prototype	53
3.2.1 Results of the friction measurements	53
3.2.2 Results of the cold test	54
3.2.3 Results of the seal life test	55
3.3 Radial load measurement	55
3.4 Experimental determination of seal friction	56
3.5 Material characterization	58
3.5.1 Hyperelasticity	59
3.5.2 Tensile tests of a HNBR-compound	60
3.6 Frictional properties of seal materials	61
3.6.1 Pin on disc test method	62
3.6.2 Performance of the pin on disc tests and used materials	62
3.6.3 General observations	63
3.6.3.1 Observations for the FPM-compound	64
3.6.3.2 Observations for the NBR-compound	64
3.6.3.3 Observations for the HNBR-compound	65
3.6.4 Results	65
3.7 Experimental determination of the CPD	65
3.7.1 Theoretical background	67
3.7.2 Experimental setup	67
3.7.3 Measurements	68
3.7.4 Results	69

3.7.4.1 Force versus displacement plots	69
3.7.4.2 Contact pressure distributions	70
3.7.4.3 Contact widths	71
3.7.4.4 Maximum contact pressures	72
3.7.4.5 Discussion	73
3.8 Summary	73
4. RESULTS & DISCUSSION	75
4.1 Summary of the results	75
4.2 Discussion	75
4.3 Recommendation	76
APPENDIX A. DETERMINATION OF THE STATIC CPD WITH COSMOS/M	77
A.1 Introduction	77
A.2 Choice of COSMOS/M	77
A.3 FEA of the PL3-562 seal	78
A.3.1 Introduction	78
A.3.2 Geometrical parameters and parametric seal model	79
A.3.3 Finite element models for the calculations	80
A.3.4 PL3-562 contact pressure distribution	82
A.3.5 Characteristic features of the CPD	82
A.3.6 Discussion	83
A.4 FEA of the SC1401_B seal	83
A.4.1 Introduction	83
A.4.2 Meshing	83
A.4.3 The COSMOS/M input-file	84
A.4.4 Results	88
A.5 Summary	89
APPENDIX B. DETERMINATION OF LEAKAGE AND FRICTION WITH THE IHL METHOD	90
B.1 Introduction	90
B.2 Assumptions for SEALCALC	92
B.3 Procedures and algorithms	92
B.3.1 Curve fitting the discrete static CPD	93
B.3.2 Curve fitting discrete geometrical data of the deformed seal	94
B.3.3 Determination of the film characteristics for a fully lubricated contact	94
B.3.4 Determination of seal leakage and friction	95
B.4 Application of Kanters algorithms on lip seals	96
B.5 Determination of leakage and friction for seals with a strongly asymmetrical contact pressure profile	98
B.5.1 New assumptions for the film profile in the boosting and exit zone	98
B.5.2 Film profile in the boosting zone	99

B.5.3 Film profile in the exit zone	101
B.6 Elastohydrodynamic pressure profile with the new assumptions	102
B.7 Piezo-viscous calculations with SEALCALC	103
B.8 Dimensionless quantities in SEALCALC	104
B.9 Influence of the fluid pressure on the pressure and film profile	104
B.10 Quasi-stationary calculations with SEALCALC	106
B.11 Conclusions	109
APPENDIX C. A HYSTERESIS FRICTION MODEL FOR ELASTOMERIC CONTACT SEALS	111
C.1 Introduction	111
C.2 Mechanisms of elastomeric friction	111
C.3 Viscoelastic material behavior	113
C.3.1 Dynamic viscoelastic behavior	113
C.3.2 Dynamic mechanical thermal analysis of the elastomer pin materials	115
C.4 Multi-mode Maxwell model	115
C.5 Hysteresis friction model	116
C.5.1 Introduction	116
C.5.2 Shaft surface roughness model	117
C.5.3 Analytical hysteresis friction model	118
C.6 Summary	121
REFERENCES	122
NAWOORD	124
CURRICULUM VITAE	125

Summary

Over the past 35 years scientific research on elastomeric contact seals for both rotating and reciprocating shafts has led to an enormous increase of knowledge on the fundamental mechanisms and the important parameters for seal operation. In general, this increase of fundamental knowledge has however not led to important changes in the practical approach towards seal design and manufacturing.

The main goal of this work is to develop a new design strategy for shock absorber seals based upon state of the art knowledge on fundamental seal operation. The work is carried out as a research project linking the theoretical knowledge of the Eindhoven University of Technology on seal design to the specific needs for a new seal design strategy of a seal manufacturer, PL Automotive. From the implementation of the IHL approach presented by Kanters [1990] it was found that this method can not be applied to predict leakage and friction for shock absorber seals theoretically. Especially, predicted values for seal friction are much smaller than the experimental values. This makes the application of the IHL approach for actual seal design optimization less useful. In order to optimize seal design the frictionless static contact pressure distribution (CPD) is used as the design objective function. Based upon the CPD of an existing design with a good seal performance or the theoretically optimal shape of the CPD the objective function for optimization is defined. This research project has resulted in the presented and implemented practical strategy for the design of elastomeric contact seals.

The practical design strategy is divided into five stages and in each stage a number of design decisions is made, resulting in the transformation of general knowledge and data into a new seal design meeting a specific list of demands.

During the first stage of the design process - the Feasibility Analysis Stage (FA-stage) - the list of demands for the new design is defined. Operating conditions, demands on seal performance, and the necessary test procedures for the new seal design are stated and documented in close cooperation with the customer.

During the second stage - the Initial Design Stage (ID-stage) - the seal designer defines an initial seal design. The initial design is defined by a choice for the basic geometry, material and type of garter spring for the new seal. The choice for a specific combination of these three main factors is based upon the data gathered during the FA-stage in combination with the knowledge of the seal designer about existing seals.

During the third stage - the Seal Evaluation Stage - the performance of the initial design is evaluated based upon the CPD. The CPD is determined numerically with a Finite Element Analysis (FEA) tool. Based upon the deformed geometry of the seal and the theoretical shape of the CPD the seal designer can determine the radial load, the contact width, maximum contact pressures and the pressure gradient function of the seal. With these data the seal performance of the new seal design is determined and evaluated.

During the fourth stage - the Seal Optimization Stage (SO-stage) - the new seal design is optimized with respect to the specific list of demands on seal performance, defined during the FA-stage. After a number of sets with different design parameters is analyzed, the optimal set of design parameters is defined. After the features of this design are evaluated with the customer a prototype is produced.

During the fifth stage - the Experimental Verification Stage (EV-stage) - a number of standard tests are carried out to judge the seal performance. These tests are developed and standardized in close cooperation with the customer during this project and carried out in accordance with the

specifications stated during the FA-stage. These test are carried out by the seal manufacturer before the new seal design is mounted in the shock absorber by the customer.

The development and implementation of this new seal design strategy, in the practical situation of PL Automotive, has resulted in a standardization of shock absorber seal design, a better knowledge of the important geometrical seal design and operating parameters, and a shorter time-to-market for new designs.

Samenvatting

Gedurende de laatste 35 jaar heeft het wetenschappelijk onderzoek naar de werking van elastomere contactafdichtingen voor roterende en translaterende assen geleid tot een enorme toename van de kennis met betrekking tot de fundamentele werkingsprincipes en de parameters, die van belang zijn voor het functioneren van een afdichting. Over het algemeen heeft deze toename van de kennis van de fundamentele werkingsprincipes echter niet geleid tot belangrijke veranderingen van de praktische aanpak van het ontwerpen en produceren van afdichtingen.

De belangrijkste doelstelling van dit werk is het ontwikkelen van een nieuwe ontwerpstrategie voor schokdemperafdichtingen, die is gebaseerd op het huidige kennisniveau van de fundamentele werkingsprincipes van afdichtingen. Het werk is uitgevoerd in de vorm van een onderzoeksproject, waarbij de theoretische kennis betreffende de werking van afdichtingen aan de Technische Universiteit Eindhoven wordt gebruikt en getoetst met behulp van de praktische kennis van een bedrijf dat afdichtingen produceert, PL Automotive. Op grond van de toepassing van de IHL-methode, gepresenteerd door Kanters [1990], is geconcludeerd dat deze methode niet kan worden gebruikt om de lek en de wrijving van een schokdemperafdichting theoretisch te bepalen. Vooral de voorspelde waarde voor de wrijving wijkt erg af van de experimenteel bepaalde waarde. Dit maakt de waarde van de IHL-methode als beoordelingscriterium voor afdichtingsoptimalisatie minder groot. Om afdichtingen toch te kunnen optimaliseren is de wrijvingsloze statische contactdrukverdeling (CPD) gebruikt als het beoordelingscriterium. Gebaseerd op de CPD van een bestaand ontwerp met goede afdichtingseigenschappen of de theoretisch optimale vorm van de CPD wordt de doelfunctie voor de optimalisatie gedefinieerd. Dit onderzoeksproject heeft geresulteerd in het gepresenteerde en toegepaste ontwerpproces voor elastomere contactafdichtingen.

Het praktische ontwerpproces is verdeeld in vijf fasen en in iedere fase wordt een aantal ontwerpbeslissingen genomen, die leiden tot de transformatie van algemene kennis en data inzake een nieuw afdichtingsontwerp, dat voldoet aan een van te voren gespecificeerd pakket van eisen.

Tijdens de eerste fase van het ontwerpproces - de Feasibility Analysis Stage (FA-stage) - wordt het pakket van eisen voor het nieuwe ontwerp opgesteld. Hierbij worden de omgevingsomstandigheden, de eisen met betrekking tot de afdichtingseigenschappen, en de benodigde testprocedures voor het nieuwe ontwerp bepaald en vastgelegd in goed overleg met de klant.

Tijdens de tweede fase - de Initial Design Stage (ID-stage) - definieert de ontwerper een initieel ontwerp. Het initiële ontwerp wordt gevormd door de keuze van de basisgeometrie, het materiaal en het veertype voor de nieuwe afdichting. De keuze voor een specifieke combinatie van deze drie hoofdfactoren, geometrie, materiaal en veertype, wordt voornamelijk gebaseerd op de data die zijn verzameld tijdens de FA-stage in combinatie met de kennis van de ontwerper over bestaande afdichtingen.

Tijdens de derde fase - de Seal Evaluation Stage (SE-stage) - wordt de werking van het initiële ontwerp geëvalueerd op basis van de CPD. De CPD wordt bepaald met behulp van de Eindige Elementen Methode (EEM). Op grond van de geometrie van de vervormde afdichting en de bijbehorende CPD kan de afdichtingsontwerper de radiaalcracht, de contactbreedte, de maximale contactdruk en de drukgradientfunctie bepalen. Met deze data kunnen de afdichtingseigenschappen van het nieuwe ontwerp worden bepaald en geëvalueerd.

Tijdens de vierde fase - de Seal Optimisation Stage (SO-stage) - wordt het nieuwe ontwerp geoptimaliseerd met betrekking tot de specifieke eisen aan de afdichtingseigenschappen, geformuleerd tijdens de FA-stage. Nadat een aantal sets met verschillende ontwerpparameters is geanalyseerd, wordt een optimale set van ontwerpparameters gedefinieerd. Nadat de specifieke

eigenschappen van het optimale ontwerp zijn geëvalueerd met de klant wordt er een prototype gebouwd.

Tijdens de vijfde fase - de Experimental Verification Stage (EV-stage) - wordt een aantal standaard testprocedures doorlopen om de werking van het nieuwe ontwerp te kunnen beoordelen. Deze testprocedures zijn in overleg met de klant opgesteld en worden uitgevoerd volgens de specificaties die zijn vastgelegd tijdens de FA-stage. Deze testen vinden plaats bij de afdichtingsfabrikant voordat de nieuwe afdichting door de klant wordt ingebouwd in een schokdemper.

De ontwikkeling en implementatie van deze ontwerpstrategie, in de praktische situatie bij PL Automotive, heeft geleid tot een standarisatie van het ontwerp van schokdemperafdichtingen, een betere kennis van de invloed van belangrijke geometrische, materiaal en omgevings parameters op de werking van de afdichting en een kortere time-to-market voor een nieuw ontwerp.

Nomenclature

\overline{F}_w	dimensionless friction	[-]
H_{min}^m	dimensionless minimal film thickness of Moes	[-]
H_0^m	dimensionless h_0 of Moes	[-]
\overline{h}	dimensionless film thickness	[-]
\overline{p}	dimensionless pressure	[-]
$\overline{Q\eta_0}$	dimensionless $Q\eta_0$	[-]
\overline{x}	dimensionless x-coordinate	[-]
$\overline{\eta V_x}$	dimensionless ηV_x	[-]
$\overline{\tau}_v$	dimensionless viscous shear stress	[-]
Λ	lambda ratio h_0/σ	[-]
α	wedge angle in the boosting zone / low pressure angle of the seal	[rad] / [°]
β	pressure-viscosity coefficient / high pressure angle of the seal	[Pa ⁻¹] / [°]
η	dynamic viscosity	[Pa·s]
ν	Poisson constant	[-]
τ	relaxation time constant	[s]
σ	combined RMS roughness / stress	[m]/ [Pa]
ω	angular frequency	[rad/s]
δ	interference	[mm]
η_0	dynamic viscosity at atmospheric pressure	[Pa·s]
σ_d	dynamic stress component	[Pa]
$(dp/dx)_{max}$	maximum contact pressure gradient	[N/mm ³]
$(dp/dx)_{min}$	minimum contact pressure gradient	[N/mm ³]
ΔF_w	Friction difference $\Delta F_w = F_{w+} - F_w$	[N]
ϵ_{max}	maximum nominal strain	[%]
η_n	viscosity of the n th -mode Maxwell element	[Pa·s]
Δp	pressure difference over a seal	[Pa]
σ_s	static stress component	[Pa]
τ_v	viscous shear stress	[Pa]
$a_T(T)$	shift factor	[-]
b	contact width	[m]
b	damper constant	[Ns/m]
b_h	half Hertzian contact width	[m]

c_1, c_2, c_3	constants	[-]
C_{10}, C_{01}	constants in the ABAQUS Mooney-Rivlin model	[Pa]
$c _h$	clearance outside the contact area	[m]
DF	division factor	[-]
d_{shaft}	shaft diameter	[m]
E	elasticity modulus (Young's modulus)	[Pa]
E'	storage modulus	[Pa]
E''	loss modulus	[Pa]
E_d	the dynamic modulus	[MPa]
E_n	modulus of elasticity of the n^{th} -mode Maxwell element	[Pa]
E_r	reduced elasticity modulus	[Pa]
F	force	[N]
F_{adh}	adhesion component of the friction force	[N]
F_{as}	force in the shaft	[N]
F_{plough}	plough component of the friction force	[N]
F_{rad}	radial load of the seal	[N]
F_{sp}	specific spring load	[N/mm]
F_{spec}	specific radial load of the seal	[N/mm]
F_{visc}	viscous component of the friction force	[N]
F_w	friction force	[N]
F_{w-}, F_{w+}	stabilized negative and positive friction at constant speed	[N]
$F_{w,\text{min}}, F_{w,\text{max}}$	minimum and maximum measured friction force	[N]
G	dimensionless pressure gradient	[-]
g	pressure gradient function	[m ⁻²]
$g_{\text{min}}, g_{\text{max}}$	minimum and maximum of the pressure gradient function g	[m ⁻²]
H	dimensionless film thickness	[-]
h	film thickness	[m]
H'	storage modulus (analytical model)	[Pa]
H''	loss modulus (analytical model)	[Pa]
h_0	flow criterion (film thickness where $\frac{dp}{dx} = 0$)	[m]
$h_{0\text{max}}$	maximum flow criterion	[m]
H_d	dynamic modulus (analytical model)	[Pa]
Hd	height of the sealing lip	[mm]
Hf	position of the garter spring	[mm]

h_{\min}	minimum film thickness	[m]
h_{x_d}	film thickness at position x_d	[m]
k	spring stiffness	[N/m]
K_1, K_2, K_3	characteristic values of the objective function	[-]
M	non-dimensional load parameter of Moes	[-]
Mooney_A,B	constants in the COSMOS/M Mooney-Rivlin model	[Pa]
p	film pressure	[Pa]
p_{atm}	atmospheric pressure	[Pa]
p_{av}	average contact pressure	[Pa]
p_{gas}	gas pressure	[Pa]
p_h	(Hertzian) contact pressure	[Pa]
p_{hm}	maximum Hertzian contact pressure	[Pa]
p_{sur}	surrounding pressure	[Pa]
p_{top}	maximum contact pressure	[Pa]
Q	leakage	[m ³ /s]
q	flow per unit of width	[m ² /s]
R	radius	[m]
R_a	arithmetic average roughness height	[μm]
S_{th}	section thickness of the sealing lip	[mm]
t	time	[s]
T	temperature / time of a period	[$^{\circ}\text{C}$] / [s]
T_0	reference temperature	[$^{\circ}\text{C}$]
U_e	entraining velocity	[m/s]
v	velocity	[m/s]
V_{Σ}	sum velocity of the rubbing surfaces	[m/s]
V_{Δ}	velocity difference of the rubbing surfaces	[m/s]
V_{afd}	seal velocity	[m/s]
V_{as}	shaft velocity	[m/s]
W	load per unit of width	[N/m]
x_a	starting position for integration in the boosting zone	[m]
x_b	position of the begin of the CPD	[m]
x_{bend1}	low pressure side point of inflection of the CPD	[m]
x_{bend2}	high pressure side point of inflection of the CPD	[m]
x_d	position from where the relaxing pressure deviate from the CPD	[m]

x_e	position of the end of the frictionless CPD	[m]
x_f	position of the film exit	[m]
x_m	merging point of the boosting zone pressure profile and the CPD	[m]
x_{top}	x-coordinate of the maximum contact pressure	[m]
y	coordinate in axial direction	[mm]

Abbreviations

General:

AFM	Atomic Force Microscope
BEM	Boundary Element Method
CAD	Computer Aided Design
CAM	Computer Aided Manufacturing
CPD	Contact Pressure Distribution
CPU	Central Processing Unit
DMA	Dynamic Mechanical Analysis
DMTA	Dynamic Mechanical Thermal Analysis
FEA	Finite Element Analysis
FEM	Finite Element Method
TUE	Eindhoven University of Technology

Physical phenomena:

EHL	Elastohydrodynamic Lubrication
IHL	Inverse Hydrodynamic Lubrication
WLF	Williams-Landell-Ferry shift factors for viscoelastic materials

Design process:

FA-stage	Feasibility Analysis Stage
ID-stage	Initial Design Stage
SE-stage	Seal Evaluation Stage
SO-stage	Seal Optimization Stage
EV-stage	Experimental Verification Stage
SA-seal	Shock Absorber Seal

Rubber compounds:

FPM-compound	Fluorocarbon rubber compound
HNBR-compound	Hydrogenated NBR rubber compound
NBR-compound	Acrylonitrile butadiene rubber compound

Trademarks:

ABAQUS	General purpose FEA-code
ANSYS/ED	General purpose FEA-code
COSMOS/M	General purpose FEA-code
MATLAB 4.0	General purpose numerical analysis software

1. Description of the design task

1.1 Introduction

The aim of this work is to design elastomeric seals for reciprocating shafts in a systematic way based on currently available research data and numerical techniques. This systematic seal design approach is implemented in the design procedure of a seal manufacturer and results in seal design optimization with respect to seal performance and manufacturing tolerances. Optimization of seal production or implementation of new manufacturing techniques is only possible when the relations between seal design parameters and seal performance are fully understood and documented within a reproducible design strategy and production technique.

In order to seal rotating, reciprocating or oscillating shafts, pistons, valves and other types of moving parts, a large diversity of seals have been designed, manufactured and tested over the last 40 years. The problem of the seal designer is to design and manufacture a seal with no leakage and friction given a certain set of operating conditions. In order to solve this design problem all existing knowledge on seal design, sealing, and lubrication mechanisms combined with environmental, economical and manufacturing considerations must be taken into account. Some attempts have been made to address the entire field of fluid sealing products, i.e. Brink [1993] and Müller [1990], from the seal designers point of view, but in general these sources do not present a methodology which can be used and implemented directly for daily seal design. A new seal design methodology, linking practical to theoretical knowledge, is needed. This is caused by the increased demands on performance, operating conditions, reliability, and environmental safety of a new or improved seal design within a shorter time-to-market from the customer demand up to the new design.

Figure 1 presents different parts which must be incorporated in the seal design and optimization procedure and their relationships with the seal design.

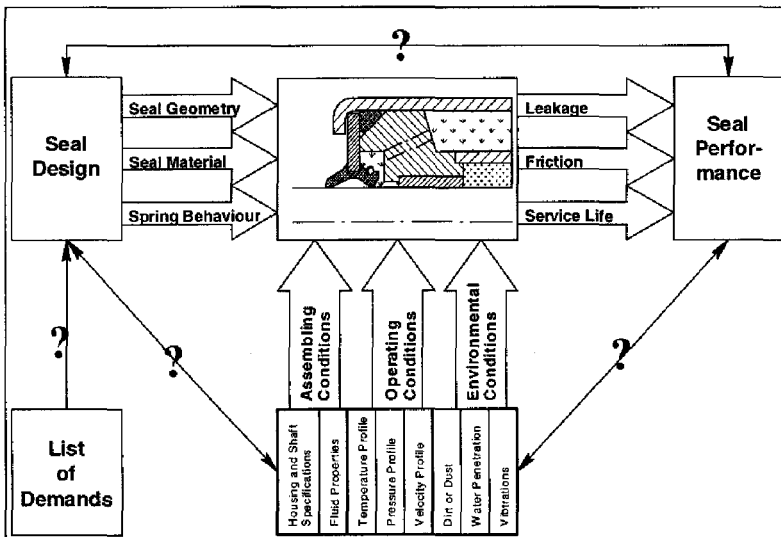


Figure 1 General aspects to incorporate in the seal design approach.

A reproducible design procedure results in a relevant quantitative description of the relationships between the list of demands, operating conditions, seal design and seal performance as presented in Figure 1. The question marks stand for the unknown relationships between the different stages of the seal design process. The theoretical knowledge of the Eindhoven University of Technology and the practical seal design knowledge of industry are combined as a part of this project. The different parts of Figure 1 are approached from the point of view of the seal manufacturer. Emphasis is given on the practical implementation of several theoretical models, within the financial, human and hardware resources of the seal manufacturer. With a flexible design procedure it is possible to create a design which is feasible for both the customer and the manufacturer within a closed period of time as opposed to the frequently applied method of trial and error using the black box approach without knowledge about how long it will take before a design is feasible..

In this thesis several times a reference is made to the customer. In order to make the influence of this important factor understandable the term customer is defined more accurately. In this thesis the customer stands for the person or company who buys the seals and uses the seals in many different applications. These applications are mainly shock absorbers. The customer expects optimal functionality from the elastomeric contact seals before they deliver their shock absorbers to the end-users in the automotive industry. It can be stated that the seal is of major importance for the functionality of the total shock absorber and thus seal research and development are of great value to the development of shock absorbers. This design project was carried out in close cooperation with PL Automotive's main customer, MONROE, and consequently the customer has an influence on the design process.

Although most fluid seals are relatively small, cheap, and simple components, compared to the complex technical system of which they are part, their sealing function can be of critical importance considering the reliability and safety of the total system. The best known example to clarify this critical importance is the failure of a simple static O-ring causing the Challenger catastrophe in 1986, resulting in the loss of human lives and a complete space shuttle. Another example, for the importance of proper seal design is the shock absorber seal. The main function of a shock absorber seal is to prevent leakage of oil from a shock absorber assuring comfortable and reliable vehicle performance on a bumpy road. If the seal fails, the shock absorber fails and by this the vehicle performance fails, endangering human life and the environment.

As an example to clarify the environmental importance of proper seal design, shock absorbers for the automotive industry will be used. Based upon data from Sobeta [1995] a rough estimate of the total number of cars on the road is made. Annual sales of passenger cars are at $4.7 \cdot 10^7$ units/year and the average lifetime of a car is 9.3 years. This results in approximately $4.4 \cdot 10^8$ passenger cars on the road. The number of other moving vehicles, like trucks and other industrial machinery, is estimated at the half of the number of passenger cars, $2.2 \cdot 10^8$ units, resulting in an approximated total of $6.6 \cdot 10^8$ moving vehicles on the road.

Every moving vehicle is equipped with a minimum of four shock absorbers and is assumed to use two sets of four shock absorbers over the lifetime. All these shock absorbers are filled with a certain volume of oil and during the life of the shock absorber a certain percentage of this oil is lost and dumped to the environment. Assuming that two sets of 4 shock absorbers are used over the average lifetime and with an estimated average oil volume of $250 \cdot 10^{-6} \text{ m}^3$ per shock absorber. A loss of 10% of the volume over the service life resulting for $6.6 \cdot 10^8$ moving vehicles in a total oil volume of 14.000 m^3 /year equivalent of a small coaster full of oil leaked into the environment. This rough estimation of the total amount of oil lost into the environment by moving machinery can be regarded as a lower bound estimate, because other sealed parts also have leakage.

These examples of the importance of seals and seal design places seal research and development in its proper global perspective from both the seal manufacturers and society's point of view. The increasing demands from society and end users have increased the importance of seal research and have led to a better understanding of the sealing and lubrication mechanisms and the parameters which influence

seal performance for both rotating and reciprocating applications. However, from the seal designers and manufacturers point of view there is an increasing need for the implementation of this knowledge into practical seal design strategies.

Although it is important to exchange information at research conferences, better and more direct results can be achieved when the results of research are coupled to and used in daily seal design strategies. This asks for a close cooperation between research and manufacturing. The work presented in this thesis is a first attempt towards an improved practical design method, which is based on results from research. This cooperation between research and industry results in a systematic approach towards seal design leading to a seal with high sealing quality, reliable performance and less pollution of the environment.

The purpose of this thesis is:

- to present the scientific principles of mechanics and tribology which are needed for a systematic design approach of shock absorber seals,
- to implement both practical and theoretical knowledge into a new radial lip seal design approach,
- and to investigate and present its practical usefulness when compared with experiments.

1.2 Sealing theory

The following presentation of concepts and ideas concerning the sealing and lubrication mechanism of elastomeric contact seals clarifies the basic principles of seal operation. The basic physical principles, important parameters and terminology are introduced and shortly discussed concerning the contact between an elastomeric lip seal and a shaft. The most important parameter influencing the seal performance is the contact area that exists between the shaft and the seal.

1.2.1 Static contact situation

The static contact situation of a seal is described by its deformed geometry and strains and stresses in the seal after assembly, pressurization and excitation due to the relative motion of the shaft. Most of the strains are induced by the interference between the shaft and the seal. The value of the interference defines the deformed geometry and as a result of this, the stress level in the seal. For radial lip type seals the garter spring also influences the stress level and its stiffness is used by the seal designer to adjust the value of the contact pressure to the desired value. The frictionless static contact pressure profile is the starting point for the determination of hydrodynamic fluid film profile, which must be formed between shaft and seal to prevent wear during relative motion.

Figure 2 presents the contact between shaft and seal and some important features of the pressure distribution that exists between the shaft surface and the deformed seal. Both the macroscopic and microscopic contact assumptions are presented. A complete physical description of the dynamic phenomena which take place in the contact area between shaft and seal resulting in a single model describing the relationships between design parameters, operating parameters and seal performance is extremely complex and not known at the moment. This means that a number of assumptions concerning the dynamic shaft to seal contact has to be made in order to simplify the model and make modeling of the sealing, lubrication and friction mechanism possible.

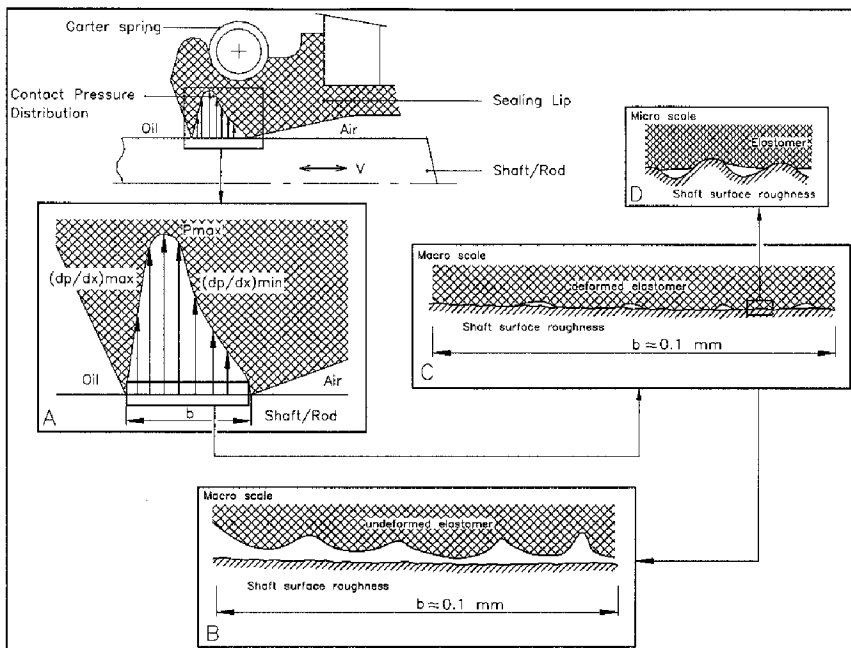


Figure 2 General shape of a shock absorber seal and assumed roughness profile in the contact area, van Klooster [1996].

The general assumptions made for the contact area are:

The contact between the shaft and the seal may be regarded as axisymmetrical, isothermal and stationary resulting in the solution of a static two dimensional line contact problem.

The contact pressure distribution (CPD) between the shaft and the seal is not influenced by temperature, shaft movement and fluid film formation resulting in the assumption that the static isothermal, contact pressure distribution is a constant parameter during seal operation.

The relationship between the hydrodynamic pressure profile and the fluid film profile can be described by the Inverse Hydrodynamic Lubrication (IHL) theory, Kanters [1990].

The seal and shaft surface roughness are neglected resulting in perfectly smooth surface profiles, which are used to determine the macroscopic CPD and fluid film profile.

Knowledge of the static CPD is important for a number of reasons, e.g.:

- the presence of tensile stresses in a seal can result in cracking and by this in seal failure.
- the static CPD must exhibit a maximum pressure that is larger than the fluid pressure to prevent leaking under static conditions. The absolute value of this pressure is not known at the moment, but is an important characteristic for the seal designer. An estimation of the minimal value for the maximum CPD has to be presented.

- the static contact situation influences the lubrication of the contact during relative motion. When the influence of the pressure distribution is given by a model a tool for quantitative seal design has been found.

The calculation of the static CPD of an elastomeric seal requires the solution of a non-linear problem. The non-linearities arise from:

- the large displacements and strains involved (in some applications up to 25%), so that the equilibrium equations may not be referred to the undeformed geometry of the seal. For the seal designer the undeformed geometry is the starting point, so that this non-linearity can not be excluded during optimization of the seal geometry.
- the non-linear relation between stress and strain or the elongation factors (physical non-linearity). The material behavior of the elastomer is important, but until now it has been difficult to incorporate a good time- and temperature-dependent material behavior into the calculation of the CPD. This is mainly due to the fact that experimental determination of the constants, which describe the material behavior for certain loads, still lacks accuracy.
- the contact phenomena involved (non-linear boundary condition).

In Kuiken [1993] it is concluded that in order to find the optimal geometry for a seal the demands on the CPD must be defined precise. Otherwise the objective function will allow a large number of seal geometry's which can be used and not one optimal geometry. However, a problem occurs because the static CPD can not directly be used for the calculation of the fluid film between the shaft and the seal. This is caused by the fact that for fluid film formation the pressure gradient function g is the most important parameter. For a static CPD the value of g will always reach infinity at the edges of the contact, resulting in zero film thickness. Based upon results from literature and the theoretical parameters influencing fluid film formation the optimal shape of the CPD is defined.

1.2.2 Sealing mechanism

The sealing mechanism of seals for reciprocating shafts can be described by two different types of sealing: static and dynamic sealing. The different types of sealing are distinguished by the movement of the shaft. Static and dynamic sealing depend upon the existence of an interference fit between the shaft and the seal resulting in a contact pressure and under dynamic conditions the formation of a fluid film to separate the contacting surfaces, while maintaining the pressure distribution.

1.2.2.1 Static sealing

During static sealing there is no relative movement between the shaft and seal surface. The sealing function of the seal is guaranteed by the static CPD if the maximum pressure, p_{top} , is higher than the fluid pressure. Furthermore, the elastomeric seal material must fill the rough shaft surface, thus preventing an oil flow from the high pressure to the low pressure side through small channels in the contact area.

1.2.2.2 Dynamic sealing

During dynamic sealing there is a relative movement between the shaft and seal surface and oil is dragged into the contact zone forming a fluid film and passing the contact zone in the direction of shaft movement. The fluid film separates the seal surface from the shaft surface, this reduces friction and wear, but also causes oil to pass through the contact area. This amount of oil can be regarded as leakage, but due to the reciprocating shaft movement, the direction of the oil flow changes with changes in the direction of shaft movement. In Figure 3 the direction of the oil flow through the contact zone for the instroke and outstroke situation is presented. The difference between the amount of oil transported through the contact zone during instroke and outstroke of a reciprocating shaft motion is called leakage.

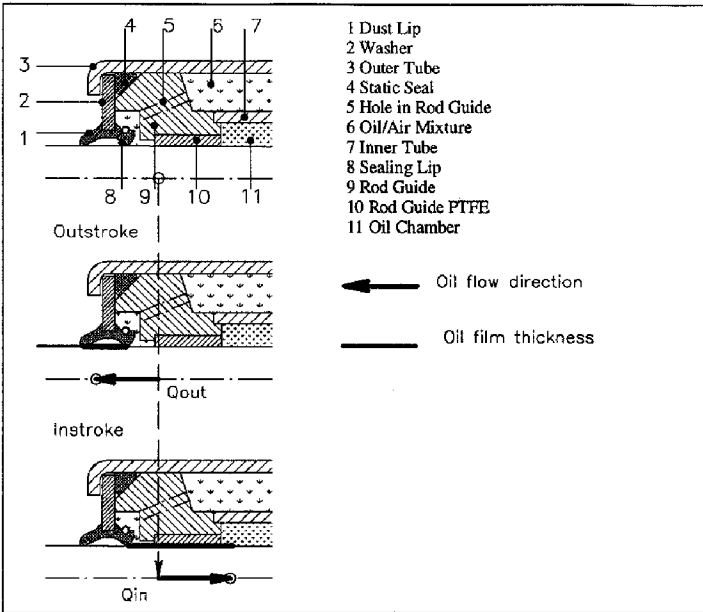


Figure 3 Definition of instroke and outstroke for a shock absorber seal.

The thick line through the contact areas between shaft and seal in Figure 3 denotes the film thickness during relative movement. The area between the sealing lips and the dust lip can be filled with grease or oil, while the film thickness in the visible area at the air side of the dust lip must be minimal. During instroke all oil that was transported through the contact zone must be transported back into the shock absorber.

In order to quantify the oil flow as a function of seal geometry, oil viscosity, temperature and other operating parameters the fluid film formation in the contact area must be described by a hydrodynamic lubrication model.

1.2.3 Basic principles of hydrodynamic lubrication

In Figure 4 the lubricated contact areas between a shock absorber seal and the moving shaft are presented schematically. In general two or more contact areas exist and in between the contact areas chambers exist. These chambers can be filled with fluid or fat. The state of lubrication for each contact area and the boundary conditions in the entry and exit zone depend on the size of the chamber and the amount and type of fluid in the chamber.

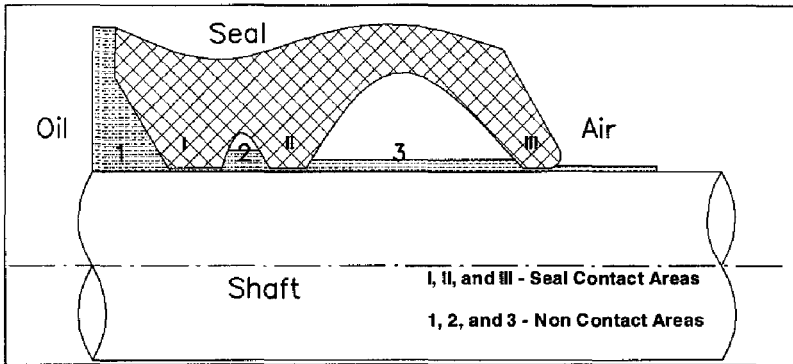


Figure 4 The lubricated contact areas of a shock absorber seal.

The theory of hydrodynamic lubrication was first published by Reynolds [1886]. Reynolds provided the first analytical proof that a viscous liquid film can physically separate two sliding surfaces by hydrodynamic pressure resulting in low friction and theoretically zero wear. All hydrodynamic lubrication can be expressed mathematically by a differential equation which was originally derived by Reynolds and is commonly known throughout the literature as the 'Reynolds equation'. Hydrodynamic lubrication only occurs when two surfaces are moving relatively to each other with sufficient velocity for a load-carrying lubricating film to be generated and when the surfaces are inclined at some angle to each other. For most engineering applications the controlling processes are too complicated to be easily described by exact mathematical equations. In order to derive the Reynolds equation, a number of simplifying assumptions is made. These assumptions are: body forces are neglected, pressure is constant through the film, no slip at the boundaries, the lubricant behaves as a Newtonian fluid, the flow is laminar, fluid inertia is neglected, fluid density is constant, and the viscosity is constant throughout the fluid film.

Due to the assumption that the shaft to seal contact problem may be regarded stationary and axisymmetrical the hydrodynamic lubrication problem reduces to a stationary line contact problem. This simplifies the Reynolds equation, while both the pressure profile, $p(x)$, and the film profile, $h(x)$ are only a function of the axial coordinate x . For analytically formulating the problem the following quasi-linear first order partial differential equation is used:

$$\frac{\partial}{\partial x} \left(h^3 \cdot \frac{\partial p}{\partial x} \right) = 12\eta U_e(t) \cdot \frac{\partial h}{\partial x} + 12\eta \frac{\partial h}{\partial t} \quad (1.1)$$

where $h = h(x,t)$ represents the film profile sought in terms of the coordinate x in the direction of the axis of symmetry of the seal system concerned and t the time elapsed. The remaining influencing quantities are:

η , the viscosity of the lubricant,

$U_e(t)$, the "entraining" velocity, being defined by the combination of the translating velocity of the rod and the seal housing, the tube, with respect to the film, where $U_e(t)$, may be considered a given function of time,

$\partial p / \partial x$, the distribution of the pressure gradients, that is imposed upon the film by the CPD in the contact area between shaft and seal.

The contact pressure between the shaft and the seal is assumed constant in time, independent of friction, shaft velocity and operating temperature and this means that Reynolds equation can be solved inverse with a known pressure profile and an unknown film profile resulting in an analytical equation,

Kanters [1990]. In appendix B the method of Kanters [1990] is expanded by Van Dijnsen [1995] to determine the film profile, leakage and friction of radial lip seals for reciprocating shafts.

1.3 PL Automotive

An important part of this work is formed by the implementation of the theoretical knowledge as a tool for seal design and optimization of PL Automotive. A number of decisions concerning the morphology of the design process and the software used is made based upon the available financial and human resources of PL Automotive. Because of this a short description of the company is presented as a part of the introduction.

PL Automotive is a company with approximately 200 employees and a turnover of 30 million guilders per year. PL mainly produces shock absorber and waterpump seals and can be regarded as one of the key manufacturers of seals for automotive applications. Due to the increased competitiveness on the automotive market PL has invested in fundamental research as a part of the design approach. In order to be able to make this research financially attractive PL has worked together with the Eindhoven University of Technology for both waterpump and shock absorber seals. PL produces approximately 150.000 seals per day.

1.4 Shock absorber

The Shock Absorber Seal (SA-seal) is an important component of a complex dynamic system. The dynamic changes of the operating conditions of the shock absorber due to vehicle movement result in dynamic changes in the seal operating conditions. This dynamic interaction between the vehicle and the shock absorber must be expressed in changes in the relevant operating conditions for the SA-seal, like operating temperature, fluid pressure, and shaft velocity profile. Some models to describe the dynamic behavior of the shock absorber exist, but they are not accurate enough to present the operating conditions for the SA-seal.

In automotive applications, a suspension system supports vehicle weight and controls tire motion. Springs hold up the vehicle on conventional suspension systems, such as parallel arm suspensions. Conventional shock absorbers, excluding spring and air assisted shock absorbers, do not support vehicle weight. Shock absorbers are called motion damping devices because they help to reduce or "absorb" the motion between two points, such as the up-and-down movement of a moving vehicle. A shock absorber is a velocity sensitive device, which means that the speed and the resulting control force are directly proportional.

The various parts of the shock absorber work together to dampen motion within a system. A variety of factors determine how the shock absorber is constructed to meet the specific needs of an application. These factors include physical orientation during operation, operating environment, length of stroke, load, and velocity or frequency. The function of a shock absorber is to absorb and dissipate energy when mounted between two points that move relatively to one another. A shock absorber is designed to work in parallel with a spring force, because the shock absorber alone will not support a static load. The damping mechanism in the shock absorber is hydraulic. This means that damping - the reduction of tire and suspension motion - is achieved by the controlled movement of fluid under pressure. It is the motion of the piston inside the shock absorber that pressurizes the fluid. The resistance to this movement (kinetic energy) produces heat (thermal energy) which is dissipated into the atmosphere through the shock absorber housing. The principle of fluid displacement works in both shock absorber cycles: compression or instroke and rebound or outstroke. The extension cycle controls motion of the vehicle body sprung weight. The compression cycle controls the same motions of the lighter axle and tire unsprung weight.

Figure 5 presents two different types of shock absorbers, mono-tube on the left and twin-tube on the right, and a schematic representation of the shock absorber used to model the oil flow in the tube.

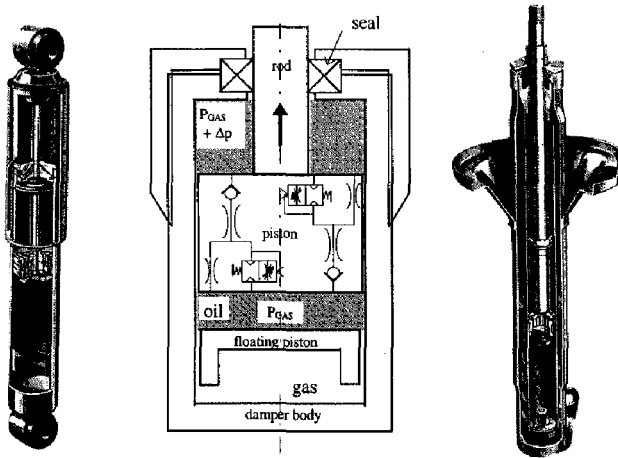
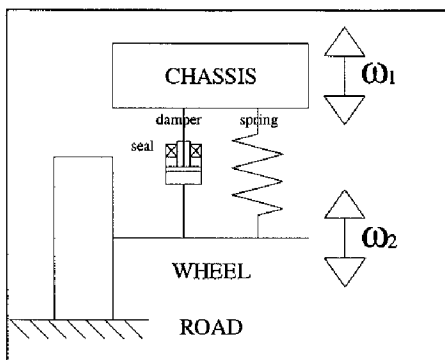


Figure 5 Schematic representation of the shock absorber.

The functionality of the shock absorber is determined by controlled fluid movement and consequently the volume and properties of the oil inside the shock absorber. Therefore, changes in the amount of oil or the composition of the oil will affect shock absorber operation. The seal performance determines leakage and contamination of the oil. As shock absorber operation is of main importance to vehicle steering behavior and comfort, it can be said without exaggeration that good seal performance is of direct importance to vehicle safety and comfort.

The shock absorber is a part of the suspension system of the car. All forces and movements that are the result of a car moving over a road must be controlled by the suspension system. For the shock absorber seal, forces and movement can be distinguished in two main directions: parallel, and tangential to the shock absorber centerline, Reimpell [1989]. Tangential movements and forces are called side loads. Side loads can be regarded as non axisymmetrical seal loads. The influence of the side load is not taken into account if the sealing situation is analyzed axisymmetrically. Although, the sealing contact is assumed to be axisymmetrical in order to make seal analysis cost effective, some tests with non axisymmetrical loads must be carried out to judge the seal performance in the shock absorber for a realistic operating condition.

During the life of the seal the entraining velocity is an important parameter for hydrodynamic fluid film formation. This velocity is defined by the combined parallel movement of the rod and the seal housing. Figure 6 presents a schematic overview of the different types of parallel motion that can occur during seal service life. The entraining velocity is defined by the combined movement of the wheel and the car body. Shock absorber and thus seal life test procedures are based upon the possible types of motion for the schematic suspension system presented in Figure 6.



If $\omega_1 = \omega_2 = 0$ the shock absorber seal must function under static conditions and thus the static sealing mechanism is important.

If $\omega_1 \neq 0$ and $\omega_2 = 0$ the rod displacement and the entrainment velocity profile for the shock absorber seal can be described a mono-frequent sinusoidal profile.

If $\omega_1 \neq 0$ and $\omega_2 \neq 0$ the entrainment velocity profile for the shock absorber seal can be described a bi-frequent sinusoidal profile.

Figure 6 Schematic overview of a suspension system.

1.5 Design task

The functional demands on the design of a SA-seal can be derived from the requirements on the functionality of the shock absorber which can be translated to demands on the oil in the shock absorber. For optimal shock absorber operation during its service life, leakage and pollution of the oil volume inside the shock absorber are not allowed, resulting in the functional demands on the SA-seal as

- 1) prevent leakage of oil,
- 2) prevent contamination of the oil
- 3) the functional service life of the seal must be larger than the service life of the shock absorber.

These functional demands will now be discussed shortly and definitions of some frequently applied terms will be given.

1.5.1 Prevention of leakage

A general definition of leakage is the loss of oil from the shock absorber during operation. Thus the main task of the designer is to produce a seal which has zero leakage during shock absorber operation. Leakage of oil from the shock absorber can occur under different circumstances and two types of leakage are identified as static leakage and dynamic leakage.

1.5.1.1 Static leakage

Static leakage is defined as the loss of oil from the shock absorber at places where no relative movement between the elastomeric seal material and the steel from the shaft or housing takes place. This type of leakage can occur in the contact areas between the housing and the seal and in the contact areas between the shaft and the seal during standstill of shaft. The main cause for static leakage is the pressure difference between the oil and the ambient pressure, resulting in a pressure penetration of oil between steel and elastomer when the fluid pressure exceeds the static contact pressure. Another cause of static leakage can be the existence of microscopic channels in the contact area between steel and elastomer resulting in an oil flow due to the pressure difference over the channel combined with capillary suction effects which allow oil to pass the contact area resulting in leakage.

1.5.1.2 Dynamic leakage

Dynamic leakage is defined as the loss of oil from the shock absorber during relative movement between shaft and seal through the area where relative movement takes place between the elastomeric seal material and the steel from shaft or housing. For SA-seal the dynamic contact areas are formed by the "static" elastomeric seal material and the moving shaft surface.

1.5.2 Prevention of oil contamination

Contamination of the oil is caused by the fact that during shock absorber operation water and dust from the surrounding are transported into the shock absorber by the movement of the shaft. Water and dust in the oil lead to significant changes in shock absorber operation and can not be tolerated. Dust and sand cause changes in flow through the small channels inside the piston of a shock absorber and increase wear of these channels significantly, while water inside the shock absorber changes the compressibility and properties of the oil, resulting in an unwanted change of shock absorber operation.

1.5.3 Seal service life

The functional service life of the seal is defined as the period of time in which the seal operates within a specified set of limits on the seal performance, leakage, friction and contamination. Although ideally seal performance should remain unchanged over the service life of the seal, seal performance changes due to the dynamic operating conditions and by wear of the seal. Changes in the seal performance can be expressed in terms of thermal and chemical aging of the seal material and by wear of the seal material in the dynamic contact area. Aging of the seal material can be minimized by a good choice of the rubber compound in relation to the sealed fluid and the operating conditions, but the amount of wear is mainly determined by the friction in the dynamic contact area between shaft and seal. Seal friction and wear are caused by the interactions between the moving shaft and the 'static' seal material. This is a complex process depending on a large number of influencing parameters. However, a generally accepted rule in seal design is that in order to minimize wear seal friction must be minimized.

The influence of friction on seal life is clear and in general it can be stated that the higher the value of the friction the higher the wear and the shorter the life of the seal. This means that the seal designer has to control friction and abrasion while maintaining minimal leakage. In order to achieve this goal several possibilities exists:

- 1) Changing the seal geometry.
- 2) Changing the shaft-seal material combination.
- 3) Changing the surface roughness
- 4) Changing or modifying the operating conditions.

Summarizing, it can be stated that an optimal seal design from the functional point of view has constant seal performance over the service life of the shock absorber with zero leakage of oil, zero penetration of external contaminants and has no friction in the dynamic contact area. As for a radial lip seal on a reciprocating shaft it is not possible to create a seal which combines zero leakage with no friction, seal design optimization with respect to optimal seal performance can now be defined as minimization of the static and dynamic leakage, minimization of the amount of external contaminants, which can enter the shock absorber and minimization of friction.

1.6 Design morphology and methodology

An engineering design process starts with the awareness of a specific human need or want and the aim of a good design method is to find a solution in a systematic and cost effective way. The

chronological order of a design method is often called the morphology of the design method. The morphology of the design method is represented by the main phases which a design project must pass. For a general engineering design procedure four steps can be distinguished, as given in Figure 7.

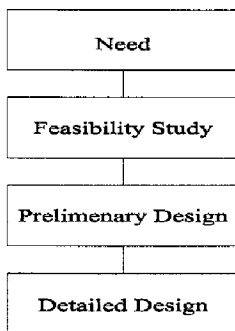


Figure 7 The morphology of design (Moore 1993).

In order to create a systematic practical seal design strategy the four steps of Figure 7 must be specified as standard procedures incorporating knowledge about seal design parameters and seal performance. In order to make the design procedure useful, the time-to-market from a specified need to the optimal product has to be well-defined, predictable and, if possible, constant and the performance of the final design has to meet the specified need.

The seal design process starts with a certain list of demands specifying the need for a new or improved seal design in terms of the minimal requirements on seal performance (leakage, friction and service life), the optional requirements, for example special geometrical features, and the seal operating conditions qualitatively and if possible quantitatively. As elastomeric contact seals are already being applied in large numbers and under different operating conditions, some general consensus exists on the overall list of demands on seal designs, expressing possible leakage, friction and service life for an existing seal design and a given set of operating conditions.

Depending on the list of demands an initial or basic design is chosen. Any new design can initially be regarded as a black-box, which has to meet the given list of demands, but this approach would exclude the knowledge of the seal designer from the design process. In general, this first choice is mainly based upon experience of the designer. This experience combined with creativity is required in order to synthesize a combination of design parameters into an initial design meeting the list of demands.

In Figure 8 the black-box point of view towards seal design is given. In order to analyze and optimize the initial design, the designer has to disclose the black-box, following a certain design procedure, in which the relationships between all seal design parameters and seal performance are described. This procedure results in a design, meeting the given set of demands with optimal efficiency. The efficiency of the design procedure can be judged based on the final design performance and resources consumed by the design process. However, the final design of any seal is also influenced by economical and marketing boundary conditions. In this work these factors will not be taken into account as major influences on the final design of the seal and are only mentioned when relevant with regard to decisions made during the seal design procedure.

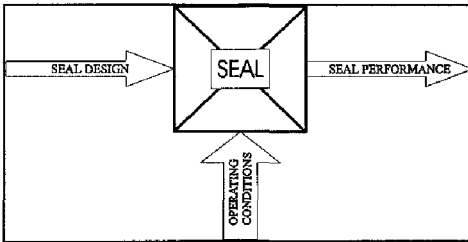


Figure 8 Black-box point of view towards seal design.

For a large number of practical sealing problems the choice of a seal from a catalogue is a standard engineering procedure and for these situations the black-box approach is accurate enough and economically efficient. Although for a large number of engineering applications standard seal designs meet the required seal performance, for special applications, like high pressures and high shaft velocities, the seal design has to be optimized with respect to its performance. However, for the seal designer and manufacturer optimization is not trivial, as the number of seal design parameters influencing seal performance is large. Due to increasing environmental and customer demands, the seal designer has to be able to predict accurately the relationships between seal design parameters and the seal performance of a new design.

The quality of a seal can be expressed in terms of leakage, friction and service life and the final definition depends largely on the point of view taken by either the designer or the client. In order to theoretically quantify leakage, friction and service life of a new seal design the known sealing, lubrication and friction mechanisms from literature will be investigated and used when possible.

The quality of the seal is of major importance for survival in a competitive market, but quality is an attribute which can be described from different directions. Quality multidimensional, it involves more dimensions in the evaluation of the product (for example performance, features, reliability, consistency, serviceability, durability, security, aesthetics, perceived quality, etc.), quality is not absolute but relative, because its value is not compared with an absolute value, but with what the customer perceives, quality is dynamic, its value changes with time, quality is global, it involves internal and external functions of the company. For this reason, good structuring of the design process of new or modified seals up to its preliminary phases, involving the customer as primary part is of fundamental importance.

The main aim of any seal designer is to find the optimal solution for a certain set of surrounding conditions within the area limited by the possible combinations of seal, shaft and lubricant. In order to find the influence of different design parameters a mathematical model of the relations between the different components must be formulated. The interaction between shaft, fluid and seal can be seen as a viscoelastic-hydrodynamic contact problem. A generally valid model describing all the relationships has not yet been found and is not expected to be found in the near future. This is caused by the complexity, the strong non-linearity and the time dependence of the models needed to describe the processes involved.

In order to describe the sealing system, a number of simplifying assumptions for the tribological system has to be made and consequently the final results can only be applied in the area where the assumptions are valid. For a geometrical optimization of the seal the relation between changes of geometry and changes in seal operation must be found. Any model that can be used for optimization of the geometrical design parameters of the seal must describe the relationships between seal geometry and seal performance as accurately as possible.

An ideal operating radial lip seal is a tribological system with zero leakage and zero wear. As these demands contradict, the optimal solution given a certain set of requirements must be found through an

optimization process, in which the influence of different design parameters on the final results can be taken into account. The tribological system is built up by three major components :

- 1) the seal, with its prescribed geometry, surface roughness and material behavior,
- 2) the shaft, with a given diameter, surface roughness and material behavior,
- 3) the lubricating fluid, with its own characteristic pressure-viscosity-temperature relationship.

1.7 Literature review

In order to capture the currently available research data concerning seal design and sealing mechanisms a literature review has been carried out. As this work is focused on the development of a practical seal design strategy also the literature review was focused on theoretical and experimental work with possible practical relevance for implementation in a daily seal design strategy. This means that complex theoretical work has been studied, but if no direct practical application could be found the models were not applied. The literature review has not been restricted to literature about seals and sealing mechanisms for reciprocating shafts, but also incorporated seal design and sealing mechanisms of seals for rotating shafts in order to present a general overview of the current scientific knowledge on dynamic fluid sealing. From the seal geometry point of view there is not so much difference between radial lip seals for rotating shafts and reciprocating shafts, although the sealing mechanisms are different.

The experimental and theoretical scientific knowledge has to be used and combined with the existing practical and experimental knowledge of the seal designer a seal design strategy will be defined. However, the existing practical knowledge has been poorly documented due to lack of a systematic and standardized approach of the experiments. The results of the literature review and an summary of existing practical knowledge about seal design will be given in three sections: Seal Design in General, Seal Design for Reciprocating Rod Seals, and Practical Seal Design.

The aim of this literature review is to summarize the state of the art knowledge concerning the relationships between the different components of the sealing system shaft, seal, housing, and lubricating fluid, and the seal performance, leakage, friction and seal life.

1.7.1 Seal design in general

Müller [1990] explains various types of fluid sealing and different sealing mechanisms, for rotating and reciprocating shafts. A good overview of the state of the art knowledge on seals and seal design is given. In this work it is concluded that the most important parameter for the performance of reciprocating shaft seals is the CPD. Furthermore, it is stated that the relationship between the contact pressure profile and the film profile can be determined with the inverse hydrodynamic lubrication theory. Müller [1990] has mainly dealt with high pressure seals, like U-ring seals, compact seals, and step seals. A distinction was made between full film lubrication of the contact area and boundary or mixed lubrication of the contact zone. The easiest solution of the inverse hydrodynamic lubrication theory is found when the contact area is supplied with enough oil to generate the maximum possible oil film. For this situation the film thickness only depends on fluid viscosity, shaft velocity, and the maximum value of the pressure gradient in the direction of motion.

Müller [1990] defines that no leakage for reciprocating shaft seals is found when the seal is able to transport more oil back into the pressurized fluid chamber, as it can transport out of the pressurized chamber during outstroke. An important aspect of non leaking seals is the asymmetrical CPD with the maximum pressure gradient at the high pressure side. Müller also defines the optimal CPD as a triangular shaped contact pressure profile, with the maximum contact pressure as close as possible to the edge of the contact zone on the high pressure side. Also different steps of the design optimization of a PTFE step seal for a reciprocating rod are given and regarding the CPD, it was found that the

optimal solution has a small contact width with a highly asymmetrical, nearly triangular, contact pressure profile with the maximum contact pressure on the high pressure side.

Kanters [1990] modeled the tribological process in the seal contact area and verified experimentally the theoretical predictions of leakage and friction. The tribological process in the contact area depended mainly upon the deformed geometry of the seal and the stresses in the seal material after mounting and pressurization. The static frictionless CPD was determined by the FEA of the seal. Subsequently, the inverse hydrodynamic lubrication theory was applied to the frictionless static CPD to determine seal leakage and friction.

Kuiken [1991] has tried to use the same approach for rotating shaft seals as presented by Kanters [1990] for reciprocating shaft seals. It is concluded that the CPD between the shaft and the seal is a parameter which can be influenced and analyzed by the seal designer, but for rotating shafts the shape of the CPD could not be directly coupled to seal performance characteristics. Even though this direct relationship between the shape of the CPD and the actual seal performance could not be proven, seals were designed based upon a design objective function expressing the optimal shape of the CPD. Gabelli [1992], has already questioned the need for an asymmetric pressure distribution in the contact area. However, if the optimal CPD does not correspond with the demands used for optimization, the objective function can be modified easily and a new set of calculations can be carried out to find the optimum given the new objective function.

The method presented by Kanters [1990] and the design objective function presented by Kuiken [1991] will be combined into the practical seal design strategy. The CPD between the shaft and the seal can be investigated both theoretically and experimentally. The theoretical determination of the CPD by means of FEA and changes in the shape of the CPD as a function of changes in geometrical parameters is presented by Kuiken [1991].

In general, it can be said that the determination of the CPD for any given seal geometry based upon a parametric model of the seal geometry is completely automated and can now be carried out by non-expert users. This approach towards seal design was developed for the design of rotating shaft radial lip seals. The direct link between the shape of the CPD and the seal performance was not described by a theoretical model. On the theoretical side of the sealing mechanism of radial lip seals no major break through is found over the last two years. In the beginning of the project of Kuiken [1993] it was expected that the optimal CPD would be found from the lubrication theory. The model describing the relations between all three components under dynamic sealing conditions, which was being developed in another project has not been able to come up with the results which are needed to come to a better definition of the goal function. This is mainly due to the fact that the development of the two-dimensional VEHD-theory, Stakenborg [1988], has raised so many questions with respect to the usability of the model that further theoretical development has been postponed. The only possible way to expand the geometrical optimization of radial lip seals is by including demands on the CPD from the lubrication side of the problem. As for rotating seals still no general mechanism describing the relation between fluid film and contact pressures has been found, it is necessary to restrict ourselves to seals for translating shafts of which the mechanism for fluid film formation can be described mathematically. As a result of this the CPD, leakage and friction can be determined theoretically and optimization like for the LIPS seal, Kuiken [1993] is possible with respect to both leakage and friction.

Some researchers, like Salant [1995] and Van Bavel [1995], have modeled the complete dynamic sealing action for rotating shaft seals by describing the influence of the deformed shape of the seal surface roughness due to shear stresses as the most important mechanism for good seal performance. These models present results on the influence of shaft speed, fluid viscosity, temperature, seal surface roughness profile on the seal performance characteristics, like reverse pumping action and frictional torque. However, this type of theoretical work seems capable of explaining and describing the sealing mechanism, the practical usefulness of the sometimes extremely complex models, using surface roughness profiles to explain seal behavior cannot be used for daily seal design at the moment.

1.7.2 Seal performance of reciprocating rod seals

An extensive literature review on seals for reciprocating rods has been presented in Kanters [1990]. The main conclusions and relevant facts about radial lip seals, for the sealing of a shock absorber, will be summarized. In Kanters [1990] the main part of the work was concentrated on a good theoretical determination and experimental verification of both leakage and friction. Kanters has presented a model that allows studying of different influences on both leakage and friction. However, some questions remained whether or not this model could be applied for practical seal design, especially the assumptions of stationary rod motion and full fluid film are not always valid for practical sealing systems.

In soft highly deformed contacts the entry and exit regions are only a small fraction of the total contact zone. A soft highly deformed contact, under lubricated conditions, may be divided into three regions. At the leading edge there is a short entrainment zone in which the film thickness is generated. This region controls the overall behavior of the contact. The film thickness generated there is then dragged through the central region at a speed close to the instantaneous entrainment velocity, with only minor modifications in the process to emerge at the trailing end. At the trailing end is the exit zone where the film thickness undergoes a short-lived reduction as it passes through an exit restriction before leaving the contact.

In most soft contacts the extents of the inlet and exit zones are extremely small. Thus, although the inlet zone is critical in generating the fluid film and the exit produces the lowest clearance, these end zones only are a minor part of the total contact and the majority of the contact lies inside the central zone. When non-steady motion of the contact is considered, the situation becomes more complicated. Firstly, under some conditions as for example in reciprocating contacts, the film thickness may emerge through the end where it was generated. Under these circumstances it is possible for the contact to consist, for a short time, of two exit zones. Secondly, squeeze-film effects have to be considered in both the entry and exit regions and in the central zone. Finally, the clearance profile under the contact is no longer smooth but may contain substantial, localized, variations and it is possible that these may significantly change the pressure distribution from its dry contact profile.

The clearances of a seal for reciprocating rods lack symmetry in their clearance profile due to the pressure of the sealed fluid. The difference of the shape of the dragged restrictions for two halves of the cycle is due to the lack of symmetry. In general, the clearances on the non-fluid side of the seal are smaller than the clearances on the pressurized side.

The value of the minimum film thickness can of course be found by carrying out a full dynamic elasto-hydrodynamic lubrication (EHL) analysis. This is, however, time consuming and is unsuited for use in design packages except, perhaps, as a final checking procedure. For most of the time in these contacts the use of the quasi-static analysis is adequate. It is only in the periods immediately adjacent to the reversal of entrainment that serious errors occur. If the quasi-static approach is supplemented by a rapid calculation of the minimum film thickness at this point then reasonable estimates of the minimal clearance between shaft and seal throughout any operating cycle could be produced.

During relative motion of the shaft friction will occur in the contact area. In order to reduce friction and by this wear the contact is lubricated, so that the seal will perform its task during a maximum period of time.

The definitions of the different directions of relative motion are defined by Kanters [1990]. This means, that for an instroke the motion, from a seal's point of view, is directed from the low to the high pressure side and during an outstroke in the opposite direction. The difference in oil flow between an instroke (in-leakage) and an outstroke (out-leakage) is called the net-leakage. It is clear that low friction and at the same time zero leakage are wanted. As these two demands contradict an optimization problem is defined by the fact that the optimal compromise between leakage and friction has to be found, given a certain set of surrounding conditions.

1.8 Strategy for seal design optimization

Based upon the assumptions made in the previous sections, it is now possible to define a strategy to design and optimize the geometry of radial lip seals for reciprocating shafts based upon the shape of the CPD between the shaft and the seal. Figure 9 presents a schedule of the different steps which are needed to optimize seal designs for shock absorber seals.

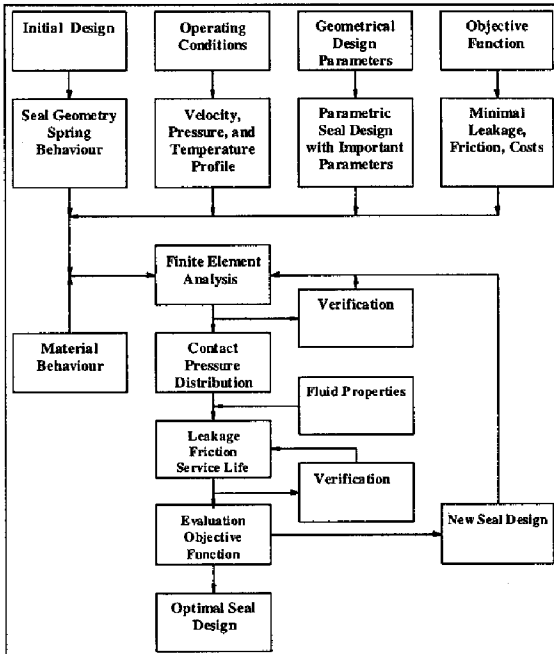


Figure 9 Seal design optimization schedule.

At this point it can already be stated that the definition of the detailed or optimal design is not an unique and static feature of the new seal design as several interests must be combined into the final new design. Whereas the customer demands optimal seal performance with respect to mainly minimal leakage under all possible operating conditions, the seal manufacturer is looking for optimal seal performance against minimal manufacturing costs.

So each new or modified design has to be checked on its performance in relation to the costs. Costs are not only defined by the actual costs of production, but also the costs of seal rejection during manufacturing and failure during operation must be included in this optimization criterion.

Summarized, this means that two optimization criteria exist. One of the customer, which demands optimal seal performance and service against a minimal prize per seal and secondly, out of the seal manufacturer which asks for maximal profit against optimal seal performance. For the seal manufacturer this means that he must obtain minimal overall costs from design to the end of the seals service life. This includes labor, materials, transportation, and claims on seal failure.

As these criteria are never static and always subject to economical interests of both manufacturer and customer, the only solution lies in a flexible design strategy based on fundamental knowledge about the mechanisms which control seal performance, but with enough flexibility to adjust to the

constantly changing market of questions and demands on seal design. The seal design optimization strategy is focused on the geometrical optimization of shock absorber seals, but based upon the same approach different features of the seal design can be judged.

1.9 New design approach

Determination of the optimal seal geometry, with respect to leakage and friction, given a certain set of operating conditions, can be performed with the new radial lips seal design approach. Proper theoretical and experimental verification of the results will be carried out during the design process according to a number well defined experiments.

In Figure 10 the stages of the old existing design procedure are compared with the new design approach and this comparison is made based upon the new five stage design procedure which is developed during this project and implemented for daily seal design.

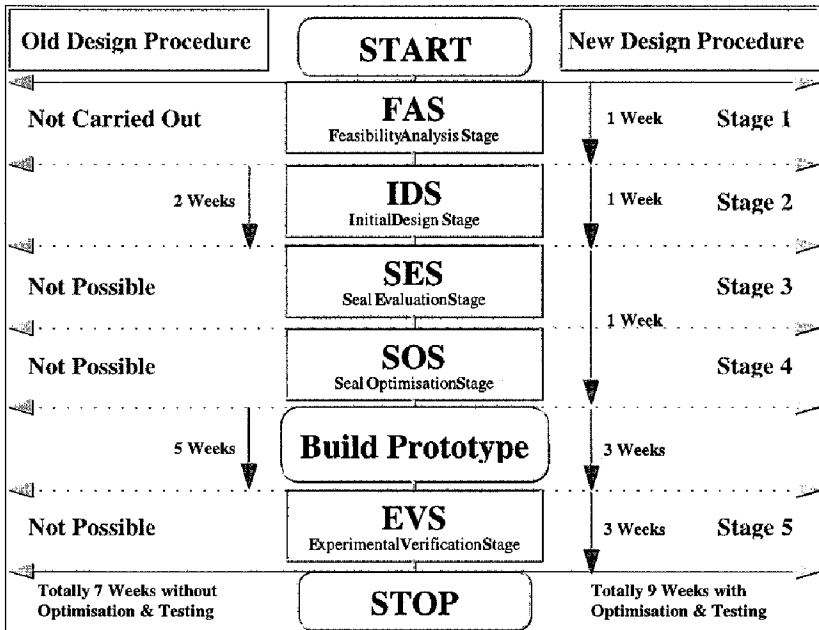


Figure 10 Comparison of the old and the new seal design procedure.

The lead-time of the product, as presented in Figure 10, has gone from 7 to 9 weeks and thus no improvement seems to have been made. However, the lead-time of the old procedure is the time for the first product and in general two or three prototypes had to be produced before the customer was satisfied. The time for testing of and communication about the new product resulted in lead-times of 21 to 30 weeks, which were far too long. With the new approach it is possible to predict the lead-time for a *fit-for-use* seal design and to optimize/reduce this lead-time depending on the customer needs.

The morphology of the new design procedure is based upon the layout presented in section 1.5 and each stage of the design procedure will now be shortly discussed. During the first stage, the Feasibility Analysis Stage (FA-stage), the need for a new or improved seal design is expressed and the list of demands on seal performance, leakage friction and service life, given a certain set of operating

conditions, temperature, pressure and shaft velocity profile and the properties of the sealed fluid are documented in close cooperation with the customer, who expresses the need for the new seal. Based upon the data gathered during the FA-stage an initial design is proposed during the second stage, the Initial Design Stage (ID-stage). The definition of the new design incorporates the choice of the seals main geometrical features, the seal material, and the garter spring. During the third stage of the design process, the Seal Evaluation Stage (SE-stage), the performance of the new seal design is evaluated theoretically based upon the shape of the static CPD for different operating conditions. During the fourth stage, the Seal Optimization Stage (SO-stage), some geometrical features of the design are changed and the influence of these changes on the seal performance is investigated theoretically and based upon the results with regard to seal performance the optimal design is determined. A prototype of the new design is produced and this prototype is experimentally tested according to a set of test procedures.

The important aspects of the different stages during this design procedure will be discussed in this thesis by a practical example.

Chapter 2 presents the new design methodology as a design tool for a new shock absorber seal and the decisions made during the different design stages will be discussed. The influence of seal geometry, seal material behavior and spring behavior will be discussed and design optimization guided by the use of existing CPD's of seals with good performance characteristics is shown. Furthermore, design optimization based upon the Taguchi approach and an objective function of the static CPD of the new seal design will be presented.

Chapter 3 presents the experimental methods to support seal design. Also the experimental verification of some theoretical results is presented.

Chapter 4 presents a discussion of the implemented seal design approach and final conclusions and recommendations are given.

2. New seal design approach

2.1 Introduction

Delivering reliable, high quality seals, design and production processes at low cost has become the key to survival in today's global competition. Driven by the need to compete on cost and performance seal manufacturers are increasingly focusing on the optimization of product design. This reflects the realization that quality can not only be achieved economically through inspection. Designing in quality is cheaper than trying to inspect and re-engineer a product after it hits the production floor or worse, after it gets to the customer, Gunter [1987]. Thus, a new seal design philosophy and advanced numerical tools must be employed to design high quality seals at low cost.

The old design process can be regarded as a trial and error method, because the problem definition, solution strategy, and optimality criteria were not or ill-defined. The seal designer took design decisions without accurate knowledge about the influence of these decisions on the seal performance. On the other hand seals were designed and manufactured and seal performance was regarded satisfactory based upon test procedures of the customer. An optimal seal design was a seal which performed satisfactory during the different test procedures of the customer and which could be produced for a price lower than the market price of the product. However, due to the increasing demands on shock absorbers, the demands on shock absorber seals have also increased. The level of knowledge of the seal designer has not changed and the number of problems has become larger. The time to solve a problem, new design or seal failure, is a critical factor in a competitive market. A fast and accurate solution of a sealing problem can only be based upon knowledge about the seal performance as a function of the seal design parameters in combination with the operating conditions.

In order to improve the existing situation a new seal design procedure is generated based upon the existing theoretical models concerning seal design and seal performance. In order to optimize design decisions the seal designer needs to know the seal performance characteristics as a function of the design parameters. The performance characteristics for a seal can be expressed in terms of the functional demands on leakage, friction and service life. As the performance of a radial lip seal for a reciprocating shaft is determined by the shape of the CPD in the contact areas between shaft and seal, Kanters [1990], the seal designer needs to know the relationships between design parameters, CPD, and seal performance. These relationships must be determined by tools which are incorporated into a well-defined design process.

A seal designer needs to know how different design features influence seal performance and customer satisfaction in order to make choices in the selection of different design features. Owing to the complexity of the relationships between design features and seal performance and the minimization of product lead time the seal designer will often rely upon ad-hoc decision procedures resulting in an arbitrary quality of the seal design. This randomness in design procedures and design features will be perceived by the end user and reflects bad on the customer perceived product quality. The only way to resolve this problem is by means of a *fit-for-use* design process, in which each step and decision taken is documented and understood by the customer, resulting in customer trust in the new seal design before it is actually produced.

2.2 Seal design process

Any design process can be regarded as the transformation of knowledge and information into concrete product specifications, Kaas [1995]. The seal design process can thus be regarded as the change from abstract information gained during the initial stage of the design process, from the functional specifications and the list of demands, to the design specifications, describing the final seal design. A design methodology, a standardized seal design procedure, defines the different stages of the design process in such a way that this design procedure can be reproduced and optimized.

2.2.1 Design in general

The early design phase of a product or process has the greatest impact on life cycle cost and quality. Therefore significant cost savings and improvements in quality can be realized by optimizing product designs. The three major steps in designing a quality product are: system design, parameter design, and tolerance design.

System design is the process of applying scientific and engineering knowledge to produce a basic functional prototype design Kackar [1985]. The prototype model defines the configuration and attributes of the product undergoing analysis or development. The initial design may be functional, but it may be far from optimum in terms of quality and cost. In the new design procedure the major steps for system design are carried out during the feasibility analysis and initial design stage.

Parameter design is an investigation conducted to identify the settings of design parameters that optimize the performance characteristic and reduce the sensitivity of engineering designs to the sources of variation (noise), Kackar [1985]. Parameter design requires some form of experimentation for the evaluation of the effect of noise factors on the performance characteristic of the product defined by a given set of values for the design parameters. This experimentation aims to select the optimum levels for the controllable design parameters such that the system is functional, exhibits a high level of performance under a wide range of conditions, and is robust to noise factors. The steps needed for parameter design are carried out during the seal analysis and seal optimization stage.

Tolerance design is the process of determining tolerances around the nominal settings identified in the parameter design process. Tolerance design is required if robust design can not produce the required performance without costly special components or high process accuracy. It involves tightening of tolerances on parameters where their variability could have a large negative effect on the final system. Typically tightening tolerances leads to higher cost. At the moment tolerance design is not really a part of the new design process. In the near future the presented design procedure can be used to investigate the influence of manufacturing tolerances on seal performance and by this optimize the seal tolerance field with regard to manufacturing costs.

2.2.2 Seal design for reciprocating shafts

The new design procedure can be applied to any type of elastomeric contact seal for a reciprocating shaft. For reciprocating shafts a large variety of geometrical solutions has been presented in literature and in Figure 11 these solutions are placed in available space between the shaft and the housing. Four basic geometrical principles can be found O-ring type solutions, U-shaped type solutions, lip seal type solutions and step seal type solutions.

Although, until now the seal designers did not use a standardized design methodology a large number of seals has been designed and produced over the last 10 years. The practical geometrical knowledge about seal design can be found in the existing designs and an inventory of the geometrical features of these designs has been made and several important features have been analyzed in combination with the operating conditions for a specific design by Maes [1996]. This inventory resulted in three different groups of current basic lip seal design principles and a list with standardized dimensions of all current seal designs. The three different seal types of PL Automotive presented in Figure 11 are: A) Shock Absorber Seals, B) Gas Spring Seals, and C) Valve Stem Seals, although each of the three seal types can be designed with the same methodology only SA-seal will be regarded in this thesis. The knowledge about existing problems with current seals in combination with this inventory is especially important for an estimation of the feasibility of a new design by the engineer. This inventory allows several features of the seal design to be combined with the practical knowledge of the engineer concerning specific problems with a seal under specific operating conditions.

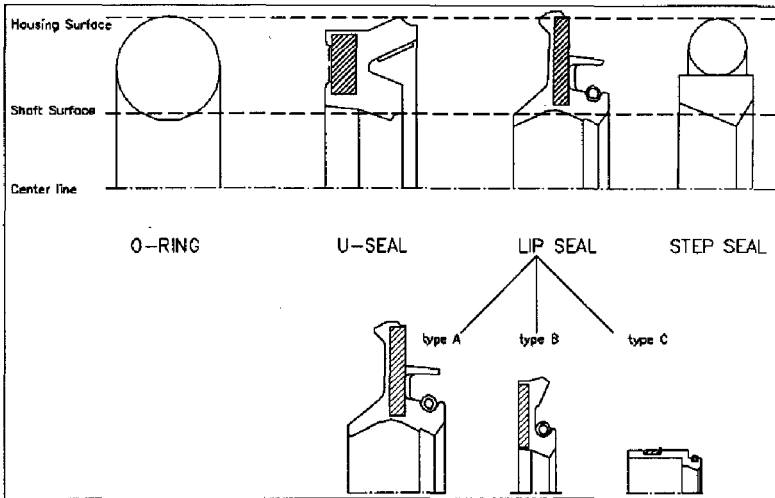


Figure 11 Different seal types for reciprocating shafts.

Type A is the basic geometry of a shock absorber seal, type B is the basic geometry of a gas spring seal and type C is the basic geometry of a valve stem seal. The choice for the type of seal which will be used depends on the application and a number of operating parameters. The choice for a certain shape is mainly determined by the combination of the application, the pressure profile and the shaft velocity profile. Low pressure (0-0.5 MPa) and low velocity sealing problems can be solved with all types of seals, but due to its simple shape and standardized dimensions an O-ring is preferred. For fluid pressures between 0 and 2.5 MPa lip seals of type A can be applied and for pressures applications between 0 and 10 MPa seals of type B can be applied.

In this chapter radial lip seals for shock absorbers are studied and the implementation of the seal design procedure will be clarified by the development of a new design of a radial lip seal for the reciprocating shaft of a shock absorber given a specific demand on seal performance. All stages of the design process will be shortly discussed and the choices made in these stages are explained and documented. The name of the new seal prototype is the SC1401 and this seal will be used for a shaft diameter of 11 mm. As this shaft diameter is the most common shaft diameter and most seals are produced to seal this shaft diameter the result of this design process is of practical importance for more than just one seal and it may in the near future result in the definition of a standard design for the 11 mm shaft.

In order to communicate about seals and seal design a standard nomenclature for SA-seals of type A is used, Maes [1996], and in Figure 12 the nomenclature for a SA-seal is explained by assigning names to different features of the seal design. Some names depend upon the customer and the application, the metal insert can also be called washer or shell and the gas lip is often mentioned as the non return valve expressing the function of this lip for shock absorber seals.

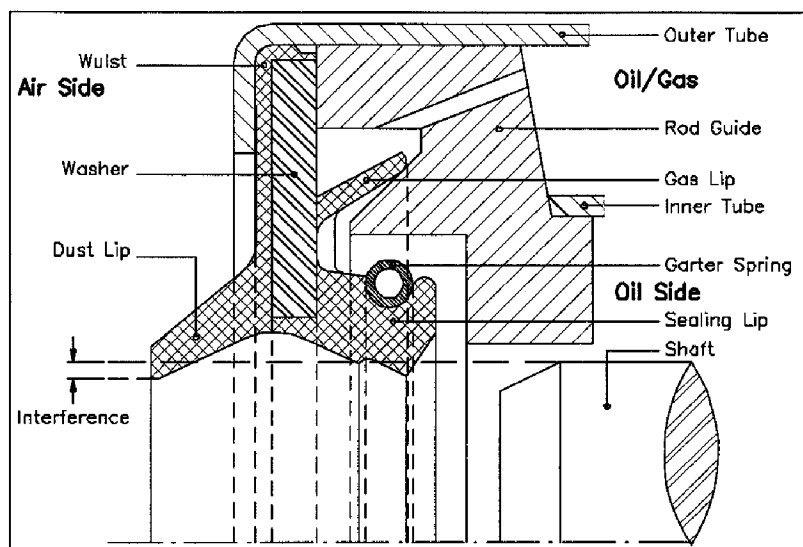


Figure 12 Nomenclature for a Shock Absorber Seal (SA-seal).

As the overall geometry of a SA-seal is complex, the first step towards simplification and standardization is to reduce this complexity by defining a small number of geometrical features. These features are identified based upon the list of functional demands resulting in six components describing a complete seal design. These components are 1) washer, 2) sealing lip, 3) dust lip, 4) seal ridge, 5) gas lip, and 6) garter spring. During the FA-stage an overview of the needed seal features has been documented and all necessary features are included in the new geometry resulting in a design drawing, presented in Figure 13.

2.2.3 Demands on state of the art seal design

The new design procedure must enable seal design optimization. In general optimization of a function or process can be defined by the minimization of an objective function given a certain set of boundary conditions. Optimization of well defined mathematical problems can already be complex, but the general definition of an optimal design procedure given a number of people and machines is almost impossible. In order to judge the new seal design methodology a number of criteria is needed and these criteria can be regarded as a list of demands for the new design approach. In the following paragraphs the list of demands will be stated and the derivation of these demands based upon a short description of the old design approach will be given. Some of the problems concerning the old design procedure will be identified, resulting in a complete list of demands for the new design procedure.

The new design procedure must use the existing practical knowledge about seal design. Millions of shock absorber seals are already being produced each year and this means that the current knowledge of seal production results in good seal performance and cost efficient production of shock absorber seals. This knowledge must not be neglected, but incorporated in the decisions which are made during the new design procedure. It has proven to be difficult to access this knowledge in a systematic way and seal design changes were made randomly depending on the problems encountered during prototyping, testing and production of the seals. It was also found, that due to the missing relationship between seal design and seal performance, information about the existing design procedure with regard to optimizing seal performance lacked completely and thus seal design optimization was not possible. Feedback data concerning seal failure could hardly be interpreted and translated into design

modifications by the seal designer. In order to document the existing knowledge about seal design an inventory of the geometrical features of all existing seal designs has been made, Maes [1996]. This inventory can be used as a tool for the definition of an initial seal design.

The new design procedure must increase knowledge about seal performance and seal design for the seal manufacturer. Seal performance was tested by the customer resulting in a long time between the prototype and feedback to the seal designer from the test results. The seal designer and manufacturer were not able to test the seals directly after prototyping. Evaluation of the customer test results is difficult, when the actual test procedures are not known. The existing knowledge about seal design was completely scattered over all areas of the design process. No design guideline was available, leading to constant design improvement by incorporating the knowledge of the seal performance of existing designs into the development of new designs.

Summarizing, it can be stated that in the old design procedure almost all design decisions were made by the customer, but the actual problem solving was left to the seal designer. The initial design was proposed by the customer, the seal prototype was tested by the customer and changes in the design concerning improvements in the seal performance were proposed by the customer. So the relationships between the final seal design and seal performance were not completely understood and could not be influenced by the seal designer. This resulted in the conclusion that not only the theoretical knowledge about seal design must increase, but the seal designer must also be able to perform functional tests on new seal designs to validate seal performance.

The different stages of the new design procedure must be clearly identified and documentation for each stage must be standardized. From experience it is known that errors, mistakes, and miscommunication combined with incomplete specifications of the new product result in problems during building of the prototype and approval of the new seal design for productions. A time consuming communication process had evolved due to the fact that the customer proposed changes in the seal design after prototyping, testing or production. This resulted in a wrong distribution of the responsibilities towards the new seal design, mainly guided by the customer instead of the seal designer. The overall time-to-market of this process which was used so far is estimated between 1 and 2 years. It is hard to improve the time-to-market, because different stages in the design process, the responsibilities and the needed results from each stage were not defined. Furthermore, a poorly documented trial and error process resulted in an undefined time-to-market. This trial and error process can not be optimized, resulting in customer dissatisfaction and increased problems to get crucial information from the customer.

The new design procedure must be based upon the current state of the art scientific knowledge concerning sealing and lubrication mechanisms, which must be made accessible for the seal designer. Theoretical knowledge concerning seals and sealing mechanisms has been available for more than 35 years, but in general it has proven to be difficult to translate the results from research into actual changes of the seal design. Some researchers, like Müller [1990], have combined the practical and theoretical approach in their research, but due to the complex numerical methods and theory used these results are hardly being used in practical design procedures. The only way to achieve such a combination between scientific knowledge and daily seal design is by applying the scientific knowledge in a practical design procedure and prove the benefits to the seal designer. The underlying ideas concerning the relationships between seal design and seal performance must be explained and transformed into tools which can be used for design analysis. Beneficial to the seal designer is an increased understanding of the important seal design parameters, which results in better overall seal design, and more effective design changes when faced with sealing problems.

The new design procedure must fulfill customer needs for improved seal design and gain customer trust resulting in better communication and faster decisions concerning design changes. One of the major problems so far has been to convince the customer that it is necessary to define the demands on the new seal design as accurately as possible. This was mainly caused by the fact that the customer

was not convinced of the capabilities of the seal designer to incorporate the accurate knowledge of the operating conditions into the new seal design procedure resulting in a better design.

The new, implemented five stage seal design procedure presented in paragraph 1.6 meets all the above mentioned demands and has brought the advantages which were expected. This new design approach will now be clarified on the basis of an actual example for the development of a new standardized FPM-compound shock absorber seal for an 11 mm shaft.

2.3 Implementation of the new seal design procedure

The design procedure always starts with a specific need or want. In this example the customer wants a new standardized shock absorber seal design for an 11 mm shaft. The most important aspect in any standardized design strategy is communication. In order to develop a new seal design which satisfies the customer it is necessary to know and document exactly what the customer wants. In order to achieve this a questionnaire with all relevant information concerning the functional demands, operating conditions and specific demands for the new seal design is answered by the customer. This document also includes the test procedures which will be applied to the prototype to experimentally validate the seal performance. All these test procedures are standardized and can be carried out both by the customer and the seal designer. The results of the most important tests have been compared, resulting in the fact that the seal designer is now capable of testing the new design.

The development of a new seal design for an 11 mm shaft of a SA-seal of type A will be presented, with a specific demand on the seal material to be used and the visible leakage of oil during the cold test.

The cold test is a standard test procedure where the seal is mounted in the shock absorber and the total shock absorber is cooled to -40°C , taken out of the refrigerator and mounted on the life cycle test rig and a 1 Hz frequency is applied to the shaft. Due to friction and the surrounding temperature the temperature of the shock absorber and the seal rise and this rise in temperature is monitored in combination with a visual inspection of the oil film on the shaft. At a certain temperature the film on the shaft will not be small or not visible anymore and at this temperature the seal is tight. For NBR-compounds the minimal temperature where there is not too much leakage lies near -40°C , but for the current generation of FPM-compound seals the minimal temperature is -15°C . Due to the material properties of FPM-compound the same performance as an NBR-compound during the cold test is not expected, but by geometrical changes the cold test performance is improved as much as possible. Consequently, the aim of the new seal is to minimize the cold temperature for a FPM-compound seal material.

As the overall geometry of a SA-seal is complex, the first step towards simplification and standardization is to reduce this complexity by defining a small number of geometrical features.

2.3.1 Design task

The design task is the development of a radial lip seal for an 11 mm shaft using a FPM-compound, which performs well during the cold test and the life test.

Requirements on the new seal design are:

- * the minimal sealing temperature has to be less than -25°C , and
- * the life cycle test has to be passed without problems, meaning less than 10% oil loss of the original oil volume in the shock absorber.

Design improvements will be judged on a comparison with existing seal designs and by the results from a number of well prescribed experiments.

The result of the cold test is expressed as a minimum temperature for which the seal shows no oil leakage. The problem which has to be solved is the fact that the rubber material tends to harden when the temperature is lowered resulting in a less flexible sealing lip and thus a smaller capability to follow eccentricities resulting in oil leakage. This test is carried out according to internal test specification 0003.SDD, described in Maes [1996].

The result of the life test is expressed as a change of the weight of the test cylinder, which is a measure for the total leakage during the lifetest. This total amount may not exceed 10 % of the initial oil mass in the shock absorber, because otherwise the quality of the shock absorber is not guaranteed anymore. For these tests also a comparison with existing seal designs will be made. It is impossible to account for all the different influences which might play a role during the cold test and the life test, but carrying out the tests in accordance with the test specifications will result in data which can be compared for different seals.

In order to tackle this problem the design methods developed and implemented during the research project are used. The design optimization is carried out by an employee of the seal manufacturer as a final study for a technical high school degree. This approach assures the implementation of the proposed design methods and the transfer of knowhow from the scientists level to the designers level resulting in a scientific approach of the new seal design. During several stages of the design process experimental data will be used to verify the theoretical results. All data is gathered from within the company surrounding and possibilities of the seal manufacturer resulting in a stand-alone design procedure, without dependence on experiments or data from third parties.

2.3.2 Feasibility analysis stage (FA-stage)

Before approaching the new seal design, the designer should assess, at least approximately, the conditions in which the seal will be working. It is desirable to know the range of temperature for any seal and for dynamic seals the range of pressures and speeds during one working period, Gawlinski [1977]. During the FA-stage the list of demands for the new design is generated in close cooperation with the customer. The most important demands on any design are the functional demands. For a seal the functional demands are expressed in terms of leakage, friction, and lifetime.

A good definition of these values poses a lot of problems, because a quantification for both leakage and friction has never been used in the initial stages of a new seal design. No knowledge about the desired quantities exists resulting in the impossibility to meet optimal demands of zero leakage combined with zero friction over an endless period of time. In order to solve this problem the functional demands on a seal design are presented in the form of a number of tests. These tests are carried out by the shock absorber manufacturer, but to increase the knowledge about seal behavior under different conditions it is important for the seal designer/manufacturer to be able to carry out these tests himself. In order to verify the functional demands the following tests must be carried out: determination of the leakage, friction and sealing quality of a seal design. The test procedures and test rigs used during the experimental verification stage will be discussed in chapter 3.

One important feature of seal design standardisation is the recognition of a finite number of basic components which can be used to solve any sealing problem presented. Whether or not these components should be present in the new seal design is determined by the description of the functional demands on the feasibility analysis form. So, the initial shape of the seal is largely determined by the functional demands. An analysis of the existing seal designs has presented the list of basic geometrical components, Maes [1996], which can be used. For simple seals, like O-rings, all functional demands are met by only one component. This has the advantage of a simple design, but the disadvantage of small flexibility when one specific task causes problems.

Furthermore, the analysis of the existing seals designs, Maes [1996], has presented a good overview of the existing seal geometries in combination with their specific sealing quality. Several designs have performed well and it would be a waste of knowledge to overlook these facts. This specific part of the

design process must be regarded as designer specific knowledge, because seal failure registration in combination with certain design parameters influencing the specific complaint has not been carried out yet. This is mainly caused by the lack of information on the documentation of the specific seal features. One of the most common complaints is the failure of the seal to perform well during the cold test.

The general functional demands on a SA-seal design can be summarized as, Maes [1996]:

- 1) primary sealing, defined as static and dynamic sealing in the contact area between the moving shaft and the static seal,
- 2) secondary sealing, static sealing and prevention of contamination between the static seal and housing,
- 3) prevention of oil contamination by water, dust, or sand, statically and dynamically, and
- 4) generation of enough mechanical strength or geometrical boundary conditions to keep the seal in its place during operation.

The specific list of demands for the new shock absorber seal, based upon customer demands stated in the standard form and nomenclature can now be given:

Seal geometry

Feature:

Static sealing on the outer diameter	→	Seal ridge
Dynamic sealing of the gas chamber	→	Gas lip
Static and dynamic sealing of the oil reservoir	→	Sealing lip
Prevention of oil contamination by dirt or water	→	Dust lip
Seal must be filled with grease	→	Grease chamber

Seal material : FPM-compound (Code LM801372)

Spring behavior : to be specified by the designer

Assembling conditions

Shaft diameter	:	10.949/10.962	
Housing diameter	:	31.15 ± 0.1 mm	
Maximum seal width	:	8.4	mm
Concentricity shaft/tube	:	0.04	mm

Operating conditions

Temperature profile	:	min.: -40°C and max.: 140°C
Pressure profile	:	min.: 0 bar and max.: 25 bar
Velocity profile	:	min.: 0 m/s and max.: 3 m/s
Frequency	:	unknown
Amplitude	:	min.: 0 mm and max.: 150 mm

Environmental conditions

Vibrations	:	Standard conditions
Water penetration	:	Standard conditions
Dirt or Dust	:	Standard conditions

Seal performance

Leakage	:	max.: 10 % of the initial oil volume / 1 million strokes.
Friction	:	min.: 0 N and max.: 20 N
Lifetime	:	1 million strokes

All the unknown input of Figure 1 is now quantified allowing the seal designer to start the design process. In order to follow the different stages of the design process the new seal design is assigned with a name. For this example the standardized 11 mm FPM-compound radial lip seal the name SC1401 is used. During the optimization of the design each new design will be given an extra letter added to this name. Thus different stages of the optimization process can be followed by the name of the design, SC1401A, SC1401B, etc.

2.3.3 Initial design stage (ID-stage)

During the ID-stage the seal designer has to make three main decisions concerning the initial features of the new seal design. It is the aim of the designer to define an initial design which is already feasible, this means meeting the functional demands stated during the FA-stage. These three main decisions are:

- I) Determination of the initial seal geometry,
- II) Determination of the seal material,
- III) Determination of the garter spring.

The choices are made based upon the data available from the FA-stage and are combined with the experience from earlier designs. The most important aspect of this stage is the fact that the first design has to be a feasible one. This means that the initial design must be able to fulfill the given list of demands on leakage and friction.

As the shape of the new seal design is not known a priori the influence of a number of operating parameters is taken into account based upon the experience of the designer. These parameters are: operating temperature, sealed pressure and shaft velocity profile. The designer's knowledge of existing seal designs and problems encountered for specific operating conditions combined with the quantitative values given during the FA-stage are transformed into a definition of the possible feasible solutions. The influence of these parameters on the feasibility of some seal design solutions during the ID-stage will be shortly discussed.

2.3.3.1 Temperature profile

The operating temperature is the shock absorber temperature. For the seal this is the temperature of the shock absorber under static and dynamic conditions. For static conditions the operating temperature is the surrounding temperature and this temperature lies between -40 and 40 °C. The dynamic operating temperature is the result of the energy dissipation of the shock absorber, the surrounding temperature and the cooling of the shock absorber by the air flow resulting from the velocity of the vehicle. For this type of data the seal designer has to rely on the experience of the shock absorber manufacturer. In general a maximum temperature is specified. The standard operating temperature is 80 °C, but for specific applications it can rise up to 175 °C. This explains the need for different seal materials.

Based upon the given temperature range, -40 to 140 °C, and the data in table 1 a HNBR-compound could be applied for this new design resulting in lower material costs for the seal, but this solution is not feasible due to the specific customer demand for a FPM-compound material.

2.3.3.2 Pressure profile

The value of the sealed pressure is important for the shape of the seal. From practical seal design it is a well known fact that the length of the sealing lip must be shorter for seals which are applied under higher pressure and that the thickness of the lip must also increase as the sealed pressure increases. Radial lip seals are self-acting. This means that the contact pressure distribution changes as a function of the sealed pressure. For the seal designer it is important to know the maximum value of the sealed pressure.

In general, the given value of the fluid pressure is not constant and it may vary as function of the shaft movement and the resulting pressure in the shock absorber. However, no knowledge of the actual value of the sealed pressure exists and the given maximum value will be applied as a constant pressure over the seal. Furthermore, the value of the sealed pressure gives a criterion for the contact pressure distribution.

In order to prevent leakage, or lifting of the seal by the fluid pressure the maximum contact pressure must be higher than the fluid pressure. There is no general consensus about the needed pressure difference between the maximum contact pressure and the fluid pressure. For high pressure seals an arbitrary engineering rule states that the maximum contact pressure must be approximately 1.5 times the fluid pressure. For lip seals the maximum contact pressure is approximately 10 or 20 times the fluid pressure.

There are significant changes in the absolute value of the maximum contact pressures of a radial lip seal during the first 24 hours due to relaxation. Relaxation effects can be taken into account easily by means of a changing modulus of elasticity as a function of time. The contact pressure distribution also changes by wear. Wear is a more complex phenomenon which results in changes in the seal geometry. Based upon the present seal design approach it is possible to incorporate the influence of changes in the seal geometry on the contact pressure distribution in the seal design process. It is difficult to predict seal wear over the life of the seal, but for the SC1401 prototype the seal wear pattern will be investigated by means of a comparison between original seal cross section and the seal cross section after a life test.

The seal designer can incorporate the fluid pressure in the tool for the determination of the leakage and friction presented in appendix B. A faster method to predict the influence of fluid pressure on the seal performance is by means of a qualitative analysis. It is possible to derive some qualitative engineering rules expressing the influence of relaxation and wear on the seal performance, but it is difficult to present generally valid models, which give the relation between sealed pressure, relaxation, wear, and seal performance quantitatively.

2.3.3.3 Shaft velocity profile

This parameter influences the dynamic sealing behavior of the radial lip seal. The influence of a specific velocity profile on seal leakage and friction can be investigated with the tool for the determination of leakage and friction based upon the IHL approach. This tool is developed and tested by Van Dijnsen [1995] and in appendix B some characteristic results for a sinusoidal motion are presented.

For this design procedure and the tests which are carried out with the new seal design the following data concerning the shaft movement must be given in the FA-stage. The maximum and minimum shaft velocity, the amplitude of the shaft movement and the shape of the shaft movement, being linear, sinusoidal, bifrequent or random. The combination of the amplitude and the frequency data results in a maximum value of the shaft acceleration and this gives the designer some insight into possible inertia effects during the lifetime of the seal.

2.3.3.4 Determination of the initial seal geometry

Determination of the geometry can be seen as putting dimensions to all the features needed for the new seal design. Any design of type A can be regarded as a combination of a metal insert, a sealing lip with a primary and a secondary sealing lip, a dust lip, a seal ridge, and a non return valve. The space that is available for the new seal design is determined by the shaft diameter, the housing inner diameter, and the rod guide design. All these dimensions are specified by the customer during the FA-stage. The surrounding conditions for the new type A seal design are compared with existing seal designs of type A and the optimal features of all designs are combined into the new initial design. For example, the optimal dimensions of the seal ridge were already determined for another seal design and these dimensions are now used in this new design, resulting in the conclusion that static sealing and mounting will be optimal for the given mounting procedure of the customer. The dimensions for the dust lip were taken from another design, thus including all the developments which took place over the last five years into the new design. The most important feature of the new design is the sealing lip geometry, because leakage during the cold test is mainly caused by loss of contact between the shaft and the seal due to stiffening of the material in the sealing lip. The first choice for the sealing lip geometry is based upon the sealing lip of another seal design made of an NBR-compound. This seal which performs well during the life test and the cold test. However, if the same seal is made with an FPM-compound, the performance during the cold test is bad.

The combination of the needed features with the dimensions for each feature result in the drawing proposal for the initial seal design. This design is based upon the knowledge about existing designs as documented by Maes [1996] drawing proposal is presented in Figure 13.

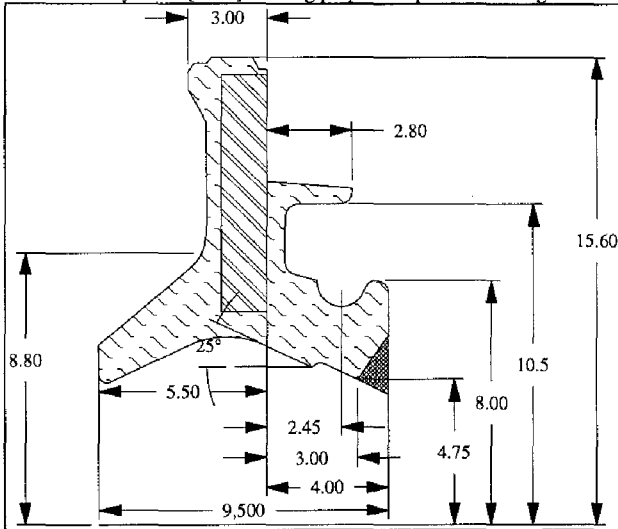


Figure 13 Some initial dimensions of the SC1401 design.

These dimensions are discussed with the customer after the initial design performance is evaluated. Before the new design can be evaluated two other decisions have to be made, determination of the seal material and determination of the garter spring features.

2.3.3.5 Determination of the seal material

In general, the seal material for shock absorber seals is a specific compound. A compound is a modified rubber or polymer or blend of polymers and other materials with optimized properties to meet a set of performance parameters or a given service application. The service application and the performance parameters of the seal material are specified during the FA-stage.

For the seal designer the choice of the elastomeric seal material is guided by the fact that feasible materials are all coded and part of some type of standardized material library. The contents of this material library change continuously because of the development of new compounds. The seal designer judges these complex compounds on a small number of overall features, without exactly knowing the chemistry of rubber compounding. For shock absorber seals this choice is made based upon the needed temperature range, chemical stability, oil swell, wear resistance, and costs. The last factor is important because shock absorber seals are a mass product and any reduction in the material costs results in an effective total price reduction of the product.

In general, data about seal materials is found in seal material databases allowing the seal designer to make a good choice for the material for both excellent mechanical material behavior and manufacturability of the seal material.

In Table 1 an overview of some parameters, which are important to make some initial design decisions is presented. This overview is far from complete and in general the seal designer has much more available data, but Table 1 is complete enough to present the concept of existing knowledge.

Table 1 Overview of relevant parameters for the choice of the seal material.

Designation according to ISO 1629	Basic Polymer	Compound name	Chemical compatibility	Resistance to abrasion	Temperature range [°C]	Vulcanization time [min]	Specific weight [g/cm ³]
NBR	Nitrile	LM80402	good	good	-40 / +120	4	1.37
HNBR	Nitrile	LM80602	good	good	-45 / +120	4	1.36
		LM71319	good	good	-35 / +150	10	1.24
FPM	Fluorelastomer	LM801378	excellent	excellent	-25 / +250	6	2.12

Compound name	Maximum strain [%]	Tensile strength [MPa]	Modulus 50% [MPa]	Modulus 100% [MPa]	Hardness Shore A	Hardness Shore A After aging test in air 94 h at 150 °C
LM80402	300	16.2	-	-	77.5	85
LM80602	263	13.5	-	-	78	84
LM713197	300	23.1	2.41	4.28	74.5	79
LM801378	193	9.88	-	5.13	78	78

The mechanical behavior of rubber like materials is dominated by its relatively near incompressibility and its ability to undergo large elastic deformations. For engineering purposes rubber like material is chosen as the best material for shock absorber seals. The use of elastomers in this dynamically loaded and critical part of the shock absorber and the potential financial damage upon failure has resulted in a growing need for improved computational tools and material characterization.

In order to describe the behavior of the seal material a constitutive model for the elastomer, describing the stress-strain relationship must be found. In general, constitutive models for rubber like materials are formulated by a strain-density or strain energy function. This function is often expressed in terms of a strain measure that is invariant for rotation of the body axes, the so called stretch invariants. Most literature sources on rubber like material behavior stress the necessity of verification of constitutive models for rubber like material by experimental evidence for a wide range of deformation conditions. The predictive value of a numerical analysis is dominated by the employed constitutive model and the procedure followed to determine the model constants. In appendix A several methods to describe different features of the seal material are discussed.

2.3.3.6 Determination of the garter spring

Shock absorber seals are equipped with a garter spring to generate additional radial load when the seal is installed on the rod. The spring also compensates for radial load changes that occur when the elastomer properties change due to exposure to heat and oil. It controls the sealing lip finished inner diameter by pulling the elastomeric lip until the coils of the spring touch each other. The garter spring also adds additional radial stiffness which allows the seal to follow eccentricities, Brink [1993].

Brink [1993] also presented some design recommendations for the garter spring of radial lip seals for rotating shafts, but the same recommendations are valid for shock absorber seals. The spring should be designed to fit tightly into the spring groove and should not be dislodged during handling and installation. It is desirable to design the garter spring with the smallest possible wire diameter to ensure the highest possible initial tensile force within the allowable torsional stress limits for the spring material. The lower the spring rate, the less variance there will be in the total radial load due to changes in the deflection of the spring. The high initial tensile force is needed to ensure that the coils of the spring touch each other and make contact with the bottom of the spring groove in the sealing lip. This ensures control of the inner diameter of the finished seal.

2.3.4 Seal evaluation stage (SE-stage)

Seal evaluation is carried out in a number of evaluation steps. The new seal design is theoretically evaluated by means of the FEM and the results of the different FEA steps are compared with the results from experiments as described in chapter 3.

2.3.4.1 Material characterization

In general it can be said that the choice of the constitutive law depends largely on the time scale which is important for the effects which have to be studied. For a study of the deformations of the seal under static loading, both from the interference with the shaft and as a result of pressurization the most common assumptions for the seal material behavior are that the material behaves isotropic and incompressible. Especially, incompressibility is considered a proper approximation since for most seal materials the bulk modulus is several orders larger than the Young's modulus.

Because the seal operates under relatively low fluid pressures, the rubber material can be regarded incompressible. However, changes in the volume of the rubber of the sealing lip can occur as a result of swell of the rubber by absorption of oil. The amount of swell depends upon the combination of the sealed fluid and the applied seal material, but for some combination a volumetric swell of 20 % can occur. It is possible to incorporate the effect of swell in some FEA codes, but COSMOS/M does not offer this possibility. Thus for the optimization of the seal geometry this effect is not taken into account.

Another effect, which is primarily time dependent is the relaxation of the seal material, which means that the initial value of the stress in the seal reduces dramatically within the first 24 hours after assembly. Although this effects the contact pressure distribution largely, the effect can be regarded as a change of the material stiffness over time. The influence of relaxation on the shape of the contact pressure distribution was investigated by Jebbink [1995] and it was found that the contact width did not change and that only the absolute value of the contact pressures changed.

According to Kanters [1990], elastic material models for elastomers have either been derived from considerations about the molecular structure of the material or by considering the elastomer as a continuum. For the new design strategy attention will be focussed on continuum models describing the macroscopic behavior of the seal material. The Neo-Hookean and Mooney-Rivlin model derived from the strain energy function by definition of a number of constants C_{01} , C_{02} , etc are often used for the description of seal material behavior. For these type of material models the constants can be easily derived from experiments. During these experiments the influences of time and temperature on the elastomer behavior must be eliminated to obtain isothermal, elastic material constants.

For a general state of deformation, these type of material models yield good results when the material constants are determined by data from tensile tests. Tensile tests can be carried out at different temperatures to compare different seal materials and designs over a large range of temperatures. However, if the loading of the seal is not static or quasi-static visco-elastic effects must be taken into account. Especially, in the contact area visco-elastic properties of the seal material are believed to have a large influence on the actual seal behavior. Parallel to this project a project with the aim to experimentally determine the visco-elastic material properties and implement these properties in a finite element calculation was carried out. This project resulted in a method to characterize and model the visco-elastic material properties accurately for finite element calculations, but at this moment calculations of this type are not used in the seal design procedure. Not only dynamic seal behavior, but also seal friction can be influenced by the viscoelastic properties of the seal material. In Appendix C an attempt to determine seal friction by a combination of the shaft surface roughness and the viscoelastic seal material properties is presented.

In Figure 14 the set of tensile tests to determine the Mooney-Rivlin constants of the FPM-compound at room temperature, 20 °C, are presented. These tensile tests are conducted on material that is

produced under lab conditions, and with different speeds of elongation and maximum strains. The test pieces are cut parallel and perpendicular to the flow direction of the rubber material in the mold.

FPM_A cut parallel and elongation speed at $v = 2$ mm/min until $\epsilon_{\max} = 50$ %,

FPM_B cut parallel and elongation speed at $v = 20$ mm/min until $\epsilon_{\max} = 50$ %,

FPM_C cut perpendicular and elongation speed at $v = 200$ mm/min until $\epsilon_{\max} = 210$ %,

and FPM_D cut parallel and elongation speed at $v = 200$ mm/min until $\epsilon_{\max} = 150$ %.

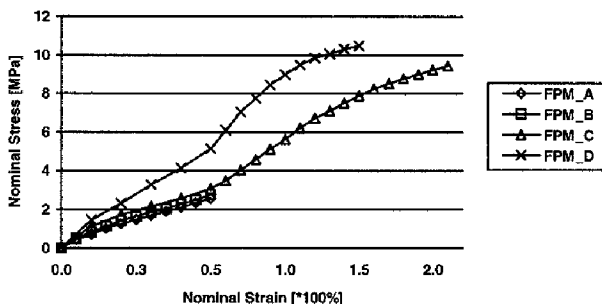


Figure 14 Tensile tests conducted for determination of Mooney_A and Mooney_B for the FPM-compound.

Some influence of the flow direction in the mold on the material characteristic was found, but it is difficult to determine the actual flow direction of the seal material in the seal. The Mooney constants were determined for all data sets and based upon a comparison of the measured and calculated radial load for the seal the best set of Mooney constants was determined.

The tensile test data from Figure 14 is used to determine the Mooney constants needed for the description of the mechanical behavior of the seal material in the FEA package. COSMOS/M 1.75 is equipped with an automatic fitting procedure, which can determine the Mooney constants based upon a nominal stress versus nominal strain curve. Table 2 presents the Mooney constants determined by the COSMOS/M fitting procedure.

Table 2 Mooney_A and Mooney_B determined by COSMOS/M 1.75 fit procedure.

Tensile Test Name	Mooney_A	Mooney_B
FPM_A	0.4442	1.0431
FPM_B	0.3029	1.3717
FPM_C	1.5590	0.1205
FPM_D	2.4150	0.0727

The final design, SC1401_F of the initial optimization procedure based upon the existing seal designs, has been used to verify the results by making a comparison of some characteristic features of the seal for the different sets of material constants.

Table 3 presents the results of these calculations.

Table 3 FEA results for the different material constants *Mooney_A* and *Mooney_B*.

Measured Characteristic	FPM_A	FPM_B	FPM_C	FPM_D	Experimenta l
Inner diameter sealing lip with spring [mm]	9.21	9.27	9.27	9.43	9.29
Radial load of sealing lip with spring [N]	36.0	38.5	38.2	49.1	33.6
Radial load of the dust lip [N]	18.8	21.2	21.4	31.7	18.9

As the maximum strains in the seal are between 30 and 40 % the choice for the best curve was made between the FPM_A and FPM_B curve. Based upon a comparison with measured radial loads the FPM_A curve yielded best results. The accuracy of the theoretical values lies within 10 % of the measured values. These material constants were used for all the calculations carried out for the two different optimization approaches.

2.3.4.2 Determination of the SC1401A spring behavior

In order to prevent the seal from failure during the life test a garter spring is used which gives an additional radial load which is constant and independent of time and temperature effects. This is an important feature, because the elastomeric material behavior is dependent on time and frequency. The stiffness of the garter spring is given as a function of the spring initial length, coil diameter and spring diameter and from measurements it is known that the radial spring stiffness can not be derived directly from the theoretical spring stiffness according to models used by other authors. Gabelli [1992] also used experimental data for the determination of the radial spring behaviour.

2.3.4.3 Determination of the SC1401A CPD

The accuracy of this stage of the design proces is dependent on the accuracy of the data and the models which are used to describe the mechanical behavior of the seal as a function of the surrounding conditions. An important step in the generation of a FE model is the assignment of the boundary conditions, which account for the external loads, shaft displacement, fluid pressure and garter spring loading.

The first component which can introduce a significant error is the description of the geometry of the seal. In order to prevent these errors the geometry of the seal is directly taken from the initial drawing of the seal. Although, the final seal geometry is the result of a pressure moulding proces this is at the moment the best guess that can be made for the actual geometry of the seal. In order to compare the final shape of the seal with the original drawing and to investigate the influence of wear on the seal geometry it is necessary to compare the original/drawing, new, and run-in shapes of a number of seals during the life tests. The method for the determination of the shape of a certain cross-section of the seal is already a standard procedure and this procedure can be used for the comparison of the different seal geometries.

The output of these analysis will always be the contact pressure distribution between the shaft and the seal and the deformed geometry of the seal. The data of the contact pressure distribution and the deformed geometry forms the input for the determination of both leakage and friction.

In order to model the mechanical behavior of a lip seal a non-linear FEM code COSMOS/M is used and different stages during the life of the seal can be analyzed. The initial seal design is equipped with a number of basic components, which are the result of the functional demands on the seal. During this stage of the design procedure it is possible to split the analysis into different parts of the seal which do not or hardly have any influence on each other. In general, three major parts of the seal can be analyzed: 1) the sealing lip, 2) the dust lip, and 3) the wulst, or static seal. For any shock absorber seal these basic functional elements must be present and as leakage and friction are mainly determined by the sealing and the dust lip the FEA will be focussed on the combination of these two components.

2.3.4.4 Determination of leakage and friction

During the seal evaluation stage the seal performance of the initial new design is evaluated.

In order to do this a two step approach is used:

- 1) Determination of the deformed geometry and the CPD - COSMOS/M.
- 2) Determination of the seals theoretical leakage and friction - SEALCALC

To determine the deformed geometry and the CPD of a seal design a non-linear problem has to be solved. Several attempts have been presented in literature to find an analytical solution to this problem, but the accuracy and general applicability of these methods was not satisfactory. As the seal's deformed geometry and the CPD between the shaft and the seal belonging are important, a tool to find these two features must be available. The CPD between the shaft and the seal is determined with the FEM and the code COSMOS/M, which can be run on a PC. A short description of the choice of COSMOS/M and some calculations is given in Appendix A.

In order to theoretically evaluate the seal performance of the new design, a tool is required that can determine both leakage and friction for different elastomeric contact seals for reciprocating shafts. This design tool can be used for evaluation and optimization of different seal geometries.

In order to determine both leakage and friction of an elastomeric contact seal the approach presented by Kanters [1990] using the Inverse Hydrodynamic Lubrication (IHL) theory is modified and applied. This approach solves the Reynolds equation by assuming the CPD to be known and constant, resulting in a film thickness profile for a given shaft velocity and oil viscosity, and thus the oil flow through the contact area and the viscous friction in the shaft-to-seal contact area. The algorithms presented by Kanters for the entry and exit zone could not be directly applied for the CPD of radial lip seals. Furthermore, the program was written in FORTRAN on a workstation and could not be run at a PC. In order to make the design tool accessible for daily seal design the FORTRAN code was translated into a MATLAB 4.0 program called SEALCALC, which can be run on a PC. This program determines both leakage and friction of an elastomeric contact seal for a given shaft velocity profile when the discrete static isothermal CPD and the discrete deformed geometry belonging to it are presented as input. Leakage and friction can be determined for both an isoviscous and a piezoviscous oil viscosity relationship. The derivation and application of the program SEALCALC is described in detail in Appendix B and by Van Dijnsen [1995].

For an accurate prediction of the dynamic seal behavior, it seems impossible to neglect the viscoelastic nature of the seal material. Finite element calculation makes it possible to incorporate viscoelastic effects of the seal in the design procedure without having to make changes to the basic layout of the design procedure. A description of some results is presented by Jebbink [1995].

2.3.5 Seal optimization stage (SO-stage)

In order to define an optimal solution for a design problem the most important step is to define an objective function which has to be minimized as a function of the design variables. In case of the new shock absorber seal design, the number of design parameters is large when all dimensions of the seal must be taken into account. In order to describe a complete shock absorber seal parametrically 75 or more independent parameters are needed. Next to this, the model to describe the seal is complex and does not allow much geometrical freedom, because of the relationships between the design parameters and the prescribed geometry of the seal. The approach of parametric design and design optimization can be and is used for simple seal geometries, but is not beneficial in case of complex seal geometries.

In order to optimize the seal design a number of design optimization strategies can be applied, but in general they all follow the same approach to define the problem. This is the definition of some measurable value, which can be used to judge the design and compare this design with other designs. In order to do this in a structural way, three basic components of design optimization must always be present

2.3.5.1 Design parameters

The notion of optimizing a structure asks for some freedom to change the structure. In general the potential for change is expressed in terms of permissible changes of a group of parameters. Such parameters are called design variables. Design variables can be parameters controlling the geometry, material properties, or operating conditions and they can take continuous or discrete values.

For the definition of the optimal seal design the following set of design parameters has been chosen based upon a number of FEA on different types of radial lip seals. This was done in order to establish the parameters with the greatest influence on the shape of the contact pressure distribution. These parameters are:

- shaft to seal interference - δ [mm]
- high pressure angle - β [degrees]
- low pressure angle - α [degrees]
- section thickness - S_{th} [mm]
- position of the spring - H_f [mm]
- height of the primary sealing lips - H_d [mm]
- Type of spring or the specific radial springload - F_{sp} [N/ π *D]

In Figure 15 the initial seal design is presented together with the position of the design parameters.

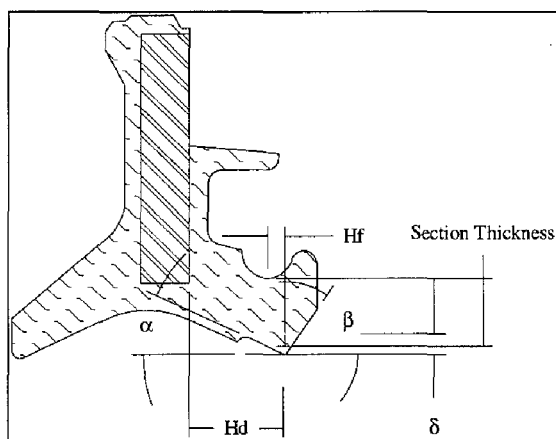


Figure 15 Design parameters for the SC1401 design.

2.3.5.2 Objective function

The notion of optimizing a design also implies that there are some merit functions that can be improved and can be used as a measure of effectiveness of the design. In general, such a function is called an objective function and for structural optimization problems weight, displacements, stresses, vibration frequencies, buckling loads and costs, or combinations of these can be used as objective functions.

The quality of the seal must now be defined in order to derive a quantitative value for the seal performance. As the seal performance is mainly determined by the contact pressure distribution, it seems logical to take this distribution as the objective or quality characteristic. However, it is difficult to compare complete contact pressure distributions and this is why the shape of contact pressure distribution for a specific seal design is described by a number of characteristic parameters. One of the

major demands on a quality characteristic for a Taguchi analysis is measurability. Therefore, a number of relevant quality characteristics must be defined, which can be measured accurately and still are characteristics of the contact pressure distribution.

Based upon these criteria the first quality characteristic of a radial lip seal is the radial force of the seal. The radial force of the seal is defined as the force which is applied by the seal to the shaft, when it is mounted and pressurized. Any parameter influencing the radial force also has a large influence on the contact pressure distribution and can therefore be seen as an important design factor.

Important characteristics, which can be found from FEA on radial lip seals, describing the contact between the shaft and seal are:

The specific radial force, F_{spec} , the three contact areas 1, 2, and 3, the maximum contact pressure, p_{top} , the average contact pressure, p_{av} , the contact width, b , and the extremes of the pressure derivative, $(dp/dx)_{\text{max}}$ and $(dp/dx)_{\text{min}}$, for each contact area.

In general for a shock absorber seal there are three areas of contact between the shaft and the seal. These are defined as the primary sealing lip contact, the secondary sealing lip contact and the dustlip contact area. The demands on the shape of the contact pressure and the local level of the radial force largely depend on which contact area is observed. The demands on the contact pressure distributions for the primary and the secondary sealing lip are those for the optimal contact pressure distribution for a reciprocating shaft. This means an asymmetrical contact pressure distribution with a maximum contact pressure which is higher than the fluid pressure and for the dustlip a symmetrical contact pressure distribution with a maximum contact pressure which is high enough to prevent penetration of small particles, dust or water.

The value of p_{top} has to be higher than the fluid pressure in the primary sealing lip during the total lifetime of the seal.

The average contact pressure, p_{av} , has to be as low as possible for each contact in order to minimize friction and wear.

The value of the contact width has to be minimized in order to minimize friction and wear.

Leakage is mainly determined by the shape of the derivative of the contact pressure distribution and it can be said that the difference between $(dp/dx)_{\text{max}}$ and $(dp/dx)_{\text{min}}$ is the main characteristic for a seal. However, the problem with the pressure derivative is the fact that it is hard to determine the actual value of the pressure derivative accurately and specifically in contact problems the pressure derivative tends to go to infinity at the borders of the contact area. This would immediately result in zero film thickness and by this no leakage at all.

2.3.5.2.1 Optimal shape of the CPD

To minimize the leakage of rod seals for shock absorbers it is essential to have a maximum contact pressure higher than the oil pressure, but it even more important to have an asymmetrical CPD between the first sealing lip (oil side) and the shaft itself. An asymmetrical shape of the of the contact pressure distribution is needed to ensure transportation of oil present on the rod after outstroke back into the shock absorber during instroke. In order to achieve such an asymmetrical CPD the seal is designed with different sealing lip angles at the oil side and the air side. In order to optimize the seal design, i.e. minimize leakage, the contact pressure gradient at the oil side has to be maximized and the pressure gradient at the air side should be minimized.

This demands on the CPD with regard to optimal sealing behavior result in the theoretical optimal shape of the CPD with an infinite pressure gradient on the oil side of the seal and minimal or zero pressure gradient on the low pressure side of the seal. First a linear approximation of the "parabolic"

contact pressure profile is presented in Figure 16. Also the important characteristics of the CPD are defined.

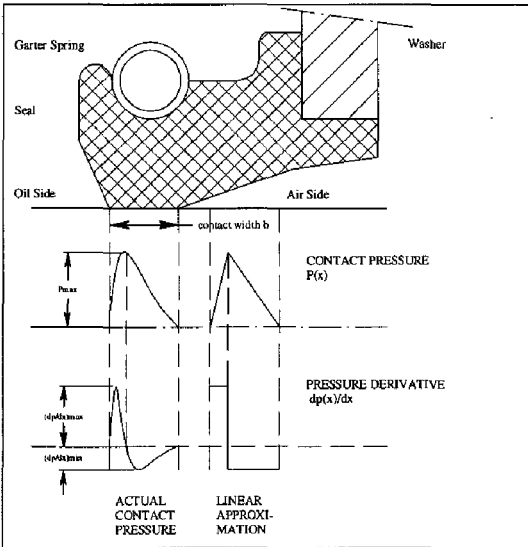


Figure 16 The definition of the CPD characteristics.

Based upon the assumption of hydrodynamic lubrication the optimal pressure distribution for a reciprocating seal is defined by a pressure profile with an infinite pressure gradient on the oil side and no pressure gradient or one close to zero on the low pressure side. The infinite pressure gradient causes a minimal film thickness (zero) to pass the contact area during the instroke and the zero pressure gradient allows a theoretically infinite film to pass the contact zone during the instroke. This ideal pressure profile, presented in Figure 17, can only be approximated by the seal designer.

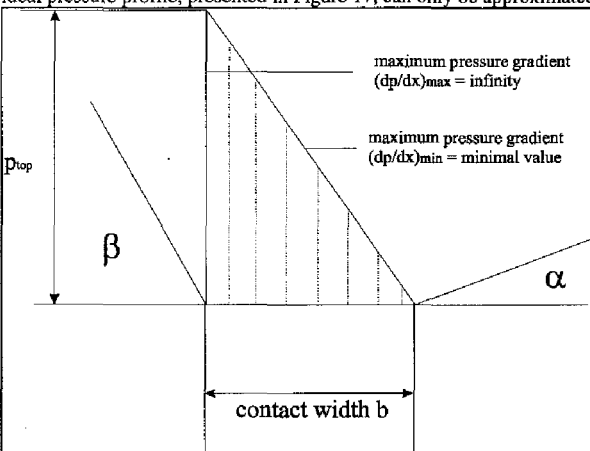


Figure 17 Theoretical optimal shape of the CPD.

The maximal value of the pressure gradient will be finite and the minimal value cannot be zero, because this would demand an infinite contact width given the fact that the maximum contact pressure must be higher than the fluid pressure. In order to use this optimal shape of the pressure as a design objective the characteristic features of the contact pressure profile are combined into a dimensionless objective function.

2.3.5.2.2 Definition of the objective function O

The actual values for the different characteristic features of the CPD are determined by FEA, but in order to use the combined effect of all characteristic features, a dimensionless seal design objective function for radial lip seals for rotating shafts has been defined by Kuiken [1993]. This design objective function, O, expresses the shape of the CPD by a number taking all important characteristics into account. The same approach as used by Kuiken [1993] is now applied to radial lip seals for reciprocating shafts, because the demands on the optimal shape of the CPD are the same.

First of all the maximum contact pressure, p_{top} , is taken into account. The optimal CPD must have a sharp peak value on the high pressure side of the contact area. The value of p_{top} will be related to the value of the average contact pressure p_{av} . When p_{top} is relatively large compared to p_{av} this means that a high pressure peak must exist somewhere in the contact area.

The average contact pressure is defined by formula (2.1).

$$p_{av} = \frac{1}{b} \int_0^b p(y) dy \quad (2.1)$$

with

- $p(y)$ = the contact pressure profile in axial direction [MPa],
 b = contact width of the contact area [mm], and
 y = coordinate in axial direction along the shaft surface.

The parameter describing the influence of the maximum contact pressure distribution in the design objective function is called K_1 and is defined by formula (2.2).

$$K_1 = \frac{p_{av}}{p_{top}} \quad (2.2)$$

For optimal performance of the seal the value of K_1 must be minimized.

The second important characteristic parameter of the contact pressure distribution is the contact width, b . In order to minimize friction and allow for maximum lubrication during small reciprocatory vibrations of the shaft, the contact width must have the smallest possible value allowing the generation of an asymmetrical contact pressure distribution. As seal friction and wear during the life of the seal tend to increase the contact width and reduce the seal performance, the initial contact width for a new seal must be kept as low as possible.

The contact width of the seal is presented in a dimensionless form by relating it to some characteristic length of the seal design in axial direction. The Hd measure of the seal is used for this purpose, resulting in the definition of the second contribution, K_2 , to the objective function is given in formula (2.3).

$$K_2 = \frac{b}{Hd} \quad (2.3)$$

For optimal performance and maximal life of the seal the value of K_2 must be minimized.

The third important characteristic is the asymmetry of the contact pressure profile. In order to express this value by a number the axial position, y_{max} , of the maximum contact pressure, p_{top} , is used.

The value of y_{\max} is measured from the start of the contact area on the high pressure side. The third contribution to the objective function, K_3 , is defined by the value of y_{\max} and the contact width b as:

$$K_3 = \frac{y_{\max}}{b}$$

For optimal asymmetry of the contact pressure distribution the value of K_3 must be minimized.

To combine the influence of these three important characteristics the dimensionless design objective function O is defined by formula (2.4).

$$O = c_1 K_1 + c_2 K_2 + c_3 K_3 \quad (2.4)$$

The constants c_1 , c_2 , and c_3 are used to give the seal designer some influence on the contribution of several characteristics to the design objective function. This allows the study of the influence of different characteristics on the optimal design. In general, the values of the constants are set to give an equal order of magnitude to all three factors.

2.3.5.3 Solution process

Because the results of the work of Van Dijnsen [1995] showed that friction of shock absorber seals could not be predicted accurately by means of the inverse hydrodynamic lubrication theory. As an accurate prediction of leakage, friction, and seal life is not yet possible for shock absorber seals based upon the inverse solution method of the Reynolds equation presented in Appendix B, the shape of the CPD was chosen as the objective function. This results in the optimization loop presented in Figure 18. In the future experimental research to link the shape of the CPD to seal performance parameters like leakage, friction, and seal life data can be carried out at the specific test rigs designed and developed during this work. At the moment the data available is not enough to be used as the design objective function.

Another important observation, making the prediction of seal friction based upon the IHL approach complex, is the fact that friction measurements on the same seal design made of different materials showed large differences in the friction value for the seal. Although the hardness of the seal material is different, the difference in the measured friction could not be explained by differences in the shape of the CPD's. Resulting in the conclusion the next to viscous shear stresses other mechanisms must be responsible for the generation of friction. In Appendix C an attempt is made to link the shaft surface roughness and the viscoelastic material behavior of the seal in a model to predict the hysteresis friction caused by the dynamic excitation of the seal material in the contact area.

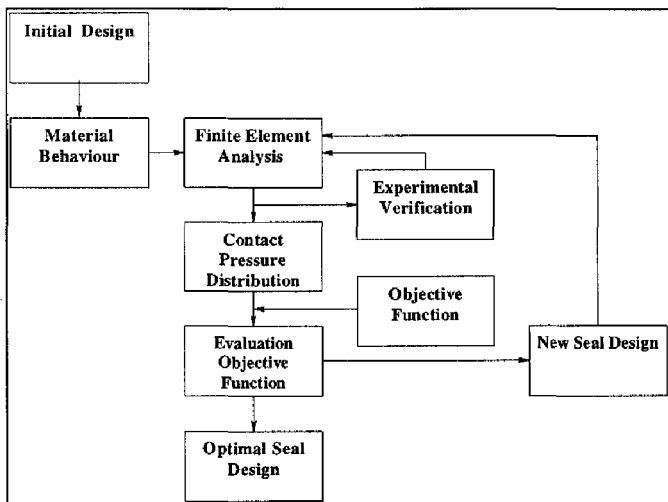


Figure 18 The optimization loop used for practical seal design.

The most important aspect in an optimization procedure is the interface between structural analysis software and optimization software. This interface includes the three major components of formulation, sensitivity, and approximation. The formulation of a structural design problem is of crucial importance for the success of the design process. The efficient calculation of derivatives of the constraints and objective function with respect to the design variables, often referred to as sensitivity derivatives is important.

In order to find the sensitivity derivatives the design parameters are changed and the new value of the objective function is determined. These values are compared to see whether or not the design has improved. Some of the more general optimization methods are mathematically complex and result in large amounts of computer time needed. In order to make the design optimization process cost efficient the Taguchi approach is chosen. This method uses the so called "orthogonal array" approach. An orthogonal array is an experimental design constructed to allow a mathematically independent assessment of the effect of each of the design factors. The arrays are a form of fractional factorial design. One important aspect is that the Taguchi method allows the gathering of the same sort of information as could be found in a full factorial experiment with significantly fewer experimental runs. The objective function is in the Taguchi approach denoted as a quality characteristic and the main aim of the Taguchi approach is to improve quality.

The new seal design approach has been tested with two different methods to come to a geometrical optimization of the new seal design. Both methods are based upon the shape of the CPD. The first method optimizes the seal design based upon the shape of the CPD of existing seal designs, which perform well for a specific set of operating conditions. The main idea behind this approach is to use the available knowledge of the existing seal designs as an objective for the geometrical optimization. The second method applied is the so-called Taguchi method. Here a number of relevant design parameters is taken at their minimum and maximum value and the resulting seal design is analyzed by FEM. The objective function is expressed by a number of important sealing characteristics.

Both methods are applied by Maes [1996] and the results will be shortly discussed and compared in the next sections.

2.3.5.4 Design optimization based upon existing seal designs

In case of the new SC1401 design not only the theoretical optimum, but also a CPD was derived from the combination of CPD's of an existing FPM-compound seal designs and there performance during the cold test. Three existing FPM-compound seal designs were found. A comparison of the geometry of these designs is presented in Figure 19.

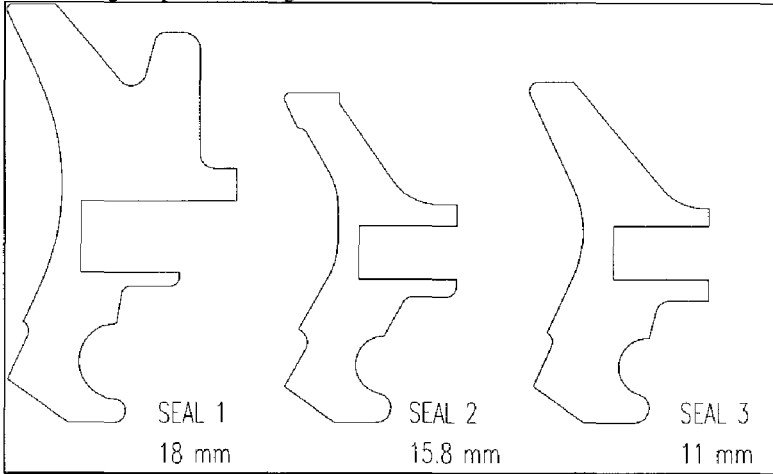


Figure 19 Existing FPM-compound seal designs used for determination of the optimal CPD.

The main dimensions (shaft diameter \times housing diameter \times seal width) and the known results for the cold test for the three designs are presented in Table 4.

Table 4 The cold test data for three existing FPM-compound seal designs.

Cold test	Dimensions [mm]	Temperature °C with side load	Temperature °C without side load
SEAL 1	18 \times 42 \times 11	- 25	- 25
SEAL 2	15.8 \times 39 \times 9	< - 20	- 20
SEAL 3	11 \times 31 \times 9	- 4	- 14

From Table 4 it can be concluded that the best results for the cold test are achieved with SEAL 1. The objective of the optimization of the SC1401 design is to generate the same CPD for the 11 mm SC1401 design as was found for the 18 mm SEAL 1 design. First of all the CPD's for the three existing seal designs were determined and in Table 5 some characteristic experimental and theoretical results for the sealing lip of three designs are summarized and compared.

Table 5 Experimental and theoretical results for three designs.

Prod.	Radial Force F_{rad} [N] with spring		Radial Force F_{rad} [N] without spring		Inner Diameter D_{in} [mm]	
	EXP	FEM	EXP	FEM	EXP	FEM
SEAL 1	58.3	62.1	28.2	30.0	15.7	15.8
SEAL 2	55.9	61.5	25.8	27.2	13.7	13.6
SEAL 3	51.5	55.7	33.3	35.0	9.19	9.25

From Table 5 it may be concluded that the correspondence between the experimental values and the finite element results is good and that the prediction of the contact forces is accurate. For the comparison of measured radial loads and FEA results the difference between theoretical and experimental values may not exceed 10%.

In order to provide the new seal with the contact pressure distribution of SEAL 1, a number of design parameters is chosen. These design parameters allow the seal designer some freedom to modify the initial design, determine the contact pressure distribution and compare this profile with the required optimal profile. The different features of the seal design which can be modified by the designer are:

- the low pressure angle of the primary sealing lip,
- the low pressure angle of the secondary sealing lip,
- the high pressure angle,
- the height of the secondary sealing lip,
- the height of the primary sealing lip,
- the height of the sealing lip,
- the height from the center line of the garter spring,
- the spring characteristic,
- the inner diameter of the primary sealing lip,
- the inner diameter of the secondary sealing lip, and
- the section thickness of the sealing lip.

Based upon the results from the feasibility analysis there is no possibility to increase the height of the sealing lip. This is constrained by the dimensions of the rod guide in the shock absorber. Due to this restriction also the standard values for the height of the primary and secondary sealing lip are taken, 3.0 and 1.4 mm respectively. The angles on the low pressure side are not modified based upon the knowledge that the design of SEAL 2, with $\alpha = 30^\circ$, did not perform better during the cold test. From this short overview of the decisions taken, it is clear that the resulting design parameters are:

- section thickness of the sealing lip
- the interference, δ , between shaft and seal.
- the garter spring characteristics.

In order to analyse the influence of these three design parameters the following designs were analysed and the resulting contact pressure distribution was compared with the needed optimal contact pressure distribution of the SEAL 1 design. Each new design is given a letter extension in alphabetical order starting from A, based upon the existing 11 mm design as:

- | | |
|---|---|
| SC1401_A design: section thickness = 2.45 mm, | spring = 1.5*0.25*44 mm and Fp10 = 2.0 N. |
| SC1401_B design: section thickness = 2.0 mm, | spring = 1.5*0.25*44 mm and Fp10 = 2.0 N. |
| SC1401_C design: section thickness = 2.0 mm, | spring = 1.5*0.30*42 mm and Fp10 = 2.3 N. |
| SC1401_D design: section thickness = 2.0 mm, | spring = 1.5*0.30*42 mm and Fp10 = 2.3 N. |
| SC1401_E design: section thickness = 1.85 mm, | spring = 1.6*0.30*42 mm and Fp10 = 2.3 N. |
| SC1401_F design: section thickness = 1.85 mm, | spring = 1.6*0.30*42 mm and Fp10 = 2.3 N. |

Remarks:

- SC1401_D: The outer contour of the garter spring lip is moved 0.15 mm inwards. This reduces the influence of the garter spring on the radial load.
- SC1401_E: The support of the garter spring lip has been enlarged resulting in a higher radial load.
- SC1401_F: The contour of the primary and secondary sealing lip have been moved outwards, resulting in the same contact profile but with less interference between the shaft and the seal.

From a comparison between the initial design SC1401_A and the final design SC1401_F is given in Figure 20 it can be seen that the final design has a thin sealing lip compared to the original design.

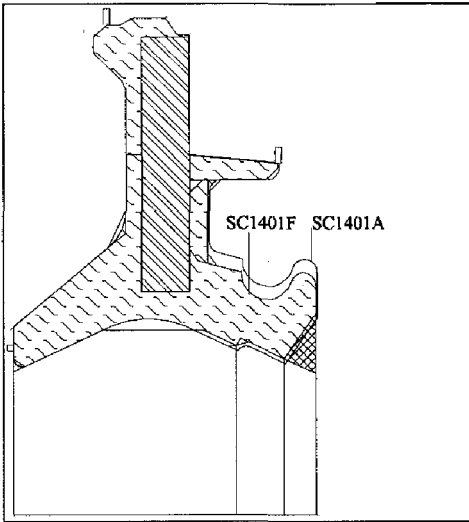


Figure 20 Comparison between the initial design SC1401_A and the final design SC1401_F.

The design SC1401_F is manufactured as a prototype and thus prototype has been tested by the new standardized test procedures. The following set of tests was used:

- verification of the seal dimensions by standard quality control,
- friction measurements of the seal in the shock absorber,
- the cold test for the seal in the shock absorber, and
- a standard life test.

The different test procedures and the results for the SC1401_F design are presented in chapter 3, but the general conclusion after the experimental verification stage was that the friction of the seal design was reduced, the performance during the cold test has increased and the seal wear during the life test is negligible. The wear of the seal was determined by comparison of images of the cross section of a new seal and the seal after the life test. No visible difference could be detected.

2.3.5.5 Design optimization based upon the Taguchi method

In order to set up an optimization experiment which is cost efficient, the Taguchi method will be applied. This method is a special approach towards optimization in general and it aims for the optimal solution in terms of minimal costs for the client after the product is shipped. It uses a number of special techniques, which can be applied to any type of procedure where a certain set of factors has an unknown influence on the result. By studying these factors in a special way a cost efficient optimization experiment is derived for a finite number of design and noise factors.

Design factors are those factors which can be changed by the designer and which have a significant influence on the quality of the seal. Based upon a preliminary study, with FEM, on the influence of different design factors on the contact pressure distribution of radial lip seals a set of factors derived, which is thought to have the biggest influence on the quality of the seal.

Noise factors are defined as those environmental factors which change during the use of the product and have a significant influence on its performance, but can not be completely controlled by the designer. For the radial lip seal the main factors of this type are operating temperature and sealed pressure. It is the aim

of the designer to design a product which is robust. This means that the quality of the seal is not influenced by changes in the noise parameters or changes in the design factors.

The goal of parameter design is to determine the parameter values of a seal so that the seal is functional, exhibits a high level of performance and is minimally sensitive to noise. A parameter design experiment typically involves two types of factors: control factors and noise factors. A control factor is a factor whose level can be set and maintained. A noise factor is a factor whose level either cannot or will not be set or maintained, yet which could affect seal performance.

Parameter design examines the interactions between control factors and noise factors to achieve robustness. In search for parameter levels for which a characteristic is stable, despite the use of inexpensive components and materials or changing external conditions.

2.3.5.5.1 Definition of quality

In this design optimization approach based upon the before presented seal design approach the definition of quality proposed by Taguchi is used. Taguchi proposes a somewhat holistic view of quality that relates quality to cost and loss in dollars, not just to the manufacturer at the time of production, but to the consumer and society as a whole.

The first and most important step in design optimization is the choice of a set of appropriate quality characteristics to measure and compare the quality of the product. This choice involves knowledge of the product, the production process and product performance under different operating conditions as well as familiarity with design of experiments. A wrong choice of the quality characteristic may result in a product which will have low performance in the actual situation where another quality characteristic seems to be more important. The most important characteristic for engineering design problems is the so called *measurable characteristic*, which can be split into three categories:

- 1) *nominal-the-best*, a characteristic with a specified target value,
- 2) *smaller-the-better*, the target is zero,
- 3) *larger-the-better*, the target is infinity.

For each of these types it is possible to develop a function to quantify the loss incurred by failure to achieve the desired quality

2.3.5.5.2 Design quality evaluation

In order to evaluate quality some kind of quality characteristic must be defined, resulting in an objective measurable quantity which can be derived from an experiment and gives a good representation of the functional performance of the seal. For a specific design the definition of the quality characteristic may change depending on the needed functional performance. Overall it can be stated that a loss of performance is not acceptable and this is why the current designs, which perform satisfactory in a large number of situations will be used as the minimal requirements.

A statistical measure of performance called Signal to Noise (S/N) Ratio can be used in evaluating the quality of the seal. The Signal to Noise ratio measures the level of performance and the effect of noise factors on performance. The S/N ratio is an evaluation of the stability of performance of an output characteristic. Higher performance as measured by a high S/N ratio implies a smaller loss as measured by the corresponding monetary Loss Function. The S/N ratio is an objective measure of quality that takes both the mean and the variation into account.

The three standard types of S/N ratio are: *nominal-the-best*, *smaller-the-better*, and *larger-the-better*.

For the design optimization experiments of the SC1401 FPM-compound seal the following quality characteristics and the type of the S/N ratio will be used for the definition of the functional performance of the seal. All these quality characteristics of the seal can be derived from the CPD between the shaft and the seal which can be determined with a finite element calculation. Because the influence of different sealing characteristics on the seal performance is different, four seal quality characteristics will be defined. These quality characteristics are:

- 1) the specific radial force of the seal, $F_{\text{spec}} = F_{\text{rad}} / \pi * D_{\text{shaft}}$ [N/mm],
- 2) the objective function, O [-],
- 3) the flexibility of the sealing lip, Dr / F_{spring} [N/mm],
- 4) the sealing criterion, $(dp/dx)_{\text{max}} / (dp/dx)_{\text{min}}$ [-] or $(dp/dx)_{\text{min}} - (dp/dx)_{\text{max}}$ [N/mm³].

The specific radial force is a *nominal-the-best* characteristic, because the radial load is set at one specific value. This value is mainly determined by the combination of the interference level and the seal material. The specific radial load is defined as the total radial load divided by the shaft circumference, and can also be determined by the integral of the CPD in axial direction.

The general seal design objective function, as defined by Kuiken [1993], is a *smaller-the-better* characteristic, because the seal design objective function expresses the a-symmetrical CPD in such a way that minimization of this function will result in optimal seal performance.

The flexibility of the sealing lip is a *larger-the-better* characteristic, because during the cold test the flexibility of the rubber sealing lip changes and becomes less due to the stiffening of the rubber material. The only way to prevent the fact that the sealing lip will stiffen is to generate as much flexibility as possible through the geometry of the sealing lip.

The sealing criterion is a *smaller-the-better* characteristic, because the best theoretical sealing quality is achieved when the maximum pressure gradient is much higher than the minimum pressure gradient.

For the optimization of the seal design it is the aim to minimize all these parameters and in order to compare the influence of different quality characteristics their order of magnitude will be scaled. The objective function for the optimal seal design is expressed in terms of the contact pressure distribution.

The undesirable and uncontrollable factors that cause a functional characteristic to deviate from its target value are called noise factors. There are three different types of noise factors that affect a product's functional characteristic, being 1) outer noise, changes in the environmental conditions and human errors, 2) inner noise, deterioration of parts, material, subcomponents, etc., and 3) between product noise, piece-to-piece variation. Noise adversely affects quality. However, eliminating noise factors can be expensive. It is not the aim of the proposed optimization method to eliminate noise factors, but to reduce the effect of noise factors. Taguchi's methods allow the designer to create a product which has a minimal sensibility to the noise factors. This characteristic of the product is called robustness and results in the conclusion the robustness is equal to high quality.

2.3.5.5.3 Control and noise factors

In order to allow for cost efficient design optimization of the SC1401 seal the following control or design factors presented in Table 6 were chosen:

Table 6 The design factors for the Taguchi design optimization.

Factor	Name	Level 1 (Min)	Level 2 (Max)	Practice
A	Interference δ	0.50 mm	1.00 mm	0.75 mm
B	High pressure angle β	40 °	60 °	55 °
C	Low pressure angle α	15 °	35 °	25 °
D	Section thickness, S_{th}	1.50 mm	2.50 mm	2.45 mm
E	Hd measure	2.75 mm	3.25 mm	3.00 mm
F	Hf measure	2.35 mm	2.65 mm	2.50 mm
G	Type of spring	weak (*)	strong (*)	both types

(*) Weak Spring: $1.5 * 0.25 * 44 F_{p10} = 2.0$ N, Strong Spring: $1.6 * 0.30 * 42 F_{p10} = 2.3$ N

The only noise factor which will be taken into account during this experiment is the pressure of the fluid and this will be taken into account as a two level noise factor, resulting in the following design of experiments, which will be judged and compared on the above mentioned quality characteristics.

Table 7 presents the combination of design parameters used for the different designs of the Taguchi experiment.

Table 7 The design factors for each experimental design number.

Design	Factor A	Factor B	Factor C	Factor D	Factor E	Factor F	Factor G
1	0.50	40 °	15 °	1.50	2.75	2.35	weak
2	0.50	40 °	15 °	2.50	3.25	2.65	strong
3	0.50	60 °	35 °	1.50	2.75	2.65	strong
4	0.50	60 °	35 °	2.50	3.25	2.35	weak
5	1.00	40 °	35 °	1.50	3.25	2.35	strong
6	1.00	40 °	35 °	2.50	2.75	2.65	weak
7	1.00	60 °	15 °	1.50	3.25	2.65	weak
8	1.00	60 °	15 °	2.50	2.75	2.35	strong

Each experimental design number stands for a finite element calculation on a geometry with the above mentioned design parameters. The results of each experiment are expressed by the value of the quality characteristics for two levels of the noise factor pressure. Figure 21 presents the seal geometry's, which are the result of the combination of factors presented in Table 7.

The level of the noise factor pressure is chosen to be 0 and 6 bar, this results in a total of 16 FEM calculations for 7 different control factors and 8 different designs.

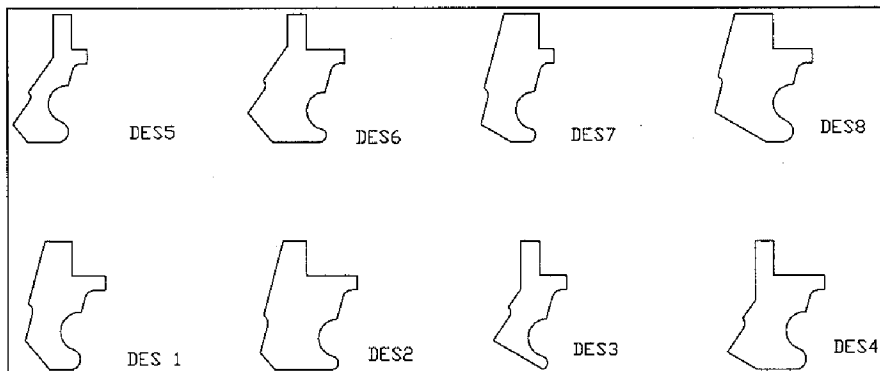


Figure 21 The Taguchi designs used for seal design optimization.

The results of the FEA calculations to determine the optimal seal geometry are presented by Maccs [1996].

2.3.5.5.4 Results and conclusions

The new SC1401 seal design is optimized for optimal performance during the cold test. From the quality analysis of the contact pressure profiles it was found that the noise factor, the fluid pressure, had no significant influence on the level of quality for the radial load and the CPD function quality characteristics. However, the value of the pressure gradient objective seems to be influenced significantly by the value of the fluid pressure. As the accuracy of the pressure gradient function is less than the accuracy of the other quality characteristics, due to the discrete nature of the contact pressure distribution, the influence of noise on the pressure gradient is neglected. The influence of the pressure gradient is also incorporated in the CPD function O and this is why the design will only be judged based upon the specific radial load and the CPD function.

The optimal set of design parameters for the specific radial load objective function is presented in Table 8.

Table 8 The optimal set of design parameters and their influence for the radial load objective function.

Design parameter	Optimal Value	Influence on Objective
Interference δ	0.75	4
High pressure angle β	60°	6
Low pressure angle α	15°	2
Section thickness, Sth	2.5	1
Hd measure	3.25	7
Hf measure	2.35	5
Type of spring	weak	3

From Table 8 it can be found that the section thickness of the sealing lip has the largest influence on the specific radial load, followed by the low pressure angle and the type of spring. This conclusion from the Taguchi experiment is in good agreement with the results from different FEA of radial lip seals and practical knowledge of important design parameters.

From Table 9 it can be found that the most important factors are again the low pressure angle, the section thickness, and the type of spring.

Table 9 The optimal set of design parameters and their influence for CPD objective function, O .

Design parameter	Optimal value	Influence on objective
Interference δ	0.75	5
High pressure angle β	60°	6
Low pressure angle α	15°	1
Section thickness, Sth	1.5	2
Hd measure	2.75	7
Hf measure	2.65	4
Type of spring	weak	3

From Table 10 it can be concluded that a different factor, the shaft to seal interference, has most influence on the result. However, the low pressure angle and the section thickness are again important.

Table 10 The optimal set of design parameters and their influence for the pressure gradient objective.

Design parameter	Optimal value	Influence on objective
Interference δ	0.75	1
High pressure angle β	60°	7
Low pressure angle α	15°	3
Section thickness, Sth	1.5	2
Hd measure	2.75	5
Hf measure	2.65	4
Type of spring	weak	6

As the accuracy of the results for the pressure gradient objective is influenced by the discrete nature of the contact pressure distribution the influence of this design objective on the final result is neglected. Thus, the three factors which have most influence on the quality characteristic of the seal design are the low pressure angle, the section thickness, and the garter spring.

The conclusion from the combined results of Table 8, Table 9, and Table 10 is that the best seal design, based upon the Taguchi experiment for an 11 mm shaft FPM-compound seal, must be equipped with the set of design parameters presented in Table 11.

Table 11 The optimal design parameters from the Taguchi experiment for the SC1401.

Design parameter	Optimal value
Interference δ	0.75
High pressure angle β	60°
Low pressure angle α	15°
Section thickness	2.0
Hd measure	3.0 ± 0.25
Hf measure	2.5 ± 0.15
Type of spring	weak

A FEA of the seal with this parameters is carried out and the quality characteristic results were compared with the results of the earlier experiments. The values of the quality characteristics of the new seal with the new set of design factors are indeed the best of all designs.

This set of design parameters is nearly identical to the values found through optimization of the seal design based upon existing seal designs. The only difference found is the weak spring instead of the strong spring. The new design is produced and tested and the results from the experiments, described in chapter 3 confirm the improved performance of the new seal design when compared to the old design.

2.3.6 Prototyping

Once the optimal geometry of the seal is determined and a CAD drawing of the final seal geometry is made a mold must be created to produce samples of the new design. The sample lead-time is defined as the time from a demand for a new seal to the delivery of the samples. A large part of this total time period, which should be nine weeks for a new design, is taken by the production time of the mold.

Any reduction in the time from CAD drawing to mold drawing and production will result in lead-time reduction. The general procedure is to send the drawing of the new seal design to the tooling department and the tooling department starts a procedure to design a mold based upon the given nominal seal dimensions by means of taking into shrinkage into account. The relationship between seal and tool dimensions is calculated by the tool designer and sometimes this is accompanied by errors. In order to reduce these errors it would be better if the tool dimensions could be determined numerically by means of an FEA analysis on the nominal seal dimensions.

Theoretically it is possible to perform this calculation with FEA software, but at the moment this is not a standardized procedure. The relationships between type of material, shrinkage, tool temperature and pressure are not known at the moment, but can be part of a future research project to reduce the time between the final drawing of the prototype and the production of the tool. If the tool is ready and a number of prototype seals is produced, the seal dimensions will be checked by the quality department. When some dimensions are not within the prescribed tolerance field, these dimensions will be given to the tool designer and changes to the tool dimensions must result in a good set of prototype dimensions. At the moment this process of modifying the tool dimensions is a trial and error process guided by the knowledge of the tool designer. In the near future FEA will be used to guide the tool designer.

In general, shock absorber seals are produced by a compression or injection molding manufacturing process. The number of parameters influencing this production process is large and the field of tolerance will always be specified on seal dimensions, material hardness, and some other important parameters. The seal designer has to generate a seal design with a good seal performance, which is robust with respect to the field of tolerance of the production process. Based upon the design strategy described in this chapter it is possible to define a number of critical seal dimensions and production

process parameters of which the field of tolerance must be small. Also the parameters which are less important can be identified resulting in a better analysis of the important parameters in the production process, focusing on those parameters which are actually important for the quality of the seal performance.

2.3.7 Experimental verification stage (EV-stage)

Once the samples have been produced and the geometrical quality of the product is checked a number of experimental verification tests is conducted before the product is released. The results from these tests will be described in chapter 3.

2.4 Summary

The new seal design strategy as proposed in chapter one has been applied to a practical seal design problem. Two different methods to optimize the seal design have been employed. The first optimization approach used the knowledge of the CPD of existing seal designs in relationship with the seal performance during a number of standardized test procedures. As the geometrical changes of the sealing lip for the different design steps during this procedure are only small, a second optimization approach the Taguchi method has been used. The Taguchi method was chosen because of its practical usefulness and the existing experience and knowledge about this method in the company. A set of control factors has been chosen based upon knowledge about the important parameters which influence the shape of the contact pressure profile most significantly. Three different design objective functions, the specific radial load, F_{spec} , the seal CPD, O , and the sealing criterion, the difference between the maximum and minimum contact pressure gradient, were used to judge the design.

3. Experimental methods to support seal design

3.1 Introduction

An important part of the quality of the new seal design is determined by the seal performance during a series of experimental tests, which are carried out by the customer to judge the performance of the new design. A comparison is made between new and existing designs for a number of standardized test procedures.

Experimental methods to determine the seal performance are combined with or derived from experimental methods to test the functionality of the complete shock absorber. Oil seal friction measurements are conducted to evaluate the static and dynamic friction of the seal during instroke and outstroke. Muddy water tests are carried out to examine the sealing properties of the dustlip against water and dirt ingestion into the shock absorber. Shock absorber life tests, high speed, low speed, mono-frequent, and bi-frequent, are done to evaluate the sealing properties of the seal and the lubricating properties of the shock absorber fluid. A cold test - a low temperature leakage test - is carried out to evaluate the sealing properties at different low temperatures.

For a good definition of comparable tests procedures and results the shock absorber and seal manufacturer have to agree about the experimental determination of the seal performance as a part of the shock absorber test procedures. Otherwise it will be impossible to shorten the time-to-market, because of the fact that the customer has to carry out its own experiments before a new seal design can be used. The only way to shorten the time from the feasibility analysis to a new approved seal design is to do the needed experiments during the design stage and these experiments must be carried out by the seal designer to minimize the time lost in communication. However, this asks for the trust of the customer in the results of the experiments and this is only possible if the test procedures to determine seal leakage and friction are comparable. During this project several tests have been set up and these tests were compared with existing tests of the customer. The resulting test procedures are standardized and documented, Maes [1996]. In general, the demands on any new seal design will be expressed in terms of a number of experiments which the seal has to pass satisfactory. The criteria by which the experiments are judged and by this seal performance are clearly described in the test procedures.

In this chapter some of the test rigs will be shortly discussed and the test results of some seal designs will be presented.

3.2 Experimental testing of the new SC1401 prototype

After the design of the SC1401 seal has been optimized a prototype of this seal is produced and tested according to customer specifications. The following tests were carried out:

- quality control of the dimensions of the seal,
- measurement of the friction of the seal,
- cold test of a seal mounted in the shock absorber between -40 °C and +10 °C, and a
- seal life test over 1 million strokes.

All tests are conducted according to the new test specifications and are documented according to the standardized test forms by Maes [1996] and only the results will be shortly summarized.

3.2.1 Results of the friction measurements

The test rig for the friction measurements and some characteristic results are described in section 3.3 of this chapter.

The main aim of the friction measurements was to compare the friction of the new FPM-compound seal, SC1401, with the friction of an existing FPM-compound seal design, the PL3-625. The demand on the friction value for the new seal design is that may not exceed 20 N for $p = 0$ bar and $v = 1$ mm/s. Table 12 presents the results of the friction measurements. For each seal, PL3-625 and SC1401, the average friction value of two experiments is presented and the percentage presents the change in seal friction compared to the existing PL3-625 design.

Table 12 The results of the friction measurements.

	PL3-625	SC1401
$p= 1$ bar, $v= 1$ mm/s	25 N	19.5 N (- 22 %)
$p= 3$ bar, $v= 1$ mm/s	30.5 N	26 N (- 15 %)
$p= 3$ bar, $v= 5$ mm/s	38.5 N	30 N (- 22 %)
$p= 1$ bar, $v= 2$ mm/s	-	23 N

From Table 12 it may be concluded that the friction value for the new seal design is 20 % lower than the friction values of the existing seal design and that the friction value meets the list of demands. A reduction of the seal friction is important with regard to seal life and due to the decrease of the friction value seal wear of the new design is expected to be much lower. For the SC1401 design the seal cross section after a life cycle test, 1 million strokes, was compared the cross section of a new seal and no changes of the seal geometry were found.

3.2.2 Results of the cold test

Cold tests are performed on the life test machine. A complete shock absorber is cooled to -45 °C and the cooled shock absorber is mounted on the test rig. The loading of the shock absorber is a reciprocating motion of the rod with a frequency of 1 Hz and a stroke of 30 mm. Next to the movement of the shaft a side load can be applied by the test engineer to the shock absorber. Test were conducted with and without side load. During tests with side load the worst loading of the cooled seal occurs, because this type of loading is non axisymmetrical and the seal material must follow eccentric shaft movement.

The possibility to perform cold tests at PL Automotive was developed during this project and the new standardized test procedure was applied to test complete shock absorbers, produced by the customer with the new seal design. The tests were also carried out by the customer and a comparison of the results was made. No differences in the results were found.

The results of the cold tests, two PL3-625 seals and four SC1401 seals, are presented in Table 13. The result of the cold test is expressed in a value in mm expressing the height of the visible oil ring above the seal on the shaft.

Table 13 The results of the cold tests performed for the new SC1401 design.

Seal	Result between -30 °C and $+10$ °C.
PL 3-625	> 10 mm, thus not O.K.
SC1401	≤ 3 mm, O.K.

From Table 13 it can be concluded that the new design has improved the performance during the cold test for an 11 mm shaft seal and meets the demands specified by the customer.

3.2.3 Results of the seal life test

The most important characteristic of the shock absorber is the force-displacement curve and in order to judge the seal performance this characteristic curve should be measured for several rod speeds before and after the life test. However, the test equipment for such measurements is not available and in order to quantify the seal performance during the life test the demands on the force-displacement curve are transformed into demands on the amount of oil that may be lost during the life test. The amount of leakage during the life test may not exceed 10% of the initial volume of oil in the shock absorber.

During the life test the new seal design had a leakage of 8.1% of the initial oil volume after 1 million strokes, thus meeting the list of demands.

After all specified tests for the new seal design were performed it was concluded that the new seal design meets the lists of demands specified by the customer and has improved performance compared to existing seal designs.

3.3 Radial load measurement

An important characteristic of any elastomeric contact seal is the radial load of the seal. The radial load is defined as the integral over the contact area of the contact pressures between the shaft and the seal. This force is measured with a so-called split shaft measuring device, presented in Figure 22. The same principle of measurement is also applied for the determination of the CPD in this chapter.

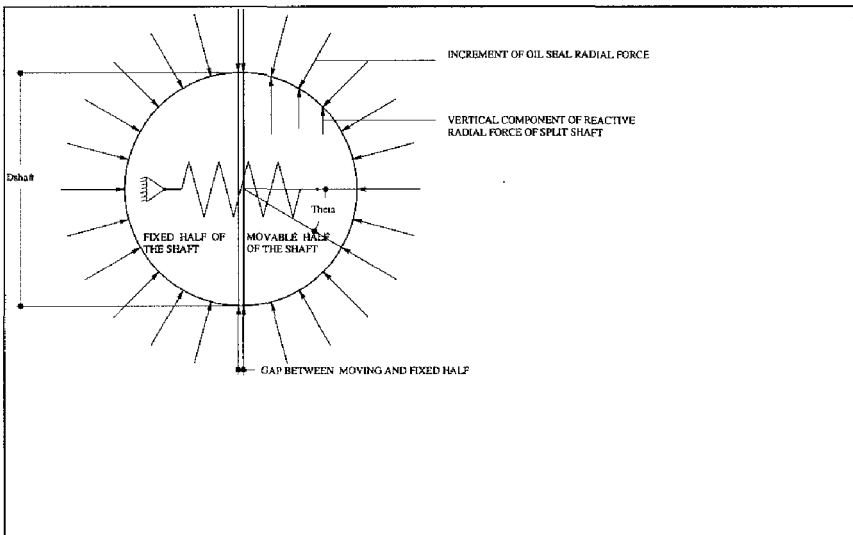


Figure 22 Split shaft principle for measuring radial force, Brink [1993].

The split shaft technique measures the total sum of the components of radial force acting perpendicular to the split line of the shaft. This resultant force P_D when multiplied by π is called the total radial load F_{rad} . Measurements of the radial force are required to estimate performance and verify mathematical models used during FEA.

Furthermore, the influence of relaxation on the radial force can be measured with the split shaft device. This data gives the designer some insight which part of the initial radial force will remain

during seal operation. In Figure 23 the influence of relaxation on the radial force of the sealing lip without garter spring is presented for the PL3-562 seal.

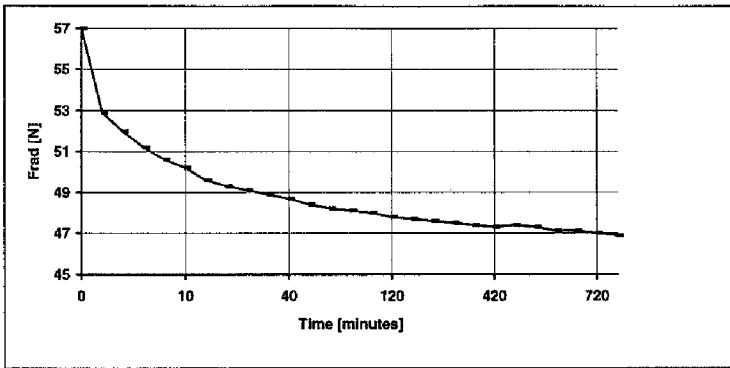


Figure 23 The influence of relaxation on F_{rad} without garter spring for the PL3-562 seal.

From Figure 23 it can be found that the radial force of the sealing lip decreases with approximately 18 % during the first 12 hours after mounting resulting in a lower radial force during seal operation. The seal designer has to take this effect into account.

The last and most important feature of the seal design, the CPD is also measured. In order to be able to determine the CPD for the PL3-562 seal a new device has been designed and tested. A comparison between measured and calculated quantities will be presented in the next sections.

3.4 Experimental determination of seal friction

To determine the friction of shock absorber seals a new test rig has been designed and manufactured. Figure 24 presents a schematic of the test rig and a more detailed drawing of the rig and the different components is presented in Figure 25.

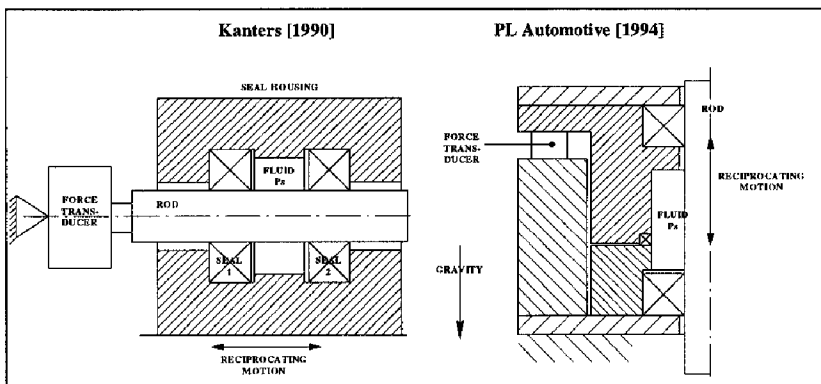


Figure 24 Schematic presentation of friction measurement test rig.

Several concepts for friction measurement of the seal were applied, but most of the test rigs were positioned horizontally. In case of shock absorber seals the dynamic seal performance is determined by a vertically positioned shaft. This is why the test rig is placed in a vertical position. Kanters [1990]

distinguished between friction measurement with moving shaft or moving housing and the type of measurement.

The principle of operation consists of moving the shaft with a given frequency and amplitude. The shaft is guided by two bearings and the friction force is measured by three piezoelectric force transducers in the stationary seal housing.

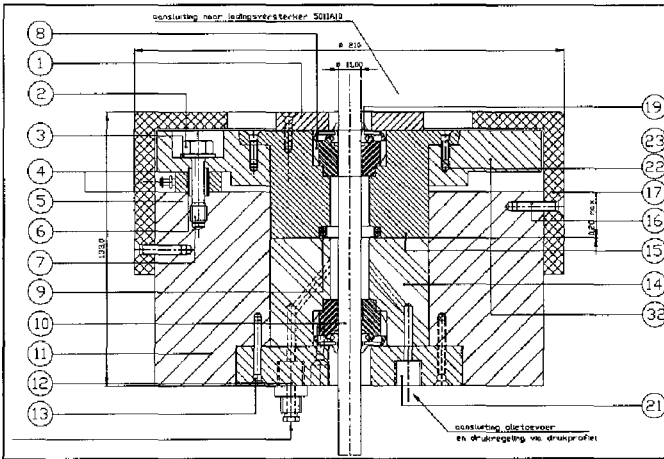


Figure 25 Test rig developed for SA-seal friction measurement.

The seal (8) is mounted with the rod guide in the upper part of the test rig and pressed into the housing by a bolted steel plate (1). The upper part of the test rig with the seal is placed in a special holder which is placed on three prestressed piezoelectric crystals. The upper part of the test rig is separated from the lower part of the test rig by a rubber seal. This seal is specially designed for this purpose and has a small stiffness in the direction parallel to the reciprocating motion of the shaft. The oil in the test rig can be pressurized and heated.

The accuracy of the friction force measurement is investigated by Van Dijnsen [1995] and the absolute accuracy was found to be 5.5 %, while the relative accuracy is ± 11 %. This relatively large error is caused by the fact that the measured friction force is the result of the difference between two measured signals. The displacement profile of the rod is measured with an accuracy of 0.13 %. From the displacement profile the rod velocity and acceleration profile can be found by differentiation, but the accuracy of these profiles is thus lower than the rod displacement profile.

In Figure 26 the cross section of the PL3-707 shock absorber seal for a rod with a diameter of 11 mm is presented. For a comparison with the theoretical results of SEALCALC the dust lip on the air side of the seal was removed, thus resulting in a single sealing lip pressed against the rod.

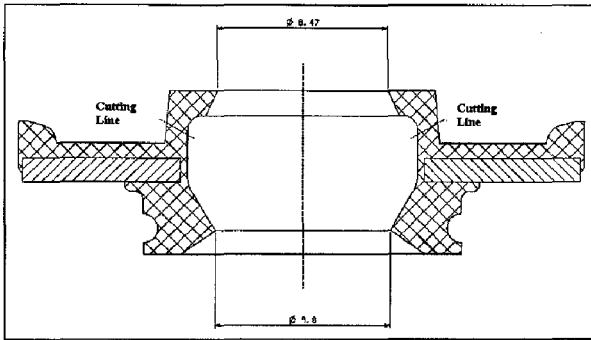


Figure 26 Cross section of the PL3-707 seal used for friction measurement.

Figure 27 presents a characteristic velocity and friction profile for the measurements with the PL3-707 seal with only a sealing lip.

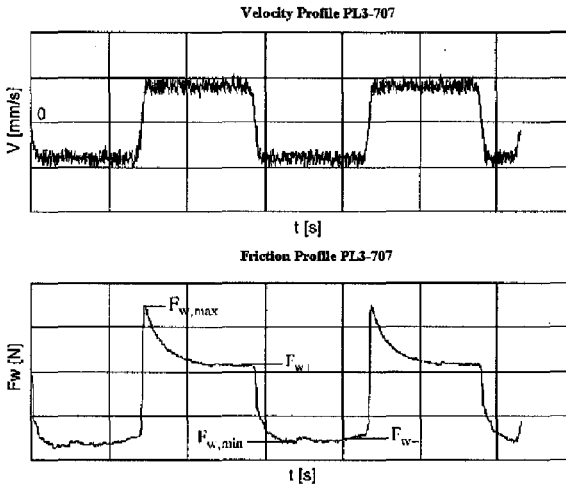


Figure 27 Velocity and friction profile for a single lip PL3-707 shock absorber seal.

In order to compare the measured friction forces with the friction forces from SEALCALC the velocity profile was taken constant for both instroke and outstroke. The noise over the velocity profile is caused by the fact that the profile is derived from the displacement profile by differentiation. Although the friction profile presented in Figure 27 is for a seal with only one sealing lip the same profiles are found for multiple lip seals. The friction profile shows a distinct maximum value during the reversal of the entrainment velocity from instroke to outstroke.

3.5 Material characterization

The large variety and ever continuing changes and improvements of rubber materials used in modern sealing technology in combination with the non-linear and viscoelastic behavior of elastomers make the generalization of rubber models quite difficult, Gabelli [1992]. A careful study of the required

accuracy of the description of the material behavior in combination with testing is therefore necessary for cost efficient and accurate finite element calculations.

Elastomeric seal materials applied by PL Automotive for all seal types can be roughly divided into 3 categories based upon the applied basic polymer. The first category consists of the so called NBR-compounds, nitrile based. Nitrile is a co-polymer of butadiene and acrylonitrile. The practical operating temperature range is -40 to 120 °C. The second category is formed by the HNBR-compounds, which is an advanced nitrile polymer based on NBR-compounds to extend the upper temperature range to -35 to 150 °C. The third category consist of FPM-compound, a fluorocarbon with excellent chemical and high temperature resistance, but approximately 15 times more expensive as the NBR-compound. Better chemical resistance, strength or temperature resistance can be achieved by using different compounds. In order to determine both stresses and strains the seal material behavior has to be described by a constitutive model. FEA-codes offer a number of possibilities, which all have their specific advantages. It is up to the designer to decide which model is used to describe the seal material behavior. For any chosen material model it must be possible to determine the material constants experimentally and verify the results from the FEA by measurements on seals.

The main aim of the designer is to apply constitutive models with enough accuracy for the computational analysis of the isothermal, static CPD in the contact area between the shaft and the seal. Several possible relationships between stress and strain can be applied and the most common relationship for engineering purposes is linear elastic material behavior. A more general way to describe the static behavior of rubber like materials is the so-called hyperelastic approach. In order to describe the dynamic behavior of the rubber like material linear viscoelastic models are used.

The contact area between the shaft and the seal is subjected to several operating conditions, which can be divided into two important states of deformation. The macroscopic (quasi) static deformation and the dynamic deformation of the seal during with the corresponding contact pressure profile the reciprocating motion of the shaft. This dynamic deformation of the seal can be divided into a macroscopic deformation of the total seal, which depends largely on the direction of the motion and the coefficient of friction in the contact zone, and a microscopic small deformation in the contact area, which is the result the deformation of the rubber surface due to the roughness asperities of the shaft surface during relative motion

The seal designer needs to establish an accurate model for the determination of the stresses and strains in the seal for different operating conditions. To establish which constitutive model and parameters describe the rubber like material behavior under static and dynamic conditions most accurately a number of experiments on the generally employed rubber compounds for seal has been conducted over a range of temperatures and for different loading situations.

3.5.1 Hyperelasticity

The constitutive behavior of a hyperelastic material is defined as a stress-total strain relationship. For this reason the basic development of hyperelasticity is somewhat different from the rate formulations used to define history dependent materials. Furthermore, hyperelastic materials are often nearly incompressible, such that mixed ("hybrid") formulations are required. In ABAQUS mixed variational principles are used to treat the fully incompressible and almost incompressible case.

The hyperelastic description of the material behavior results in some well known models to describe large strain elasticity. These are the Neo-Hookean and Mooney-Rivlin material descriptions, both resulting in a set of two or more constants, which can be derived from tensile, shear and compression experiments. ABAQUS allows for the automatic determination of the constants given a nominal stress-strain curve.

The strain-energy function W , used in hyperelastic material models, is still independent of time and thus not able to describe accurately the time- or frequency dependent material behavior, which is characteristic for most elastomeric materials. For the quasi-static determination, also temperature

dependent, of stresses and strains this model is generally used to describe the structural response of elastomers in engineering analysis.

The mechanical response of the seal material is defined by the material parameters in the strain energy potential, so that it is necessary to determine these parameters to use the material models. Since hyperelastic materials are usually fully or almost incompressible, the approach is to use data from experiments involving simple deformations to define the material constants on the assumption that the material is fully incompressible, and the to use volumetric compression data to determine D , if compressibility is important.

It is usually best to obtain data from several experiments involving different kinds of deformation over the range of strains of interest in the actual application and to use all these data to determine the parameters. The models are phenomenological (non-molecular), and it has been observed that it is necessary to fit these models using test data from more than one deformation state in order to achieve good accuracy and stability.

The superposition of a tensile or compressive hydrostatic stress on a loaded, fully incompressible elastic body results in different stresses, but does not change the deformation. This means that some apparently different loading conditions are actually equivalent in their deformations, and therefore are equivalent tests. On the other hand, the tensile and compressive cases of the uniaxial modes are independent from each other yielding independent data from uniaxial tension and compression.

In order to derive the material parameters for elastomeric seal materials uniaxial tension and compression tests will be used and the material is assumed to be fully incompressible. In order to verify this last assumption a set of volumetric test data has to be found.

3.5.2 Tensile tests of a HNBR-compound

In order to determine the Mooney-Rivlin constants for the rubber material of the seal uniaxial elongation experiments are used. As an example the Mooney-Rivlin constants for a HNBR-compound, LM713197, will be determined.

A set of five elongation experiments is conducted according to DIN 53504 at room temperature with test specimen dimensions 52 and a cross head speed of 2 mm/min. The nominal stress versus nominal strain for each experiment is presented in Table 14 and the averaged stress-strain curve is plotted in Figure 28.

Table 14 Nominal stress (MPa) versus the nominal strain.

	5%	10%	15%	20%	25%	30%	35%	40%	45%	50%
1	0.50	0.75	0.94	1.09	1.22	1.32	1.43	1.53	1.63	1.74
2	0.47	0.65	0.88	1.02	1.14	1.25	1.35	1.44	1.55	1.68
3	0.50	0.76	0.95	1.11	1.24	1.37	1.46	1.57	1.67	1.79
4	0.52	0.76	0.95	1.09	1.22	1.32	1.42	1.52	1.62	1.74
5	0.52	0.77	0.96	1.11	1.23	1.33	1.44	1.54	1.64	1.76
Average	0.50	0.74	0.94	1.08	1.21	1.32	1.42	1.52	1.62	1.74

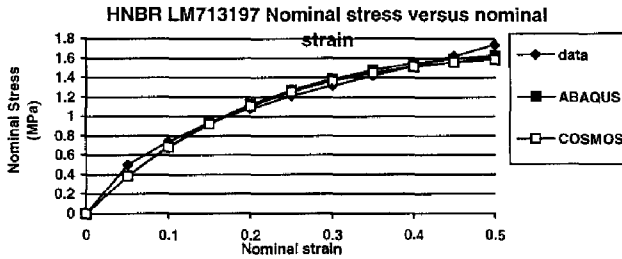


Figure 28 Mooney-Rivlin data fit from ABAQUS and COSMOS/M.

The Mooney-Rivlin constants for the curves presented in Figure 28 are determined with the automatic data fit features of ABAQUS and COSMOS/M. These two procedures did not give exactly the same values, ABAQUS found $C10 = -0.5865$ and $C01 = 2.037$ MPa, whereas COSMOS/M presented Mooney_A = -0.6181 and Mooney_B = 2.058 MPa. As can be seen from Figure 28 these constants represent an almost identical stress-strain curve. The deviation between the Mooney-Rivlin model and the measured data becomes larger for larger strain values. If the strains in the seal become much higher than 30 % a hyperelastic model with more material constants must be used to describe the stress strain relationship accurately. Both ABAQUS and COSMOS/M allow for a more accurate model to be used.

3.6 Frictional properties of seal materials

A theoretical approach towards seal friction only is not satisfactory because of the difference between theoretical and experimental seal friction as found by Van Dijnjen [1995]. Measurement of seal friction of an 11 mm and a 22 mm SA-seal produced of different materials resulted in a coefficient of friction (seal friction/radial load) between 0.15 and 0.3 for the same operating conditions. Thus a strong dependence of seal friction on seal material was found. This could not be explained based upon the assumption of full film lubrication and thus a more direct relationship between the seal material and seal friction seems to exist.

In Appendix C a model is presented to explain seal friction not only based upon viscous shear stresses, but also the shaft surface roughness and the seal material. It is useful to compare theoretically derived frictional forces based upon the hysteresis friction model of Appendix C with experimentally determined frictional forces. Next to this the knowledge about the frictional properties of seal materials in general is useful information for the seal designer.

Due to the complexity of the process of tribological interaction between two running partners and their environment the measurement of the relationship between seal material and seal friction was not carried out with complete seals. In order to determine experimentally the total frictional force, a generally accepted and commonly used tribological friction experiment is used in this study: The pin on disc experiment.

A set of pin on disc experiments is conducted with four different elastomeric pin materials performed on a smooth and a rough disc under certain applied contact load. These tests are done in order to make an estimation of the possible contribution of hysteresis friction to the measured total frictional force.

A lubricant is supported during the pin on disc experiments in order to minimize interfacial adhesion effects.

3.6.1 Pin on disc test method

In an experiment, a flat headed elastomeric pin runs against the flat surface of a steel disc under a constant load W and speed v long enough to attain a steady state, see Figure 29.

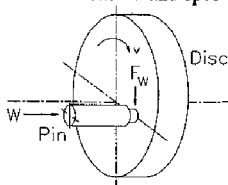


Figure 29 Basic configuration of the pin on disc test: the pin is loaded by force W onto the rotating disc; the velocity of the track amounts to v , the frictional force acting on the pin is depicted by F_w (Meesters [1993]).

The frictional force F_w and for several experiments the temperature T within the elastomer are continuously measured and recorded. The test rig is outlined in Figure 30.

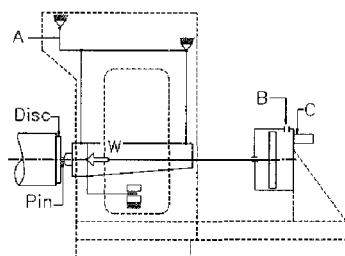


Figure 30 Overview of the pin-disc device (Meesters [1993]).

The steel disc is mounted on the main spindle of a modified lathe with continuous adjustable speed. The number of revolutions of the modified lathe can be varied between 0 up to 20 rotations/sec. The elastomeric pin specimen fits in a recess of a steel specimen holder, which is clamped into the pneumatic loading device B. The contact load W is continuously measured using a pressure gage A. The frictional force F_w is measured using a strain gage A.

3.6.2 Performance of the pin on disc tests and used materials

A set pin on disc tests at an ambient temperature of $T = 20 \pm 2^\circ\text{C}$ is conducted, in presence of a lubricant, to investigate the influence of:

- Velocity, approximately between 0.002 up to 0.4 [m/s].
- Disc roughness, for a rough ($R_a=0.2 \mu\text{m}$) and a smooth ($R_a=0.02 \mu\text{m}$) surface.
- The contact load W , respectively: 75, 150 and 225 N.
- Different elastomeric materials.

The value for the contact loads was chosen based upon the results of the FEA of radial lip seal yielding the average and maximum contact pressure between 0 and 10 MPa. A load of 75 N results in an average contact pressure over the surface of the pin of 2.6 MPa, while 225 N results in 7.9 MPa.

The following elastomeric pin materials, most provided by PL Automotive, are used in the pin on disc experiments:

- | | | |
|---|-----------|------------------|
| 1. FPM-compound | LM 801372 | Micro IRHD: 79.5 |
| 2. NBR-compound | LM 80602 | Micro IRHD: 79.2 |
| 3. HNBR-compound | LM 71372 | Micro IRHD: 79.8 |
| 4. FPM-compound, manufactured by Lips and used in maritime sealing applications | | |

The FPM-, NBR-, and HNBR-compounds are used in shock absorbers for automotive applications. FPM-compounds are materials with high chemical and temperature resistance compared to NBR-, and HNBR-compounds used for sealing applications.

The pin on disc tests were performed on a rough and a smooth disc:

1. Smooth disc surface: steel 100Cr6 with a surface roughness $R_a=0.02 \mu\text{m}$
2. Rough disc surface: steel 100Cr6 with a surface roughness $R_a=0.2 \mu\text{m}$

During pin on disc tests the supplied lubricant was:

an oil with a dynamic viscosity of 0.0152Ns/m^2 at $20 \text{ }^\circ\text{C}$, DEA-oil.

The oil mentioned above is used in shock absorber applications and provided by PL Automotive.

All tests were run long enough to attain an obvious steady state, the steady state situation could be detected from the measured frictional force signal. The tests were performed using a thoroughly cleaned pin and a cleaned track on the disc. In order to measure possible temperature rises within the elastomeric material, for several tests a thermocouple was inserted within the elastomeric pin material at approximately 0.5 mm from its running surface.

3.6.3 General observations

Possible influence of interfacial adhesion was studied by performing pin on disc tests with non-lubricated and lubricated specimens. The main observation after a set of experiments was that if interfacial adhesion behavior exerts a dominant influence on the measured frictional forces, this influence could be significantly reduced by the lubricant. To explain this more elaborately: a test was conducted with a NBR-compound in absence of a lubricant, using a smooth disc and a constant applied load of 150 N . A frictional force of 90 N for a given velocity was found. After repeating the same test, however this time with a lubricated specimen, a frictional force of 8 N was found.

Increasing the applied load W with a factor of 2, did not result in a rise of the measured frictional force level with a factor of 2. This observation results in the conclusion that seal friction can not be described by Coulomb friction.

The measured frictional force always fluctuates with periods corresponding to rotation of the disc. In order to take this effect into account bar charts are included in Van Klooster [1996], which represent the variation of the measured frictional force as a function of the velocity.

When hysteresis occurs in the seal material, the resulting work is transformed to heat and the temperature of the elastomeric pin must rise. The measured temperature rise within the elastomeric pin material is small, 1 to $2 \text{ }^\circ\text{C}$.

Measured frictional forces of a FPM-compound show a much higher level compared to the NBR- or the HNBR-compound. The HNBR-compound shows the lowest measured frictional force level. The same trend can be found by comparing the calculated hysteresis forces for the different elastomeric compounds. The calculated coefficient of hysteresis friction f_h generally shows a low value (Van Klooster [1996]).

The influence of the disc surface roughness is significant, because an increase of the surface roughness results in a considerable increase of the measured frictional force and the calculated hysteresis force level.

Now some observations of the pin on disc for the different seal materials will be shortly discussed and the calculated hysteresis force level will be compared with the total friction force of the experiments.

3.6.3.1 Observations for the FPM-compound

On a smooth disc:

The maximum measured coefficient of friction is $f=0.26$ concerning a low velocity and an applied load of 75 N.

The calculated hysteresis force levels are of a low value, though the contribution of the hysteresis frictional force varies between 1.6 % for a low velocity ($W=75$ N) up to 18 % for a high velocity ($W=150$ N). After investigation it seems that the FPM-compound operates in the transition region (considering velocities between 0.002 up to 0.4 m/s and a mean wavelength of 6.3 μm), so stiffening and asymmetry effects become significant. Due to the high applied load W of 150 N and 225 N, FPM-compound is fully squeezed around the small amplitude asperities of the model disc roughness profile. Gaps cannot be generated at all considered velocities.

The applied load of 75 N is not sufficient to squeeze the elastomeric material totally. Due to stiffening effects the elastomeric material tends to move higher upon a crest of an asperity until equilibrium is reached and therefore gaps between the model shaft roughness profile and the elastomeric material will exist. As a result less material will be deformed and therefore the hysteresis force decreases on increasing velocity.

On a rough disc:

The measured frictional forces are much higher compared to those on the smooth disc. The maximum measured coefficient of friction is $f=0,31$ concerning a low velocity.

The contribution of the hysteresis frictional force varies between 3.9 % for a high velocity ($W=75$ N) up to 17.6 % for a low velocity ($W=150$ N). As mentioned before, the elastomeric material is excited in the transition region. Due to the occurring stiffening effects within the FPM-compound, the applied load of 75, 150 and 225 N is insufficient to squeeze the elastomeric material totally around the "high" amplitude model roughness profile. Therefore gaps will certainly exist. Due to the increase of the gap size, less material will be deformed at higher velocities, so the hysteresis force level decreases.

It should be noted that the behavior of the FPM-compound (Lips) is similar compared to the FPM-compound of PL Automotive resulting in the conclusion that differently manufactured FPM-compounds have remarkably similar frictional characteristics.

3.6.3.2 Observations for the NBR-compound

On a smooth disc:

The measured frictional forces are much lower compared to a FPM-compound on a smooth disc. The maximum measured coefficient of friction is $f=0.06$ and the maximum calculated coefficient of hysteresis friction is $f_h=0.0023$.

The definition of the coefficient of hysteresis friction, is not always valid. It is stated that when the elastomeric material already fully drapes around the surface roughness profile due to a high applied load W , the hysteresis force level remains constant in case of a further increase of the applied load, thus the hysteresis force becomes independent of the applied load. As a result, the coefficient of hysteresis friction f_h is not representative for the occurring hysteresis friction. Nevertheless, the results of the coefficient of hysteresis friction, f_h , are presented even when the elastomeric material is already fully squeezed around the model roughness profile.

The contribution of the hysteresis force varies between 0.18 % for a low sliding velocity ($W=225$) up to 15.9 % for a high velocity ($W=75$ N). The NBR-compound operates in the rubbery and partly transition region, resulting a nearly elastic material behavior and a low stiffness. Therefore, the NBR-compound is fully squeezed around the model roughness profile even on increasing velocity, due to the applied load of 75, 150 and 225 N. As a result, the hysteresis force level remains constant in spite

of the applied load (75, 150 or 225 N). Increasing frequency or of course sliding velocity, leads to more energy dissipation, thus an increase of the hysteresis force.

On a rough disc:

The measured frictional forces are much lower compared to a FPM-compound on a rough disc. Surprisingly, the measured frictional force curve at an applied load of 225 N is of a lower level compared to those with an applied load of 75 and 150 N. The maximum measured coefficient of friction is $f=0.26$ and the maximum calculated coefficient of hysteresis friction is $f_h=0.014$.

The contribution of the hysteresis force varies between 0.56 % for a low sliding velocity ($W=75$) up to 30 % for a high velocity ($W=225$ N). The elastomeric material drapes fully around the model roughness profile as mentioned before.

3.6.3.3 Observations for the HNBR-compound

On a smooth disc:

This material exhibits far the lowest measured frictional force levels and the lowest calculated hysteresis force level. The frictional force suddenly increases at a sliding velocity of 0.33 m/s and an applied load of 75 N. This could be a possible result of typical hydrodynamic lubrication effects. It can be seen that the measured frictional force maximum fluctuates 48 percent! concerning a low velocity and an applied load of 75 N.

The contribution of the hysteresis force varies between 0.09 % for a low sliding velocity ($W=225$) up to 8 % for a high velocity ($W=150$ N). The HNBR-compound operates, in exactly the same manner as NBR, in the rubbery and partly transition region. Therefore again the elastomeric material drapes, due to the applied load, fully around the model roughness profile as mentioned before.

On a rough disc:

The same observations as the rough disc in combination with the NBR-compound. The maximum measured coefficient of friction is $f=0.27$ and the maximum calculated coefficient of hysteresis friction is $f_h=0.033$.

The contribution of the hysteresis force varies between 0.62 % for a low sliding velocity ($W=150$) up to 90 % for a high velocity (compare the measured frictional force generated with an applied load of 225 N and the calculated hysteresis force at a sliding velocity of 0.44 m/s). Furthermore the material drapes fully around the model roughness profile as mentioned before.

3.6.4 Results

The coefficients of friction found during the pin on disc experiments are in good agreement with the coefficients of friction found for complete shock absorber seals, making the pin on disc experiments a useful tool for the determination of the characteristic friction values of seal materials. The hysteresis friction model of Appendix C is not capable to predict the absolute value of elastomeric friction, but a relationship between the viscoelastic properties, storage modulus, and the friction coefficient of the rubber materials was found.

An accurate theoretical determination of seal friction for a SA-seal is still not possible, making a further investigation into the physical nature of seal friction necessary.

3.7 Experimental determination of the CPD

One of the basic design parameters for the evaluation and optimization for lip seals is the CPD. Numerous efforts to calculate or measure this pressure distribution are undertaken to gain insight in the sealing function. Finite Element Analysis (FEA) facilitates calculation of pressures under the lip of the seal, and is therefore a helpful tool in seal design. Despite the increased power and accuracy of FEA, measurements under the sealing lip are still necessary, in order to check the results.

Several researchers have tried to determine the shape of the contact pressure distribution experimentally, but due to the relatively small dimensions of the contact area and the small pressure values most of these attempts failed. The main problem in measuring static or dynamic contact pressures in the contact area is the lack of standard measurement transducers for these purposes. Although a good option might be to scale the sealing problem to get bigger contact areas, the main aim of this work was to design a device that can measure the static and dynamic CPD in the contact area of an existing shock absorber seal.

Determination of the static CPD is already difficult, but for the determination of the dynamic CPD abrasive wear is another problem to be considered when seal and rod are not completely separated by means of a lubricating oil film. Furthermore, during dynamic measurements an effect not to be neglected is the influence of temperature increase in the contact zone. A large group of resistance measurement principles is seriously affected by alternating temperatures, and would thus measure temperature instead of pressure.

A solution to meet all the above mentioned problems is thought to be found with the *divided shaft transducer*. In this type of transducer, a hollow shaft contains an elastic body that supports a set of strain gauges to register strains that can be related to forces. These forces are initiated by the mounted seal and act on the shaft's upper half, which is resiliently jointed to the stiffer lower half. Measurements with this transducer are presented in this section, and the results will be discussed. A schematic of the divided shaft is depicted in Figure 31.

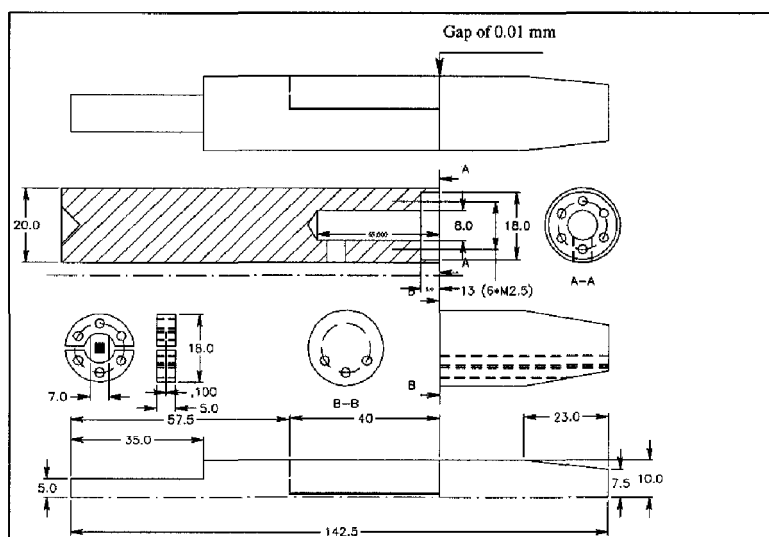


Figure 31 The new divided shaft radial force transducer.

3.7.1 Theoretical background

A seal mounted on a shaft will result in a radial force acting on the shaft. This radial force results from a certain pressure distribution in the contact areas between shaft and seal. The force can be calculated from the integral of pressure profiles working over the contact areas. An infinitely small load sensor, traveling through the contact zone, will therefore register the radial force working on a corresponding small area as a function of the coordinate of displacement. Thus the measured force as function of displacement in axial direction x , can be used to calculate the CPD using equations (3.1) and (3.2).

$$F_{rad} = \pi d \int_x p(x) dx \quad (3.1)$$

$$p(x) = \frac{dF}{dx} \cdot \frac{1}{\pi d} \quad (3.2)$$

3.7.2 Experimental setup

A lathe is chosen to construct the test rig. The seal is mounted with the use of a special housing in a four-jaw chuck such that rotation of the seal is possible. This rotation enables reduction of the friction in direction of displacement when the shaft is moved through the contact zone.

The divided shaft is mounted in the drill spindle carriage. Accurate position of the shaft is possible using the spindle of the carriage. To eliminate effects of the clearance, the carriage is pre-stressed using a simple rubber belt. Figure 32 presents a schematic of the test rig.

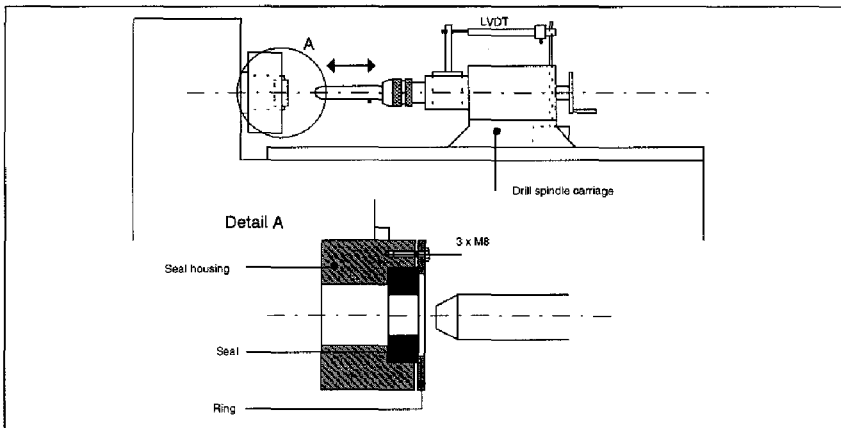


Figure 32 The experimental set up for the measurement of the contact pressures.

The position of the shaft is measured using a linear variable displacement transducer (LVDT). The transducer is calibrated with the use of the spindle, and found to be linear within 0.1 percent. Because of derivation of the registered force against displacement, only relative displacement is relevant.

In Figure 33 the movement of the force transducer through the contact area is clarified. First the secondary sealing lip contact forces and after this the primary sealing lip forces are measured. This

results in the characteristic two leveled force displacement curves presented in Figure 34 and Figure 35.

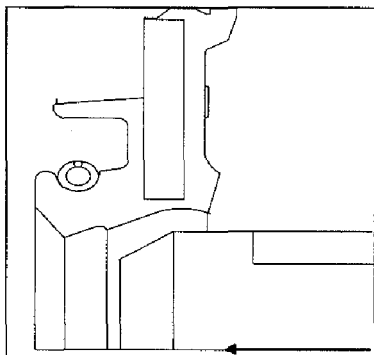


Figure 33 The sealing lip and the direction of movement of the divided shaft transducer.

The transducer for force measurements is calibrated in several ways. Dead weights and a lever were used for static calibration and investigation of linearity of the sensor. In these calibrations extra care is taken to keep the contact load exactly vertical on the upper half, such that the sensor is loaded in pure compression. Deviations from this angle lead to different loading conditions for the strain gauges, and thus to errors. The radial force induced by a seal however, will never be a point load and therefore extra calibrations are necessary to investigate the response when a force is applied over the complete circumference of the transducer. These calibrations are done using two garter springs with a known stiffness. In this way the radial force can be obtained from the output voltage of the sensor.

Both measurement signals are amplified using HBM measurement amplifiers. An AC HBM "type" is used for the displacement signal, whereas the force signal is amplified using a HBM KWS 3020 amplifier. The output signals are logged using a WORKBENCH signal processing card and are directly saved on disk. Further analysis of the signals and numerical operations are obtained from an analysis file written in MATLAB 4.0.

3.7.3 Measurements

A set of measurement runs is taken on the PL3-562 seal, under different conditions. The PL3-562 is a type of seal used in shock absorber applications for a shaft of $\varnothing 20$ mm. The material of the seal is a NBR-compound which is studied before. These studies aimed at obtaining the characteristic material parameters, necessary for FEA. The PL3-562 seal features a double lip contour and a washer. The latter was cut off to eliminate its influence on the measurements of radial forces under the sealing lips. The basic parameters that were varied are the relaxation period after mounting, and the presence or absence of the garter spring. In this way combined effects of both parameters can be studied.

The results are obtained from four different seals. Two of them have been mounted for relative long time (48 hours) on a dummy rod with the same dimensions. These seals will be referred to as numbers 4 and 5. The other two, numbers 2 and 3, are mounted on the measurement shaft just before measuring. In this way the effects of relaxation on the CPD and contact width can be studied. In both pairs of seals, with and without relaxation time, one of the seals is featured with the garter spring, whereas for the other seal the garter spring was removed before measurement or relaxation period, respectively.

Thus the measurement runs are indicated in Table 15 as:

Table 15 Overview of the measurement runs.

	Without relaxation	With relaxation
Without garter spring	SEAL2UZ*	SEAL4RZ*
With garter spring	SEAL3UM*	SEAL5RM*

Rotation of the clamping chuck leads to large deviations in the measured load signal, due to misalignment of the seal in its housing. Therefore the option of a rotating chuck is not used. To suppress the effect of friction in axial direction, the translation speed is kept sufficiently high. It appeared that when this speed was too low, the seal started to move due to stick-slip effects, thus affecting the registered force. A constant speed in axial direction will keep the frictional force working in the same direction throughout the measurement run.

3.7.4 Results

Five measurement runs were made on each seal, leading to a total set of twenty measurements. For all four seals an extra amount of oil was added between the second and third run as an extra effort to minimize friction.

3.7.4.1 Force versus displacement plots

As discussed before, the measurement runs yield plots of registered output voltage versus the axial displacement. This plot is used for further mathematical evaluation and calculation of the CPD under the sealing lips. Reproducibility can be examined by plotting five runs on the same seal in one plot. Figure 34 illustrates an example for SEAL2UZ*. It is clear that only run 3 to 5 reproduce to a satisfactory degree. Reasons for this can be the influence of time effects through relaxation, or the

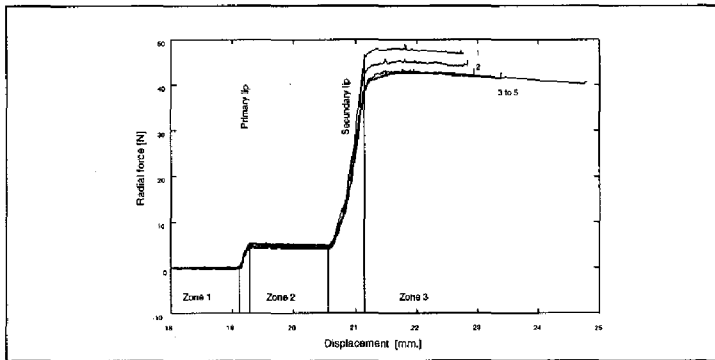


Figure 34 Radial force versus shaft displacement for SEAL2UZ*.

addition of the extra amount of lubricant.

Figure 34 clearly shows three different zones where the transducer output voltage is almost constant. These zones can be explained by the shape of the CPD for the seals used in the experiment. In zone 1 the load cell is outside and approaching secondary contact area of the seal. In the second zone the load cell has passed the secondary lip, leading to a response in measured force. In the third zone the registered load is maximal, implying that the load cell has also passed the primary lip of the seal. Transition from one zone to the next means that the load cell is directly under one of the sealing lips. The registered force should be, strictly speaking, constant in zone 2 and 3, when noise effects are

neglected. The decrease in output voltage is explained by the momentum effect due to the shaft movement and the measurement principle.

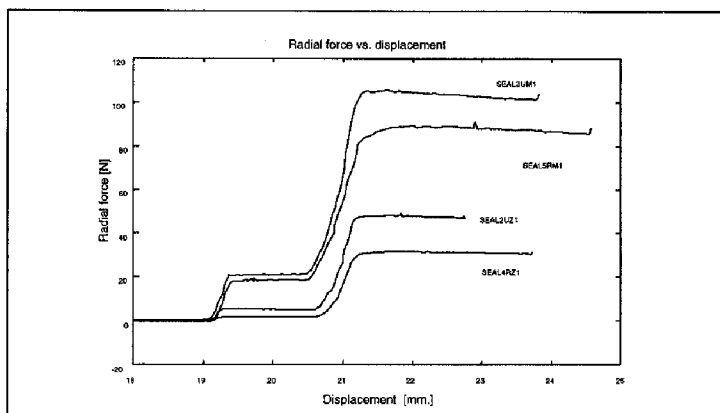


Figure 35 Influence of garter spring and relaxation on radial force.

This momentum effect is also present in the transition between two zones, but is neglected because of the small width of the transition zones. The effects of relaxation and the garter spring are demonstrated in Figure 35.

The main conclusion from Figure 35 is that the effects of relaxation and the garter spring for the radial force of a mounted seal are not negligible. To investigate this influence the quotient of maximum force is calculated for both an unrelaxed as a relaxed seal. This led to the relaxation quotients of Table 16.

Table 16 The relaxation quotients for five runs

	run 1	run 2	run 3	run 4	run 5
With garter spring	0.861	0.900	0.918	0.923	0.899
Without garter spring	0.649	0.696	0.745	0.755	0.757

The main conclusion from Table 16 is that, due to the presence of the garter spring, the total radial force under the seal remains significantly higher after relaxation. The statement that the garter spring is used to account for relaxation effects is therefore true.

3.7.4.2 Contact pressure distributions

The measurement runs are used to calculate the CPD under both sealing lips. The results from the MATLAB-file are graphically and are too elaborate to present. Therefore an analysis of the maximum occurring contact pressure and the contact width under both lips is examined and tabulated. An example of resulting output from the MATLAB-file is depicted in Figure 36.

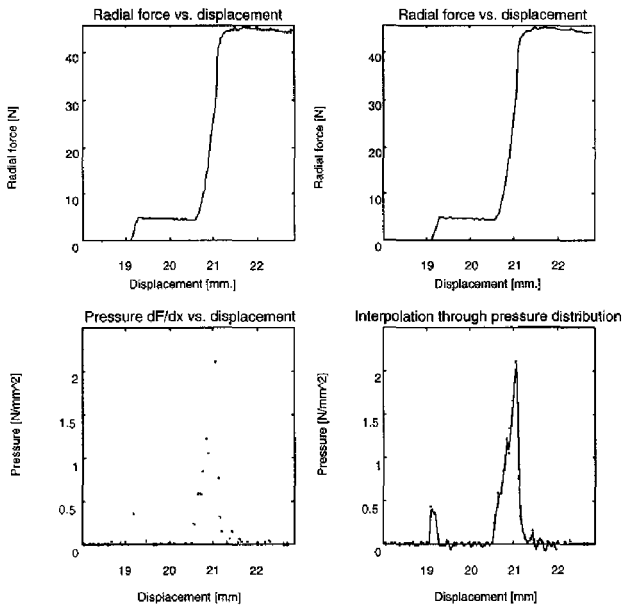


Figure 36 Graphical output from the MATLAB-file for SEAL2U22.

3.7.4.3 Contact widths

From the plots, similar to the one depicted in Figure 36, the contact width of both primary and secondary lip are calculated. Results of these calculations are tabulated in Table 17.

Table 17 The contact width for the primary and secondary sealing lip in [mm].

SEAL2	run 1	run 2	run 3	run 4	run 5	average \pm dev	spring	relaxation
primary	0.74	0.72	0.69	0.70	0.85	0.74 ± 0.064	no	no
secondary	0.32	0.36	0.28	0.27	0.52	0.35 ± 0.101		
SEAL3								
primary	1.00	1.00	0.97	1.11	1.06	1.028 ± 0.056	yes	no
secondary	0.47	0.47	0.42	0.44	0.59	0.478 ± 0.066		
SEAL4								
primary	0.77	0.74	0.73	0.76	0.67	0.734 ± 0.039	no	yes
secondary	0.29	0.26	0.33	0.41	0.22	0.302 ± 0.073		
SEAL5								
primary	0.96	0.92	1.00	1.22	0.93	1.006 ± 0.124	yes	yes
secondary	0.44	0.54	0.58	0.65	0.50	0.542 ± 0.079		

Table 17 indicates that the primary contact width is generally twice the width of the secondary lip. Another conclusion is that the contact width of the primary lip is not affected by relaxation. The effect of the garter spring is clear since the contact width of the primary lip without garter spring is 75% of the contact width for a seal with a garter spring.

The contact area under the secondary lip seems to be affected by relaxation. However, the table shows that the change is influenced by the garter spring. A decrease of the secondary contact width appears when the garter spring is removed, and an increase when the spring is left in position. Conclusions therefore should be made with extreme care.

3.7.4.4 Maximum contact pressures

After analysis of the contact width the absolute pressures are examined. Calculated maximum pressures (in N/mm^2) for the primary and secondary sealing lip of all measurements are tabulated in Table 18. The absolute value of the pressures is influenced by the division factor used in MATLAB analysis.

Table 18 Maximum contact pressures for the sealing lip in [MPa].

SEAL2	run 1	run 2	run 3	run 4	run 5	average \pm dev.	spring	relaxation
primary	1.768	2.540	1.518	1.518	1.114	1.683 ± 0.524	no	no
secondary	0.382	0.506	0.910	0.754	0.250	0.560 ± 0.270		
SEAL3								
primary	3.666	2.684	2.934	2.912	2.076	2.854 ± 0.572	yes	no
secondary	2.274	2.634	1.870	1.136	1.466	1.878 ± 0.600		
SEAL4								
primary	1.416	1.342	1.342	1.642	1.488	1.444 ± 0.124	no	yes
secondary	0.176	0.176	0.102	0.102	0.206	0.152 ± 0.048		
SEAL5								
primary	2.098	2.684	1.848	1.694	2.480	2.164 ± 0.416	yes	yes
secondary	1.466	1.312	1.218	1.592	2.530	1.620 ± 0.526		

The standard deviation is large compared to the average value, thus the method of calculating the contact pressure is rather inaccurate. Despite this inaccuracy some conclusions can be drawn from Table 18.

As could be expected, the pressures are higher when the garter spring is present. The effects of relaxation on the maximum pressure, see table V, are of the same order as the relaxation quotients from Table 16. Except for the secondary lip without garter spring where the effects of relaxation have decreased the maximum pressures significantly.

The ratio, r , of absolute pressure under primary and secondary lip is calculated for all seals and yields:

- SEAL2: $r = 3.0$ (without garter spring, without relaxation)
- SEAL3: $r = 1.5$ (with garter spring, without relaxation)
- SEAL4: $r = 9.5$ (without garter spring, with relaxation)
- SEAL5: $r = 1.3$ (with garter spring, with relaxation)

The conclusion from these ratios is that relaxation in the absence of the spring affects the maximum pressures differently than when the spring is present. This effect is mainly due to the fact that the maximum pressure under the secondary lip (table III, SEAL4) has decreased more than other pressures. When the garter spring is present, the ratio between maximum pressure under primary and secondary lip is not altered significantly.

Table 19 Ratio of maximum contact pressure before and after relaxation.

	Primary sealing lip	Secondary sealing lip
With garter spring (3/5)	$2.164/2.854 = 0.758$	$1.620/1.878 = 0.863$
Without garter spring (2/4)	$1.444/1.683 = 0.858$	$0.152/0.560 = 0.271$

3.7.4.5 Discussion

Calculation of the pressure according equation (3.2) is strongly influenced by noise and measurement errors in both force and displacement signal. The resolution in the displacement signal is found to be insufficient for accurate calculation of pressures: it appeared that even though the sample rate is taken sufficiently high, the number of discrete values of displacement varies between 2 and 5 in the secondary, and between 10 and 20 in the primary contact zone. This is not enough for calculation of a smooth pressure distribution.

An attempt to solve numerical problems due to equation (3.2), is introduction of the division factor in the MATLAB-file. This led to some improvement for the graphical presentation in Figure 36 (upper-right), smoothing of the force signal, but naturally could not solve the problem of insufficient resolution in axial direction.

Increased resolution in the measurement of displacement is necessary for improvement of contact pressure determination. From the results, displayed in Figure 36, it is concluded that the measurement method of force registration with the divided shaft transducer is promising. Results with this transducer in combination with another displacement sensor are believed to result smoother and more accurate results. The resolution needed in displacement x is at least 0.025 mm. for 10 discrete points where pressures can be calculated, in the secondary contact zone (with $DF=25$).

The division factor affects the results in calculated contact pressures. The main goal of introduction of DF is to smooth the force signal. However, another advantage of DF is that a lot of samples in x are ignored. In most cases $DF=25$ appeared to be such that no equal x coordinates are left in the measured data. This problem could have been solved by decreasing the sample rate. However, since the minimum translation speed is not guaranteed, this solution is rejected.

Contact pressures that are measured and calculated with the equipment described in this article agree with numerical results obtained by FEA. Both methods yield maximum pressures under the primary that range from 15 to 30 bar. The shape of the CPD is also in agreement with FEA, even though resolution in the measurement method is not satisfactory.

3.8 Summary

A complete seal design strategy consists of two major parts: the theoretical prediction of the seal performance and the experimental verification of the theoretical results. Several experimental methods to support seal design are presented. By a good documentation of the experimental results in combination with the wanted seal performance characteristic the level of knowledge of the seal designer will become higher in the future. The experimental determination of the material properties of the seal material must be carried out before FEA can accurately predict the CPD. Seal performance tests are carried out after the SO-stage.

4. Results & Discussion

4.1 Summary of the results

A new approach towards the design of radial lip seals was setup, implemented and tested in an industrial setting. The main results of this work are:

Seal design and seal design optimization based upon the shape of the contact pressure profile can be used for daily seal design and the results from seal research can be translated into useful guidelines for design decisions during the seal design procedure.

In order to implement and use the results from research in an industrial setting, a close cooperation and a constant exchange of information between research institutes and industrial design proved to be necessary. This cooperation is beneficial for both the research institute, who gets more information and thus better insight which research is needed in the future, and the designer, who is being equipped with better tools, more knowledge, and guidelines for design decisions.

The gap between the theoretical knowledge of the seal researcher and the seal designer at the start of this project was enormous resulting in no use of models and knowledge derived from research for actual seal design. This gap has been closed and the seal designer is now well aware of what is possible and what will be possible in the future. The increased level of knowledge of the seal designer on theoretical and experimental seal design data has resulted in faster and more accurate communication between the seal designer and the end-user resulting in *fit-for-use* product design as opposed to the original trial-and-error method.

It is difficult to use theoretical models to predict seal leakage and friction quantitatively for any given sealing system, because of the fact that the assumptions made during the validation of the model are not always valid for actual sealing systems. Especially, the assumption of seal operation in the full film lubrication regime does not hold for many practical sealing situations resulting in no practical use of predicted leakage and friction values. This problem can only be solved by testing of the actual design in its actual surrounding: the shock absorber.

The test facilities and test procedures needed for the determination of the important seal performance characteristics are developed, implemented and standardized and coupled to the theoretical side of the design process. The seal designer knows what he can do with the results from various tests and how these results can be compared with the results from models and tools used during the design process.

4.2 Discussion

One of the main factors influencing the decisions made to come to a useful seal design strategy is formed by the industrial setting in which the new strategy must function. Available human resources, hardware resources, knowledge and software tools, determine the possible solutions of a number of problems during the development of a design strategy. If the industrial setting changes the usefulness of the design approach must be checked against the new setting and some important features of tools of the current design approach might prove to be insufficient. As this situation has occurred during the final stages of this project a short evaluation of the presented radial lip seal design approach in the new industrial setting will now be given.

The original company was a stand alone seal manufacturer with 200 employees and an annual turn over of approximately 30 million guilders. The company was taken over by a world wide organization with more than 24.000 employees world wide and an annual turn over in the European shock absorber parts department of 53 million guilders. This new industrial setting provided much more backup from the point of view of the financial, theoretical, technical and theoretical knowledge on the important

steps needed for seal design. The organization has a central research center, which has done research on elastomer technology and FEA for more than 30 years with approximately 400 employees. It is impossible to compare the skill and know how of the original company with the new company and as a result some methods, tools and skills developed during this project might now seem without any value. However, the proposed approach will be adopted and implemented by the new organization, because of the fact that the proposed *fit-for-use* design strategy was not available and the new approach is demanded as the standard approach towards seal design by the main customer.

The complexity, accuracy, and customer input of several steps of the proposed design strategy can be increased easily by a synergy of the existing knowledge of a customer approved *fit-for-use* design strategy with the knowledge and know-how from 60 years of elastomer technology. The value of the standardized seal design approach has been acknowledged by the fact that the standard approach of the small company, coupling theoretical and experimental knowledge about seals in direct communication with the customer is regarded as the standard approach towards seal design for the future.

Thus proving, that although not every aspect of the seal design strategy could be investigated into full detail because of restrictions in the available resources, the usefulness of the approach is still valid if the available resources increase enormously. Making the proposed design strategy robust with respect to changes in the boundary conditions and thus valid and useful over a long term.

4.3 Recommendation

Fundamental research for reciprocating and rotating seals should be focused on the mechanisms and models to explain and predict seal friction in the mixed/boundary lubrication regime. Measured leakage or pumping action of radial lip seals can be explained by theoretical models. The fact that theoretical seal friction remains lower than measured friction values still rises doubts about the accuracy of the description of the tribological processes in the contact area.

Appendix A. Determination of the static CPD with COSMOS/M

A.1 Introduction

In the new design procedure presented in chapter one the determination of the shape of the pressure distribution in the contact area between the shaft and the seal is taken as the most important step in the process of designing and optimizing a new seal. In order to optimize the design of elastomeric contact seals changes in the shape of the CPD as a function of the relevant design parameters must be found. The shape of the CPD is the result of the interactions between housing, shaft and seal geometry, material properties and operating conditions. To find the influence of several relevant design parameters on the shape of the CPD and as a result of this on the seal performance an accurate method for the determination of the stresses and strains in the mounted and pressurized seal is required.

This appendix describes the steps of the determination of the CPD of a radial lip seal with the finite element code COSMOS/M and compares the important assumptions and numerical results with results from experiments. The first important step is an accurate characterization of the elastomeric seal material. The following steps and the general layout of static non-linear FEA are the result of the different external loads applied to the seal. Firstly, the garter spring load is applied to the seal, resulting in a change of the inner diameter of the seal. Secondly, the seal is mounted on a shaft resulting in a deformation of the sealing lip due to the interference δ (difference between the shaft diameter and the seal inner diameter). Thirdly, the seal is loaded by the fluid pressure on the high pressure side of the seal. The seal is also loaded dynamically due to friction forces in the contact area and by pressure fluctuations in the shock absorber, but the influence of these effects is not taken into account due to the fact that the exact value of the fluid pressure as a function of the shaft movement cannot be determined.

A.2 Choice of COSMOS/M

Nowadays several numerical approximation techniques to determine the response of structures to external loading are available. For structural design optimization two methods can be used, 1) the Boundary Element Method (BEM) and, 2) the Finite Element Method (FEM). BEM seems to offer some advantages from a needed automatic meshing algorithm point of view, but as the state of the art on non-linear contact and rubber analysis is more advanced for Finite Element Analysis (FEA) and the specific meshing advantages of BEM over FEM disappear in case of non-linear analysis the FEM is chosen as the mathematical technique to determine the CPD of radial lip seals.

Determination of the shape of the CPD by the FEM seems straightforward, but a number of problems must be solved concerning the accuracy of the finite element model. Most problems in engineering analysis of seals result from the non-linearity's included in this type of problem. The non-linearity's in seal design have three different physical reasons. First of all the contact problem is always non-linear, because both the distribution of forces over the surface and the contact width change and are a priori unknown. Secondly rubber like elastomeric materials show non-linear material behavior and special models are needed to describe the non-linear force-extension behavior. Thirdly a geometrical non-linearity exists due to the large displacements in a seal during mounting and pressurization. Another problem complicating the FEA is the fact that elastomeric materials show nearly incompressible behavior. Incompressible material behavior means that the elastomer exhibits zero volumetric change under hydrostatic pressure and so the pressure in the material is not related to the strain in the material.

In addition to the non-linearities the dimensions of the contact area are small, a contact width some tenth of a millimeter is common for radial lip seals, resulting in small dimensions of the elements in the contact area when the shape of the CPD has to be found accurately. Modern FEA codes are capable to solve all these problems and due to the increasing computational capabilities of PC's at the moment a number of commercially available non-linear FEA codes can also be run on a PC making the initial investments smaller and increasing the accessibility for smaller companies.

Summarizing the list of demands on the FEA code gives the minimal capabilities needed for FEA software which is to be used in the new seal design strategy.

- 1) The code must be able to deal with the combined non-linearity's of the material, geometry, and boundary non-linearity's. In order to come to geometrical optimization of seals this highly non-linear problem has to be solved cost efficient while maintaining accuracy and convergence. So, for engineering problems in seal design a non-linear FEA code capable of accurate contact and non-linear elastomer deformation analysis is needed.
- 2) The code must be capable to model and mesh different complex seal geometry's.
- 3) The code must have the possibility of automatic mesh generation, analysis and post processing for efficiency and geometry optimization purposes.
- 4) The code must run on a PC and total costs for the PC and software may not exceed fl 20.000,-.
- 5) The code must be implemented in and compatible with a design environment where AUTOCAD 12 is the standard.
- 6) The code must be easy to learn and use for AUTOCAD oriented seal designers and incorporate pre and post processing capabilities for visualization of the results.

Fansson [1996] compared three FEM-programs, ABAQUS, COSMOS/M, and ANSYS/ED, on the results of a non-linear benchmark problem, with large deformations, elastomeric material, and contact elements. Fansson deformed a rubber profile, fastened in a metal fixture, compressed by a rigid surface. Because of the strong non-linearity and the existence of experimental data, the presented problem is a good benchmark to compare the capabilities of different non-linear FEM-programs.

The results from ABAQUS reflected the experimental data good and the results from the other FEM-programs were compared with ABAQUS. The calculated contact stresses, principal stresses, contact forces, deformations and stress distributions were compared. The results for the different FEM-programs were in good agreement (within 5% of the ABAQUS results), leading to the conclusion that COSMOS/M seems capable of solving nonlinear, elastomeric, contact problems accurately.

FEA results of ABAQUS and COSMOS/M for radial lip seal geometries were compared. The difference in radial loads determined by ABAQUS and COSMOS/M with the same material behavior and mesh were less than 5%. Depending upon the accuracy of the mesh some differences were found for the maximum contact pressures, but when the tolerance of the COSMOS/M calculation was increased this problem could be solved. As the costs per year for ABAQUS are much higher and a PC should be used as the operating system COSMOS/M was chosen as the FEM package to analyse the seal deformations and contact stresses during the Seal Evaluation and Seal Optimization Stage.

Based upon this list of demands combined with the good results when compared to other FEA codes, COSMOS/M was purchased and implemented in the seal design procedure. COSMOS/M meets the list of demands completely, although the automatic meshing facilities of the code are not good. However, these meshing problems could be solved by an external meshing program and the easy to use COSMOS/M Language.

A.3 FEA of the PL3-562 seal

A.3.1 Introduction

In order to compare different finite element packages a standard has to be developed. In this thesis the PL3-562 seal is taken as the standard problem for comparison of calculated results from different FEA

codes and for the determination of both leakage and friction. The seal is designed for a shaft of 20 mm and is equipped with a non-return valve, which complicates the geometrical design. This seal will be used as a benchmark for the comparison of ABAQUS and COSMOS/M. Also the experimental results, presented in the previous sections can be used to say something about the accuracy of the finite element method to predict the static CPD of a radial lip seal.

A.3.2 Geometrical parameters and parametric seal model

To determine the CPD of the PL3-562-10 seal the parametric model presented in Figure A. 1 is used and the coordinates of the parametric points are presented in Table A. 1.

Table A. 1 Coordinates of the points of the PL3-562 geometry.

Point Number	Point 1	Point 2	Point 3	Point 4	Point 5	Point 6	Point 7	Point 8	Point 9	Point 10
1 - 10	0.0 11.05	1.5 11.05	1.5 13.25	2.0 13.25	2.0 12.62	2.7 12.50	3.5 11.50	4.3 12.30	5.1 11.60	7.5 11.60
Point Number	Point 11	Point 12	Point 13	Point 14	Point 15	Point 16				
11 - 16	7.5 10.75	5.1 10.67	5.1 10.44	4.1 9.25	2.5 9.80	0.0 10.66				

The values in Table A. 1 are determined as points from the dimensions give in the drawing of the PL3-562 seal, but in the future such coordinates can be obtained from a parametric model, which describes the relations between seal dimensions and its shape. A general setup for such a model within the COSMOS/M environment has been developed and applied to a simpler geometrically shaped radial lip seal.

The shape of the seal, given in Figure A. 1, is modified in the tip areas, where tip 1 and tip 2 are rounded-off with a radius of 0.05 mm to prevent numerical problems during the contact iterations. This rounding-off causes a small change in the inner diameter of the seal, resulting in a change from the original values of 9.25 and 9.60 mm to 9.263 and 9.617 mm for tip 1 and tip 2, respectively. This is less than 0.1% and the influence on the CPD is neglected.

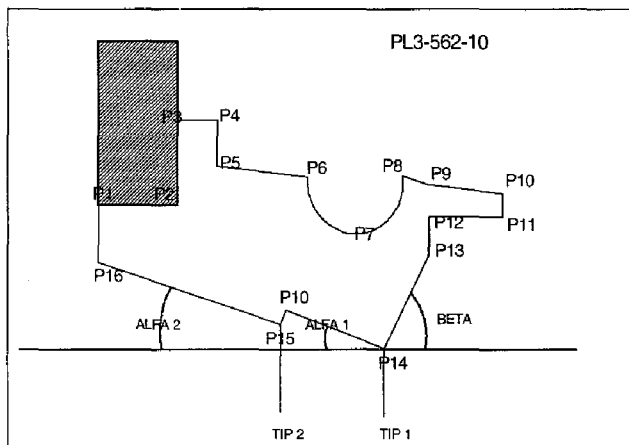


Figure A. 1 Geometry of the PL3-562 seal with parametric points.

The characteristic features of the PL3-562 seal are described by the following list:

General seal features:

Shaft diameter	D	=	20.00	mm
Inner diameter of primary lip	D1	=	18.50	mm
Primary sealing lip sharp	R1	=	0.05	mm
Inner diameter of secondary lip	D2	=	19.20	mm
Secondary sealing lip sharp	R2	=	0.05	mm
Characteristic geometrical features:				
Interference of tip1	=	0.75	mm (FEM = 0.737 mm)	
Spring leverage to tip1	=	0.60	mm	
Low pressure angle α_1	=	25 °		
High pressure angle of tip1 β	=	50 °		
Interference of tip2	=	0.40	mm (FEM= 0.383 mm)	
Spring leverage to tip2	=	-1.00	mm	
Low pressure angle α_2	=	25 °		
High pressure angle of tip2 β	=	50 °		
Spring characteristics:				
Spring stiffness F_{p10}	=	2.8	N	
Undeformed spring length	l_0	=	68	mm
Linear spring stiffness c	=	0.412	N/mm	
Radial spring stiffness c_{rad}	=	16.26	N/mm	
Radial spring position	=	11.50	mm	
Spring length	=	72.26	mm	
Spring compression	=	0.68	mm	
Spring force	=	11.1	N	

Based on this list of data two finite element models of the PL3-562 seal are created and the results of number of calculations will be presented, but before any finite element calculation can be executed a certain constitutive model for the material behavior has to be chosen. The designer of radial lip seals is primarily interested in the contact pressure distribution between the shaft and the seal and the distribution of forces in the contact area.

A.3.3 Finite element models for the calculations

The assumptions made and finite element model, which is used for the determination of the CPD between the shaft and the seal, are largely the same as used by previous researchers, like Ten Hagen [1987], Luijten [1987], Stakenborg [1988], Kanters [1990] and de Vrede [1993]. The isothermal, frictionless, axisymmetrical, static CPD will be determined using a hyperelastic, incompressible material model. The material behavior is described by the so called Mooney constants C_{01} and C_{10} for ABAQUS and Mooney_A and Mooney_B for COSMOS/M.

In Figure A. 2 the distribution of the elements for the calculations on the PL3-562-10 and the displacement boundary conditions are given.

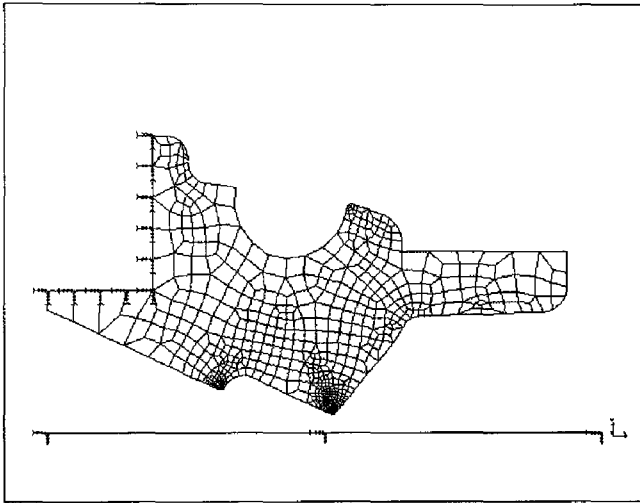


Figure A. 2 Finite element distribution and boundary conditions for the PL3-562 seal.

The model of Figure A. 2 consists of 814 isoparametric quadrilateral hybrid elements and the pressure distribution is determined with a linear elastic material model with $E=6.34 \text{ N/mm}^2$ and $\nu=0.45$.

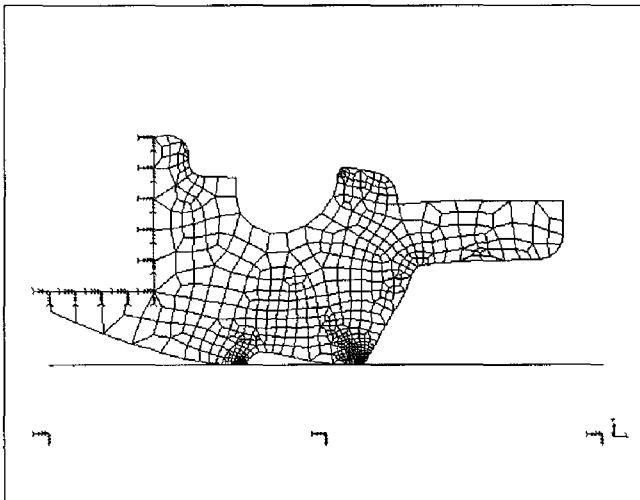


Figure A. 3 Deformed geometry of the PL3-562 seal determined with COSMOS/M.

The part of the seal which is molded to the washer, the metal part of the seal, is fully constrained. The washer is not a part of the finite element model, because modulus of elasticity of the washer is

approximately 20 times higher than rubber modulus of elasticity (Rubber approximately 10 MPa, and steel approximately 210 MPa).

A.3.4 PL3-562 contact pressure distribution

In Figure A. 4 the deformed geometry after mounting the seal to the shaft and the resulting contact pressures are presented.

For any type of elastomeric contact seal for a reciprocating shaft the functional behavior of the seal is

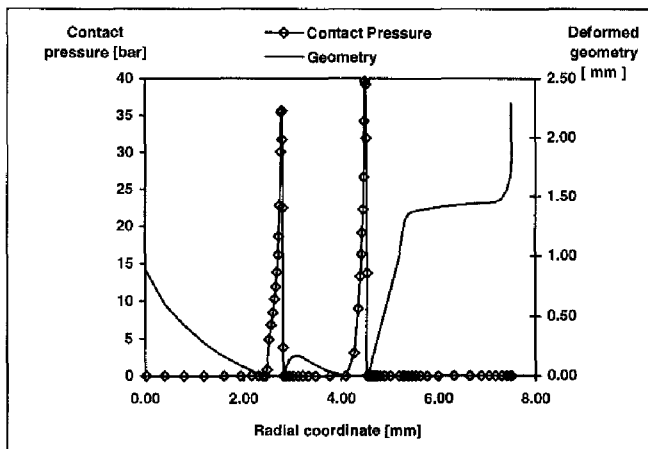


Figure A. 4 Deformed geometry and CPD of the PL3-562-10.

described by the combination of the deformed geometry curve and the contact pressures. From these two curves both leakage and friction can be determined.

A.3.5 Characteristic features of the CPD

In this section the influence of a number of parameters of the finite element analysis on the characteristic features of the CPD will be discussed. a more elaborate discussion of the influence of several parameters on the shape of the contact pressure profile and the resulting optimal parameters is discussed in Kuiken [1991].

The following nomenclature will be used to address the different features of the multiple contact pressure profile of the PL3-562 seal:

$p1_{max}$	= maximum pressure value of the primary sealing lip,
$b1$	= the contact width of the primary sealing lip,
$F1_{rad}$	= the radial force of the primary sealing lip,
$p2_{max}$	= maximum pressure value of the secondary sealing lip,
$b2$	= the contact width of the secondary sealing lip,
$F2_{rad}$	= the radial force of the secondary sealing lip,
$dp1_{max}$	= maximum pressure gradient in the primary sealing lip,
$dp2_{max}$	= maximum pressure gradient in the secondary sealing lip
F_{FEA}	= total radial force for the primary and secondary sealing lip as determined by the FEA,
F_{data}	= calculated radial force after data analysis of the CPD.

All the above mentioned parameters can be derived from the three contact areas of a shock absorber seal and based upon these values, as presented in Table A. 2, the results of different meshes and seal geometry's can be compared.

Table A. 2 Determination of the influence of the number of elements on the CPD.

Seal-elements	$p1_{max}$ [N/mm ²]	b1 [mm]	$F1_{rad}$ [N]	$p2_{max}$ [N/mm ²]	b2 [mm]	$F2_{rad}$ [N]	$dp1_{max}$ [N/mm ³]	$dp2_{max}$ [N/mm ³]	Fr_{FEEM} [N]	Fr_{data} [N]
PL3562-814	3.175	0.7576	26.96	3.456	0.4225	29.76	43.03	36.89	56.76	56.72
PL3562-2582	3.254	0.5389	26.82	3.560	0.3760	29.31	55.03	58.95	56.15	56.13

A.3.6 Discussion

From Table A. 2 it can be concluded that the number of elements used during the FEA has an influence on the characteristics of the CPD. The characteristic results for the PL3-562 seal are determined by FEA with 814 and 2582 elements. The influence of the number of elements on the radial force is small when compared to the influence of the number of elements on some of the characteristics of the CPD.

If the number of elements increases the theoretical value of the maximum contact pressure will become higher and the contact width will become smaller. Also the maximum value of the pressure derivative will become higher. For COSMOS/M the maximum number of elements is 3000, but in order to compare the CPD of different seal designs it is important to generate a mesh with the same average element size in the contact areas. This can be achieved by specifying the size of the elements in the contact area before the mesh is generated. During FEA in the SE-stage and the SO-stage at PL Automotive seal designs are always compared with approximately the same average element size in the contact areas

A.4 FEA of the SC1401_B seal

A.4.1 Introduction

In order to describe the different steps which are taken to model and analyze a shock absorber seal the SC1401_B seal design used during the optimization of the new FPM-compound seal will be presented. The software used for each step will be shortly discussed.

First a drawing of the new seal design with all the geometrical features and tolerances is made by the seal designer in AUTOCAD. The information about the geometrical features of the new design is carried by a DXF-file and the nominal dimensions of the seal design will be used for the FEA model of the seal. The drawing of the new seal design is produced at the end of the initial design stage (ID-stage) and the drawing proposal is discussed with the customer. For optimization of the design changes around the nominal dimensions used and these modifications will only be discussed with the customer after an optimal solution has been defined.

A.4.2 Meshing

The next step to generate a FEA model of the seal is to mesh the seal geometry. Due to the complex shape of the seal and the needed accuracy in the contact areas the mesh generator of COSMOS/M is not capable of meshing the seal. In order to solve this problem an external mesh generator is used. This is a small DOS-program called MESH.EXE and is developed at the Eindhoven University of Technology. This program meshes a certain area with quad or triangle elements based upon a number of points connected by straight lines and arc segments describing the seal geometry. At the moment the translation from the DXF-file to the input-file for MESH.EXE is done by the seal designer. This process could be automated, but due to the interactive nature of the program MESH.EXE complete automation of the meshing process is not possible. The designer can specify the wanted mesh density by giving the element length in the points describing the seal geometry. Some geometrical information is lost during this step, because not all parts of the seal design need to be part of the FEA model.

Some extra geometrical information is incorporated in the design, based upon experience with the FEA of radial lip seals.

A small radius of 0.05 mm is applied to the primary and secondary sealing lip to prevent numerical problems. Originally the seal design is equipped with sharp sealing edges, but these edges will result in stiffness singularities during the FEA. The tip of the sealing lip has been studied by a microscope and was found to be never completely sharp. The radius of 0.05 mm seems a good compromise to prevent numerical problems, but keep the CPD of a sharp lip. Larger radii will yield more Hertzian like pressure distributions at the high pressure side of the seal, while smaller values of the tip radius tend to increase the risk of numerical problems. The same solution has also been applied by several other researchers, like Luijten [1987] and Gabelli [1992].

The result from the program MESH.EXE is a file with the nodes and elements of the seal and this data is transformed into an COSMOS/M input-file by a specially written QBASIC program. This program is written in QBASIC because any DOS PC is or can be easily equipped with this software. The program automatically adds the needed element groups to describe the problem and after COSMOS/M has read the input file the boundary conditions can be applied.

A.4.3 The COSMOS/M input-file

```
C*
C* COSMOS/M Geostar V1.75
C* Problem : 1401B_MV
C* Date : 24-07-96
C* Time : 13:15:21
C*
C* Definition of the needed element groups for the seal problem.
C* Group 1 - Axisymmetrical 4-node hybrid elements to describe the elastomer.
C* Group 2 - Gap elements to describe the contact area.
C* Group 3 - Truss2D dummy elements to define the shaft surface and the rigid
C* connection between the spring and the seal
C* Group 4 - Axisymmetrical 4-node linear elastic elements to describe the washer.
C* Group 5 - A non-linear spring element to describe the garter spring behavior.
C*
C* Next to the type of element also some constant values are assigned to the elements
C* by the RCONST command
C*
EGROUP,1,PLANE2D,0,1,1,0,3,2,0,
EGROUP,2,GAP,1,0,0,1,3,0,0,
RCONST,2,2,1,7,0,0,0,0,1E+008,0,1,
EGROUP,3,TRUSS2D,0,0,0,0,0,0,0,
RCONST,3,3,1,2,1E+006,0,
EGROUP,4,PLANE2D,0,1,0,0,0,2,0,
RCONST,4,4,1,2,1,0,0,
C*
C* Definition of the time curves needed to describe the loading of the seal.
C* The loading of the seal is carried out in three stages (time curves):
C* Step 1 - Deformation of the sealing lip by the garter spring.
C* Step 2 - Deformation of the sealing lip by the rod.
C* Step 3 - Deformation of the sealing lip by pressurization.
C*
C* Thus three time curves are needed for the description of the loading of the
C* seal. In order to analyze the result from each step exactly at the same time
C* the total time for the loading of the seal will be set to two
C*
```

```

CURDEF,TIME,1,1,0,0,0.05,0,1,1,2,1
CURDEF,TIME,2,1,0,0,0.05,1,1,1,2,1
CURDEF,TIME,3,1,0,0,0.05,0,1,0,2,1
C*
C* Definition of the different material properties of the seal,
C* the washer and the garter spring.
C*
ACTSET,TC,0,
C*
C* Material properties of the FPM-compound seal material.
C* The Mooney_A and Mooney_B constants are determined by an
C* uniaxial elongation experiment and the nearly incompressible material
C* behavior is modeled by the Poisson constant of 0.49.
C*
MPROP,1,NUXY,0.49000001,
MPROP,1,MOONEY_A,0.4442,
MPROP,1,MOONEY_B,1.0431,
C*
C* Material properties of the dummy elements.
C*
MPROP,3,EX,30000000,
MPROP,3,NUXY,0.28,
MPROP,3,GXY,12000000,
MPROP,3,ALPX,7.4E-006,
MPROP,3,DENS,0.00073000003,
MPROP,3,C,42,
MPROP,3,KX,0.00066999998,
C*
C* Material properties of the washer.
C*
MPROP,4,EX,210000,
MPROP,4,NUXY,0.3,
C*
C* Definition of the nodes to describe the seal geometry.
C*
ND,1,1.25748,0,0,0,0,0,0,0,0,
ND,2,10.90269,0,0,0,0,0,0,0,0,
:
: The rest of the nodes is removed, but has the same information.
:
ND,1995,6.32925,1.942764,0,0,0,0,0,0,0,
ND,1996,6.298866,2.033639,0,0,0,0,0,0,0,
C*
C* The element group needed to describe the rubber part
C* and define the elements.
C*
ACTSET,EG,1,
ACTSET,MP,1,
ACTSET,RC,1,
EL,1,SF,0,4,323,3,4,324,0,0,0,0,0,0,
EL,2,SF,0,4,1752,1739,1740,1753,0,0,0,0,0,0,
:
: The rest of the elements is removed, but has the same information.
:

```

```
EL,1834,SF,0,4,24,25,34,35,0,0,0,0,0,0,
EL,1835,SF,0,4,35,36,23,24,0,0,0,0,0,0,
C*
C* Definition of the shaft surface by three nodes and two
C* dummy TRUSS2D elements.
C*
ND,1998,4.5,-7.0,0,0,0,0,0,0,0,0,
ND,1999,4.5,0,0,0,0,0,0,0,0,0,0,
ND,2000,4.5,7.0,0,0,0,0,0,0,0,0,
ACTSET,EG,3,
ACTSET,MP,3,
ACTSET,RC,3,
EL,1837,CR,0,2,2000,1999,0,0,0,0,0,0,
EL,1838,CR,0,2,1999,1998,0,0,0,0,0,0,
C*
C* Definition of the gap elements to model the contact between
C* shaft and seal surface.
C*
ACTSET,EG,2,
ACTSET,MP,2,
ACTSET,RC,2,
EL,1899,ND,0,1,60,0,0,0,0,0,0,0,
EL,1900,ND,0,1,61,0,0,0,0,0,0,0,
:
: The rest of the gap elements is removed.
:
EL,2088,ND,0,1,249,0,0,0,0,0,0,0,
EL,2089,ND,0,1,250,0,0,0,0,0,0,0,
C*
C* Definition of the contact surface for the gap elements.
C* This is the part of the contact pair that determines which surface
C* (the shaft) cannot be penetrated by the gap elements (the seal surface).
C*
NL_GS,1,2000,1998,1999,
C*
C* Definition of the non-linear calculation properties
C*
TIMES,0,1,0.05,
TOFFSET,273,
TREF,0,
NL_AUTOSTEP,1,1.0E-4,0.05,
NL_PLOT,1,20,1,0,
NL_CONTROL,0,1,
PRINT_OPS,0,0,0,0,0,1,0,0,0,0,
C*
C* Definition of the boundary conditions.
C*
DND,1,ALL,0,30,1, C* Fully constrain all nodes along the washer.
DND,1998,UY,0,2000,1, C* Constrain movement of the shaft surface in axial direction
DND,1998,UZ,0,2000,1, C* Constrain movement of the shaft surface perpendicular to the plane
DND,1,UZ,0,NDMAX,1, C* Constrain movement of all nodes perpendicular to the plane
C*
C* Activate the time curve which is coupled to the movement of the shaft and
C* define the shaft movement.
```

```

C*
ACTSET,TC,1,
DND,1998,UX,1,0,2000,1,,
C*
C* Define the position of the garter spring, the non-linear spring behavior, the nodes
C* and the spring element. Apply boundary conditions to the spring element, ensuring
C* that the spring only loads the seal in radial direction.
C*
PT,1,7.55,-2.45,0,
PT,2,9.55,-2.45,0,
EGROUP,5,SPRING,0,2,1,0,1,1,0,
MPCTYPE,1,0,
MPC,1,0,1,-1.765,-4.19,-1.275,-3.74,-0.765,-3.19,-0.275,-2.62,0,-2.31,&
0.22,-2.06,
NDPT,2500,1,
NDPT,2501,2,
EL,2500,CR,0,2,2500,2501,0,0,0,0,0,0,
CPDOF,1,UY,2,2500,2501,
ACTSET,TC,2,
DND,2501,UX,-0.000001,2501,1,,
ACTSET,TC,1,
DND,2500,UZ,0,2501,1,,
C*
C* Definition of the rigid elements that couple the spring to the seal.
C*
ACTSET,EG,3,
ACTSET,MP,3,
ACTSET,RC,3,
EL,2501,CR,0,2,2500,292,0,0,0,0,0,0,
.
.
EL,2507,CR,0,2,2500,286,0,0,0,0,0,0,
C*
C* The pressure is applied over the elements on the high pressure side of
C* the seal.
C*
ACTSET,TC,3
PEL, 3 , .6 , 2 , 3 ,1
PEL, 5 , .6 , 2 , 5 ,1
:
: The rest of the pressurized elements is removed.
:
PEL, 1529 , .6 , 3 , 1529 ,1
PEL, 1530 , .6 , 3 , 1530 ,1
C*
C* Finally the non-linear calculation is started by
C*
R_NONLINEAR

```

A.4.4 Results

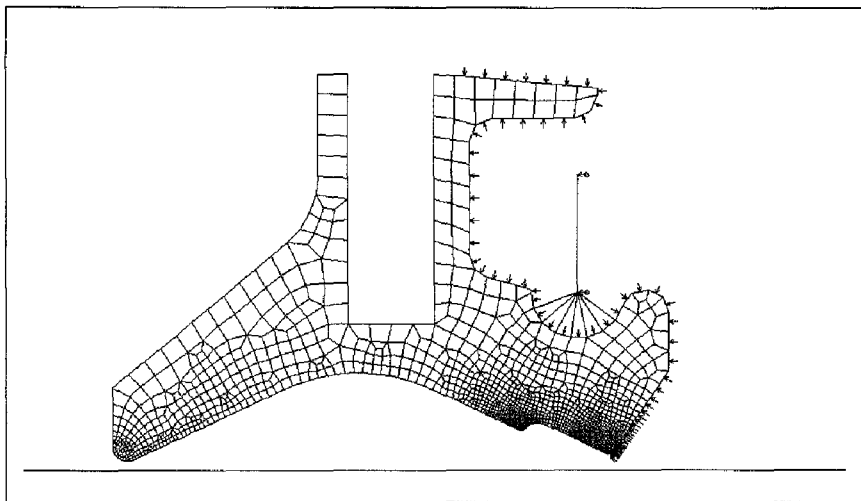


Figure A. 5 Undeformed SC1401_B seal with garter spring and pressure loading.

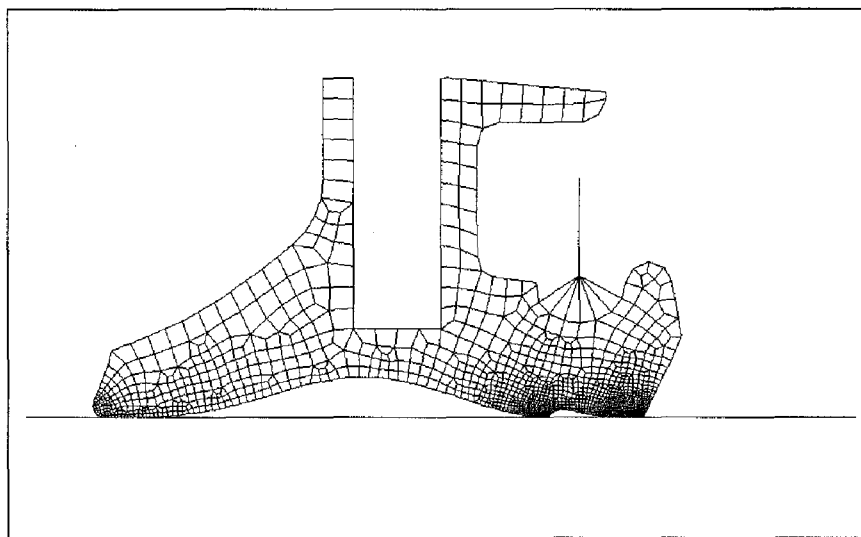


Figure A. 6 Deformed SC1401_B seal with garter spring and pressure loading.

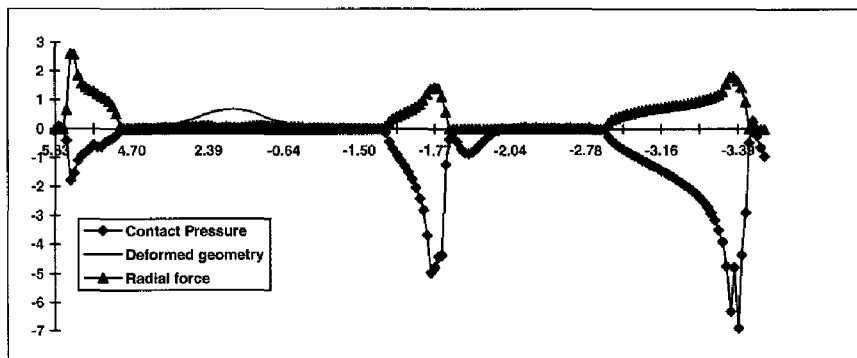


Figure A. 7 Characteristic graph of contact pressure, deformed geometry, and radial force.

A.5 Summary

COSMOS/M is used to determine the CPD of SA-seals. This FEA-code runs on a PC and the ease of use of the program made it possible to train the seal designers of PL Automotive to use COSMOS/M as a part of the new seal design strategy. Some disadvantages of COSMOS/M over other more expensive commercial FEA-codes, like ABAQUS, were found, but these disadvantages could not justify the use of ABAQUS instead of COSMOS/M for daily seal design analysis.

COSMOS/M is capable of solving the non-linear shaft-to-seal contact problem with enough accuracy to be used for seal design purposes.

Appendix B. Determination of leakage and friction with the IHL method

B.1 Introduction

This appendix presents the assumptions and models of Van Dijnsen [1995] to determine radial lip seal leakage and friction with the inverse hydrodynamic lubrication approach. The inverse hydrodynamic lubrication theory was first presented by Blok [1963].

Many seal designers have focused on the determination of leakage and friction, both theoretically and experimentally, because knowledge of these two characteristics is of direct importance to the quality of the seal. Experimental investigations provide knowledge about the actual state of lubrication in the contact area and allow for the verification of theoretically obtained results. The combination of a flexible elastomeric seal and a rigid steel shaft leads to a complex tribological system of which both leakage and friction have to be controlled.

A seal mounted on a reciprocating shaft with lubricant supply on one side of the contact can be regarded as an heavily loaded elastohydrodynamic lubricated contact. In order to determine the changes in the quality of the seal as a function of the above mentioned changes a set of governing equations describing the relationships between deformations, fluid film and hydrodynamic pressures must be solved. To derive the set of governing equations a number of assumptions is made to simplify the actual contact conditions into an approximated set of contact conditions. According to Gohar [1988] material properties, elastostatic contact theory and fluid flow theory form the basic input for an EHL contact. Different features of these theories are described by the Reynolds equation, the energy equation, the lubricant film geometry equation, the elastic deflection equation, the lubricant equations of state and the load equation. Several researchers have solved the complete set of equations and compared the results with experiments. For an engineering design problem this approach is far too complex and results in high computational efforts needed to solve the set of equations. The resulting set of equations for an EHL contact is far too complex to solve as a part of the design optimization, so a faster method has to be found to derive the important parameters leakage and friction.

The determination of leakage and friction for reciprocating shaft seals has been studied by Kanters [1990]. Kanters proposed to determine both leakage and friction with the inverse hydrodynamic lubrication theory. This theory is based upon the assumption that the contact pressure distribution (CPD) between the shaft and the seal is known and that the film thickness will not change the pressure distribution, but follow the prescribed pressure gradient function. Kanters has experimentally verified his results and found a good correspondence between theoretical and experimental results in the full film lubrication regime and he stated that the theoretically predicted leakage values would also be valid far into the mixed lubrication regime. Based upon these results and the fact that the IHL method separates the problem into the determination of the static CPD followed by the determination of the film profile for a given static CPD, which makes the method far less computationally complicated as the solution of the full coupled EHL problem, leakage and friction will be approximated based upon the IHL theory.

Figure B. 1 presents a schematic overview of the different contact areas of a shock absorber seal, with the possibility of different amounts of oil or grease in the zones between the contact areas.

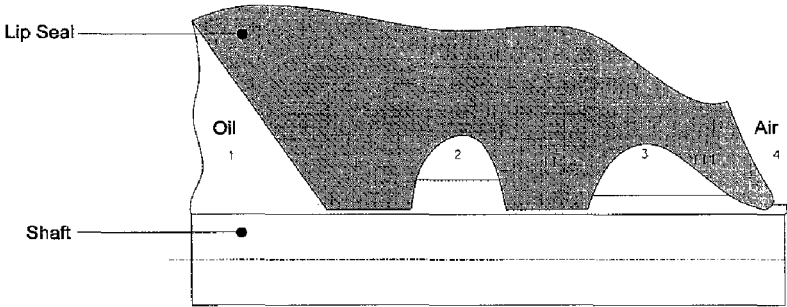


Figure B. 1 General representation of the contact areas of a seal with two sealing lips (I and II) and a dustlip (III).

One of the main ideas behind this work was that the developed tools should be implemented on a personal computer. As the software developed by Kanters was written in FORTRAN and the graphic user interface fully programmed for APOLLO workstations a number of changes had to be made to the original codes. In order to make the codes easy to access on any operating system the choice was made to develop the software for the determination of leakage and friction within the MATLAB 4.0 environment. MATLAB 4.0 is available for UNIX and DOS, WINDOWS platforms and allows for the code to be used on both workstations and PC's without having to change the code. The only necessity is the availability of MATLAB 4.0 on the computer.

Kanters used the name PROGRES for his code, because the code has been changed and in order to make a distinction between the two codes the new code for the MATLAB 4.0 environment is called SEALCALC. Figure B. 2 presents an overview of the contact nomenclature used by Kanters [1990].

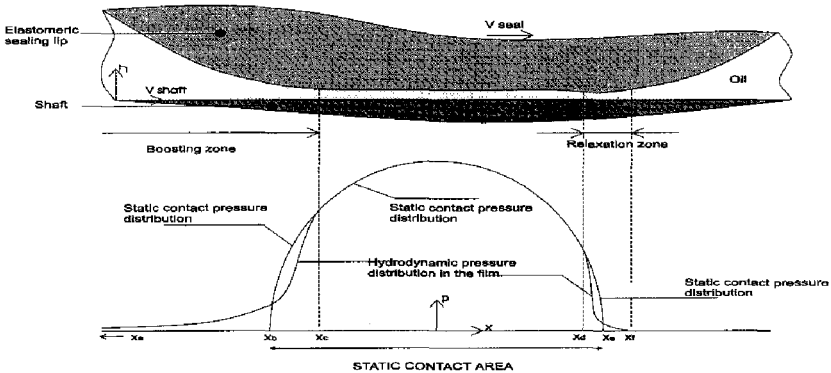


Figure B. 2 Frictionless static contact pressures and elastohydrodynamic film pressures for the heavily loaded, soft Hertzian line contact, from Kanters [1990].

For radial lip seals the general shape of the CPD differs from the CPD's of the reciprocating seals used by Kanters and the general asymmetrical shape of a radial lip seal CPD is determined in appendix A and its relation to the film thickness can be determined based upon the IHL approach with SEALCALC.

B.2 Assumptions for SEALCALC

- In order to adapt PROGRES for the determination of leakage and friction of radial lip seals a number of simplifying assumptions were made. First of all the assumptions made by Kanter used for the determination of the film and pressure profile in the boosting zone were used. However, for lip seals this lead to erroneous results and some new assumptions for the pressure profile in the exit and boosting zone were used.
- Although in general the design of a shock absorber seal is equipped with a number of sealing lips (I and II) and a dustlip (III) (Figure B. 1), the program is only capable of determining the leakage and the friction for a single contact area. When the results for a single contact area are known it is possible to connect the three contact areas by prescribing boundary conditions which are influenced by the preceding contact areas. This coupling of the contact areas leads to the determination of leakage and friction for the total seal. In literature some knowledge about an oil flow through a multiple contact zone can be found in the area of piston rings.
- It is assumed that there is always enough oil available outside the contact area of the seal to generate the maximum possible thickness of the oil film ($h_0 = h_{0,max}$). This means that not only during an outstroke, but also during instroke. In general this is not true for radial lip seals as $(dp/dx)_{max}$ is larger for an outstroke than for an instroke. This means that in general there is not enough oil during an instroke to form the maximal film thickness. It will be assumed that, although there is not enough oil to form the maximum film thickness, all oil will be used for the formation of a smaller film thickness. The flow through the contact then determines h_0 and all oil will be transported through the contact area resulting in zero leakage. SEALCALC only determines the maximum possible value for h_0 .
- It is assumed that for any given speed the stroke of the shaft is long and that the fluid film can establish itself. The stationary isothermal film profile for different shaft velocities is used for the determination of the dynamic leakage and friction of the seal.
- The pressure on the oil side and the air side of the seal are given and constant. This means that the movement of the shaft has no influence on these pressures. This assumption holds for the pressure on the air side, but especially the pressure on the oil side is not always known accurately.
- The pressure on the oil side of the seal is higher or equals the pressure on the air side of the seal.
- The influence of friction on the CPD is neglected. This means that the shape of the CPD is independent of the direction of movement and the shaft speed V_L .

B.3 Procedures and algorithms

Next to the algorithms for the determination of the fluid film profile in the contact area a number of algorithms has been written to fit the discrete static CPD and the corresponding deformed geometry of the seal to a curve for which in each point in axial direction the film contact pressure and the corresponding gap height are known. In the following flowchart a global overview of the program SEALCALC is given in Figure B. 3.

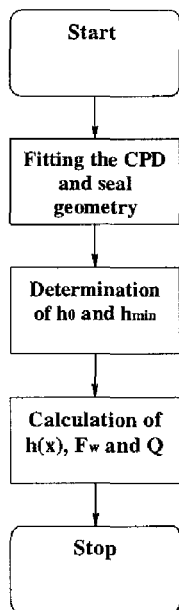


Figure B. 3 Global structure of the computer program SEALCALC.

B.3.1 Curve fitting the discrete static CPD

For the determination of leakage and friction with the IHL method it is necessary to determine the pressure gradient function accurately. While the number of points in the area of contact is limited it is difficult to use the discrete data from the finite element calculation directly for an accurate determination of the pressure gradient function. A curve is fitted through the discrete data sets of both the contact pressures and the deformed seal geometry. In this way it is possible to determine the value of the pressure gradient function in any point of the contact area. The fitted curve has to meet the following demands:

- The fit has to be continue
- The first derivative of the fit has to be continue
- The fit has to create a smooth line through the data points, which allows for some small irregularities from the finite element CPD to be taken care of.
- In any point from the discrete data where the contact pressure is equal to zero the fitted curve has to be equal to zero too.
- Oscillations in the fitted curve are to be avoided, whereas the distribution of the contact pressures must be continues..
- It must be possible to fit the data fast and independent of the user.

Several methods to fit the curve have been examined by Van Dijnjen [1995], but the final choice was to fit the data by means of a so called "smoothing spline".

The algorithms for this kind of curve fit have been implemented in an interactive fitting program that runs within the MATLAB 4.0 environment. A graphical interface in combination with quality data of the spline are used to judge the fit.

Although the proposed method is able to fit any discrete data set accurately there still are some drawbacks. It was impossible to automate the fitting procedure completely, so it is still up to the designer to judge the quality of the fit. This may lead to different results for different users, but the differences in the pressure gradient functions created by different users are surprisingly small. Another drawback is the fact that a spline presented oscillations in the boosting and exit zone were the actual value of the contact pressure is zero, resulting in positive and negative values for the contact pressure, whereas it should be zero outside the contact. This problem was solved by fitting only the area where the discrete contact pressures are larger than zero. This resulted in a continuous, but not smooth shape of the CPD, with jumps in the first derivative in the beginning and the end of the contact area. Hooke and O' Donoghue [1972] have experimentally observed these jumps for elastomeric seals in contact with a shaft so it can be assumed that the fitted derivative equals the actual contact pressure derivative.

The above mentioned adaptations of the fitting procedure result in an accurate fit of the discrete contact pressures (least squares error $< 10^{-4}$, no oscillations before and after the contact area and a difference in the maximum pressures of the fit and the discrete data less than 1 %). The proposed fitting algorithm meets the list of demands and can be used for any discrete CPD.

B.3.2 Curve fitting discrete geometrical data of the deformed seal

For an accurate determination of the flow criterion h_0 also the deformed geometry of the seal is important whereas the boosting and relaxation action are completely determined by the deformed shape of the seal. The same problem as with the discrete pressure data applies to the discrete geometrical data, but in this case the problems occur in the contact area where the initial gap height must be zero in all points. The same demands as stated in 3.3.1 hold for the curve fit of the geometrical data, but two extra demands are to be met.

- The derivative of the fit has to be equal to zero at the edges of the contact area.
- The curve fit may never penetrate the shaft surface resulting in a negative film thickness.

Especially this last demand is difficult to meet with higher order polynomials. A method using interpolating splines with an adaptive value of the derivative was used and programmed for the MATLAB 4.0 environment. This method is described in appendix B of Van Dijnjen [1995].

Just like the curve fit for the CPD the spline showed the tendency to oscillate in the contact area where the gap is constant and equal to zero. In case of the geometry this problem was solved by fitting the data selectively in the areas outside the contact area, where the shape of the deformed seal is not known. On both sides of the seal a fit is used and the three curves are combined to form a continuous and smooth profile of the deformed shape. This procedure is completely automatic and the user does not influence the result of the fit.

B.3.3 Determination of the film characteristics for a fully lubricated contact

The characteristic film parameters are the flow criterion h_0 , the position where the boosting pressure merges with the static CPD x_m , the minimum film thickness h_{min} and the position where the hydrodynamic pressure starts to deviate from the static CPD in the exit zone x_d .

Determination of the flow criterion h_0 and at the same time the position x_m can only be achieved by an iterative process. The algorithm is described by Kanters [1990] and Van Dijnjen [1995] and is programmed in the MATLAB 4.0 environment. The calculations are continued until a certain accuracy is accomplished. The choice of x_m is made with the so called interval splitting method. This method is not fast, but stable and an accurate estimation of the position x_m can always be found. For the integration of the Reynolds equation in the boosting zone a recursive integration algorithm is used. This algorithm is not fast, but the integral can be determined with a preset accuracy. This algorithm was available as standard MATLAB procedures (quad.m and quad8.m), which have been specially adapted to the needs of SEALCALC in routines (gquad.m and gquadg.m).

Also the minimum film thickness h_{\min} and the position x_d is achieved by an iterative procedure in MATLAB. The number of required iterations is determined by a preset accuracy ϵ . The new choice for x_d is also determined by interval splitting, resulting in a slow, but stable iterative procedure.

The possibility of cavitation in the relaxation zone is taken into account, by assuming that cavitation occurs if the hydrodynamic film pressure equals the surrounding pressure p_{sur} at position x_f . From the point x_f the Reynolds equation is not valid anymore and the hydrodynamic pressures can not be determined in the zone after the point x_f . However, if no cavitation occurs, the hydrodynamic pressure profile is given by Figure B. 4.

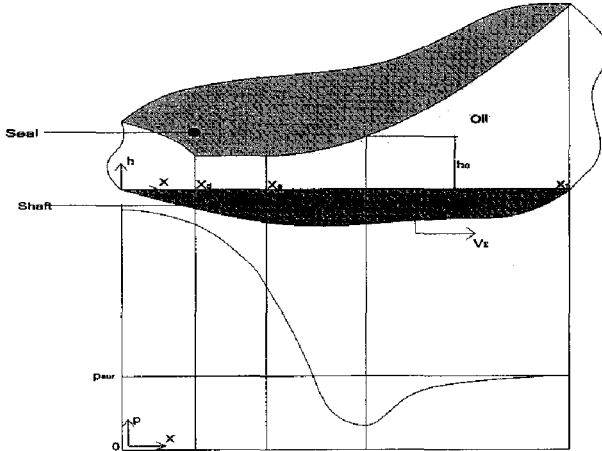


Figure B. 4 The elastohydrodynamic pressure profile without cavitation.

In case of no cavitation in the exit zone the point x_f , where $p = p_{\text{sur}}$ and $(dp/dx) = 0$, lies far from the end of the static contact area. In general, this will result in a smaller value for the minimal calculated film thickness. A problem, which remains to be solved, is a valid criterion for the occurrence of cavitation. In literature there is no consensus about this criterion and the occurrence of cavitation can only be validated by experiments. For seals these experiments are not always conducted and this why the following approach towards implementation of cavitation is chosen and implemented in SEALCALC. SEALCALC first assumes that no cavitation will occur. However, when the calculated value of the hydrodynamic pressure in the oil drops below a certain pre-set value of the cavitation pressure, p_{cav} , the calculation will be carried out again with the cavitation boundary conditions applied in the exit zone. The actual value of p_{cav} depends on the type of oil and the temperature of the oil in the contact zone. An estimation for the value of p_{cav} could be found from a analysis of the applied oil type, but in general SEALCALC will use the surrounding pressure as the cavitation pressure.

B.3.4 Determination of seal leakage and friction

When the elastohydrodynamic film thickness and pressure profile are known leakage and friction can be found from these profiles in the full film lubrication regime. The seal leakage is calculated from multiplication of the flow per unit of width and the circumference of the lubricated surface, e.g. the rod surface for elastomeric contact seals, according to equation B.1.

$$Q = \pi d_{\text{rod}} V_{\Sigma} \frac{h_0}{2} \quad (\text{B.1})$$

For a fully lubricated contact friction forces are calculated from integration of the viscous shear stresses, acting on the shaft and the seal surface. The friction force on the shaft is calculated according to equation 3.2.

$$F_w = \pi d_{as} \int_{x_s}^{x_f} \tau_v(x) dx \quad (\text{B.2})$$

with
$$\tau_v = -\frac{h}{2} \frac{dp}{dx} + \frac{\eta V_A}{h} \quad (\text{B.3})$$

B.4 Application of Kanters algorithms on lip seals

In order to verify the general applicability of the method proposed by Kanters for the determination of both leakage and friction a typical frictionless static CPD for a radial lip seal has been used. Static CPD's of radial lip seals are characteristic a-symmetrical, with a maximum value of the contact pressure on the high pressure side of the seal. A typical shape of these CPD's is presented in

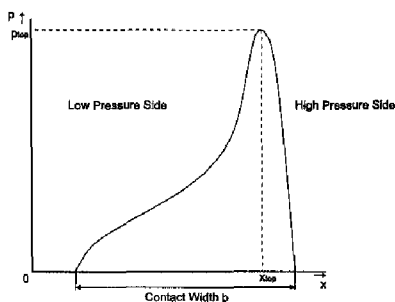


Figure B. 5 Example of an asymmetrically shaped CPD of a lip seal.

During the part of the stroke where the shaft surface drags oil from the low pressure side of the seal through the contact area towards the high pressure side, a so called instroke, the algorithm of Kanters [1990] for the boosting zone yields the result presented in Figure B. 6.

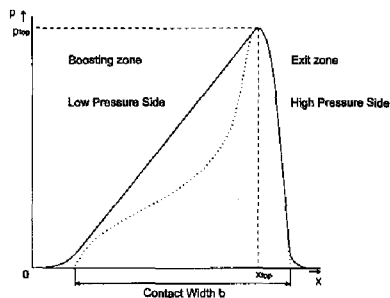


Figure B. 6 Elastohydrodynamic pressure profile for a lip seal with the boosting zone on the low pressure side of the seal.

During the part of the stroke where the shaft surface drags oil from the high pressure side of the seal through the contact area towards the low pressure side, a so called outstroke, the algorithm of Kanters [1990] for the boosting zone yields a hydrodynamic film pressure distribution presented in Figure B. 7.

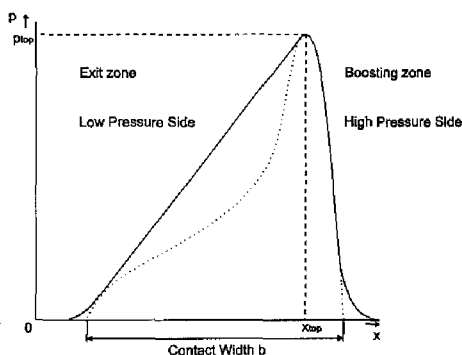


Figure B. 7 Elastohydrodynamic pressure profile with the boosting zone on the high pressure side of the lip seal.

During these calculations it is assumed that cavitation will occur in the exit zone. In Figure B. 6 and Figure B. 7 the hydrodynamic pressure profile is represented by the continuous line and the fitted discrete static CPD, which is the result of a finite element calculation and used as input for SEALCALC, is represented by the dotted line. Both figures show a large discrepancy between the initial static CPD and the hydrodynamic film pressures. This disagrees with the assumption of the inverse hydrodynamic lubrication theory that the hydrodynamic film pressure is equal to the static contact pressure over a large part of the contact area, or that the boosting and exit zone must be small compared to the contact area. In general, this means that the seal will be lifted from the shaft by the hydrodynamic film pressures and the only way to determine the fluid film profile accurately is by a coupled solution of the seal deformation and the film profile equations, resulting in a complex non-linear EHL-problem. This type of solution cannot be solved by the seal designer and on the equipment available for daily seal design. This conclusion restricts the general applicability of the algorithms

proposed by Kanters to seals where the static CPD has a Hertzian profile in both the entry and exit zone.

This is in conflict with the assumption made by Kanters [1990], which states that the areas of boosting and exit zone must be small compared to the contact width of the pressure distribution. The large difference between the static and dynamic contact pressure profile results in a component of the pressure which will lift the seal from the shaft and by this change the CPD significantly. This limits the applicability of the algorithm proposed by Kanters. The algorithm, in its unchanged form, can only be used for seal with have a Hertzian shaped CPD (Figure B. 8) and not for the asymmetrically shaped pressure profiles of radial lip seals. In order to solve this problem the algorithms of Kanters have been modified and now lips seals, with their asymmetrically shaped pressure profile, with a point of inflection in the contact area on the low pressure side of the seal can be treated with the same IHL approach as used by Kanters [1990].

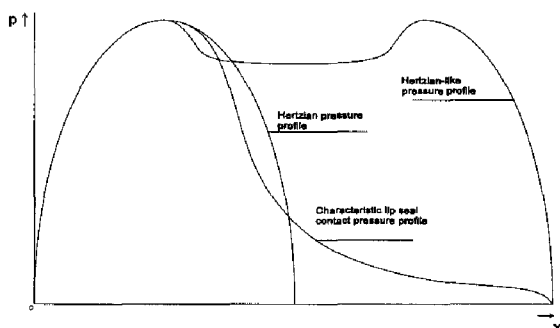


Figure B. 8 Example of the differently shaped pressure profiles.

Hydrodynamic lubrication must take care of the separation of the seal and the shaft. By means of a mechanism for load support the initial radial load of the seal is balanced by the pressure generated in the fluid film. Moore [1975] summarized the actual causes of possible load support for both smooth and rough surfaces. For smooth surfaces only three terms can contribute to the load support: the wedge, stretch and squeeze terms can contribute separately to the load support. By introducing the concept of surface roughness at least four contributions to the load support become apparent: the directional effect, the macro-elastohydrodynamic effect, cavitation and viscosity effects. The macro-elastohydrodynamic effect is the most important. The generation of pressure on the positive slopes of the flexible asperities tends to push down and distort the asperities, while the negative pressures on the pull slopes produce a distortion of the pull or suction type.

B.5 Determination of leakage and friction for seals with a strongly asymmetrical contact pressure profile

B.5.1 New assumptions for the film profile in the boosting and exit zone

In the previous sections it was found that the assumptions of Kanters for the shape of the film profile in the boosting and exit zone can not be used for the determination of the leakage and friction of a radial lip seal. As the main aim of this appendix is the determination of leakage and friction for radial lip seals, a new set of assumptions must be formulated in order to present physically acceptable

results. It must be noted that the algorithms presented by Kanters are valid for Hertzian-like pressure profiles. In general, the high pressure side of the CPD of a radial lip seal resembles one side of the Hertzian contact pressure profile, see Figure B. 9. The algorithms presented by Kanters will be applied to this side of the contact area.

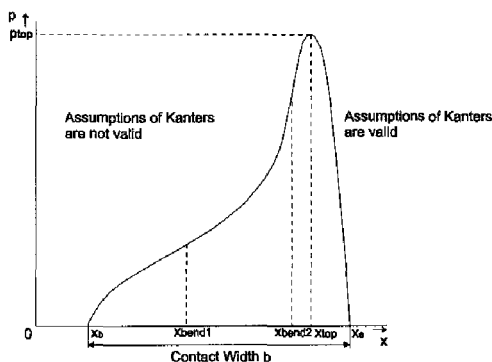


Figure B. 9 Typical shape of the frictionless static CPD of a radial lip seal.

For the CPD of Figure B. 9 it is possible to apply the algorithms presented by Kanters [1990] on the right side of x_{top} , while on the left side of x_{top} this leads to the erroneous results presented in the previous sections and another algorithm must be applied.

B.5.2 Film profile in the boosting zone

In the previous sections it was explained that the use of the assumptions of Kanters [1990] for the film profile would lead to erroneous results with the determination of the film and pressure profile in the contact area between the shaft and the seal. The calculated hydrodynamic pressure profile deviates over a large part of the contact area from the frictionless static contact pressure profile. The difference between the two pressure profiles may not be neglected and the problem should be treated as a fully coupled elasto-hydrodynamic problem, because there is no global equilibrium of the hydrodynamic and structural induced forces. As this type of coupled EHL problems are complex and the numerical procedures to solve such a problem are complicated and time consuming efforts will be made find a different set of assumed film profiles in the entry and exit zone which allow for the IHL method to be applied and the global force equilibrium to be established.

The results in the previous sections all were obtained with the assumptions of Kanters [1990] for the film profile in the boosting and exit zone. Although the results found with the algorithms proposed by Kanters [1990] did not give good results for radial lip seals this does not imply that the IHL approach can not be used for such seal types. It seems possible to formulate a different set of assumptions, which do not violate the demands on the continuity of the film and pressure profile more as the assumptions of Kanters, but allow for the global force equilibrium to be established through an iterative procedure. In the following sections these assumptions will be discussed and implemented in the program SEALCALC.

In order to verify the results for the calculated film profile $h(x)$ a number of experiments is conducted and described in Van Dijnsen [1995].

There exist two theoretical possibilities to minimize the difference between the static contact pressure profile, determined for a certain seal with the finite element method, and the hydrodynamic pressure profile determined with SEALCALC based upon the static contact pressure profile.

The first possibility is when the merging point x_m (see Figure B. 10) comes closer to the edge of the contact area x_b . Then the total length of the boosting zone becomes smaller and by this the difference between the hydrodynamic and static pressure profile forms a smaller part of the total contact area. (However, with the assumptions of Kanters [1990] the merging point x_m will always be located between x_{bend2} and x_{top}).

The second possibility is when the hydrodynamic pressure profile between x_b and x_m has the same shape as the static CPD the global force balance will automatically be resolved.

The first option was implemented in the algorithms of Kanters and this allowed for x_m to lie closer to the edge of the contact zone x_b . This resulted in the solution presented in Figure B. 10.

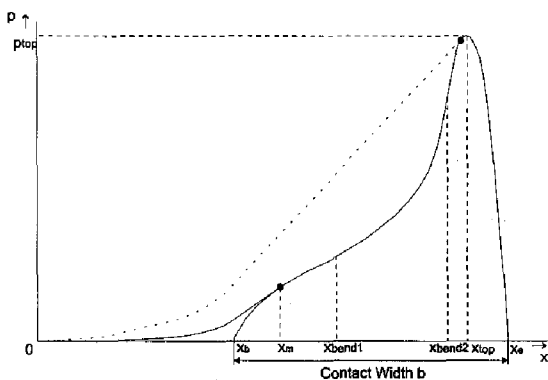


Figure B. 10 Moving the merging point x_m closer to the edge of the contact area.

The difference between the hydrodynamic and static pressure profile has indeed become smaller and for situations where the shaft speed, V_z , is small good results are found. However, a shaft speed exists which generates a high fluid pressure in the boosting zone so that the pressure profiles can not merge between x_b and x_{bend1} . This means that the merging point can only be found between x_{bend2} and x_{top} and that there will always be a shaft speed where the hydrodynamic pressure profile (and as a result of this the film profile) will behave discontinuously as a function of the shaft speed V_z . Such transitions in the pressure profile must also result in strange frictional behavior of the seal and as such results were not observed experimentally it was concluded that this solution to the problem of the global force equilibrium was unsatisfactory.

The second possibility is to adjust the shape of the hydrodynamic pressure profile in the boosting zone. This can be achieved by the following two assumptions:

- The geometry of the seal will in the boosting zone be influenced by the pressures in the film. The seal will be pressed away from the shaft by the pressures in the fluid and as a result of this a wedge between the seal and the shaft is formed. This wedge will have a certain angle α and is formed between the points x_b and x_m . This results, just like Kanters [1990] found, in a discontinuity in the first derivative of the pressure profile in x_m . However, Kanters [1990] found no negative influences of this discontinuity on the final results.

- The value of the pressure angle α is determined by the global force equilibrium in the area from x_b to x_m .

This leads to the following assumptions for the film profile in the boosting zone (see Figure B. 11):

$$\begin{aligned}
 h(x) &= \alpha(x_m - x) + \frac{3}{2}h_0 & \text{voor } x_b < x \leq x_m \\
 h(x) &= \alpha(x_m - x_b) + \frac{3}{2}h_0 + cl_n(x) & \text{voor } x \leq x_b
 \end{aligned}
 \tag{B.4}$$

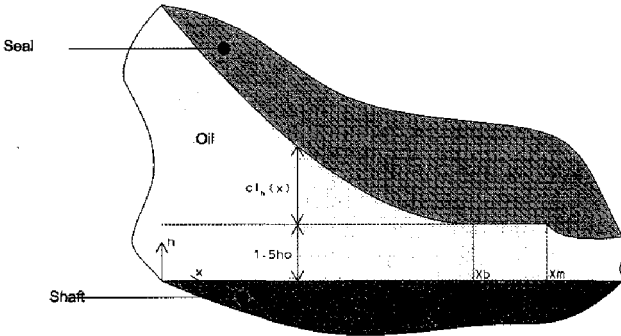


Figure B. 11 Assumed film profile in the boosting zone.

The pressure angle α in Figure B. 11 is the variable which has to be determined with an iterative procedure.

B.5.3 Film profile in the exit zone

In the previous sections also it was found that the algorithms of Kanters [1990] resulted in erroneous results in the exit zone. These errors are of the same type as in the boosting zone, a difference between the frictionless static contact and the hydrodynamic pressure profile. Also for determination of the film and pressure profile in the exit zone the algorithms of Kanters have to be adjusted. A possible solution is to shift the point where the hydrodynamic pressure deviates (drops) from the frictionless static contact pressure profile, x_d , as presented in Figure B. 12.

This time the shifting of the merging point, x_d , towards the edge of the contact area does not present the same problems as for shifting the position of x_m in the boosting zone, as long as the value of the ambient pressure outside the contact area is low enough. In general, the ambient pressure or low pressure side pressure is small enough to fulfill this requirement.

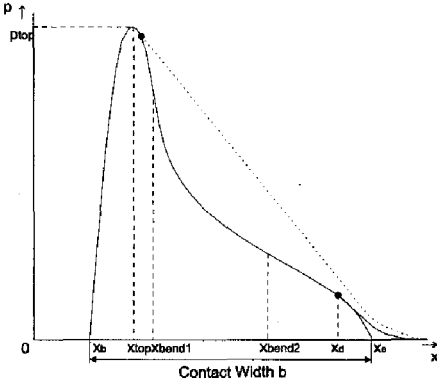


Figure B. 12 Shifting of the dropping point x_d .

For the relaxation zone the following complementary assumptions can be made:

- The film thickness h_{xd} (see Figure B. 13) exists over a finite part of the contact area, namely between x_d and x_e .
- x_d lies between x_{bend1} and x_e .

For the film profile in the exit zone it follows that (see Figure B. 13):

$$\begin{aligned} h(x) &= h_{xd} && \text{voor } x_d \leq x \leq x_e \\ h(x) &= h_{xd} + c l_h(x) && \text{voor } x_e < x \leq x_f \end{aligned} \tag{B.5}$$

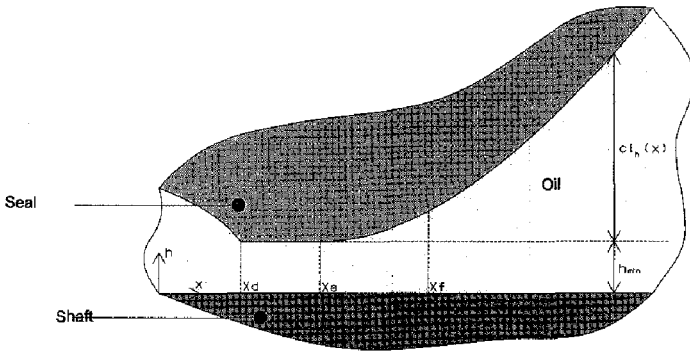


Figure B. 13 Assumed film profile in the exit zone.

B.6 Elastohydrodynamic pressure profile with the new assumptions

In the subjoined pictures the elastohydrodynamic pressure profiles which are determined with the new assumptions for the film profile of a lip seal in the entry-zone and exit-zone. In both the boosting-zone and exit-zone a global force equilibrium is achieved. In Figure B. 14 the hydrodynamic pressure profile still deviates from the static contact pressure profile, but the deviation is much smaller due to the new set of assumptions for the film profile. The force equilibrium is maintained over the total contact area.

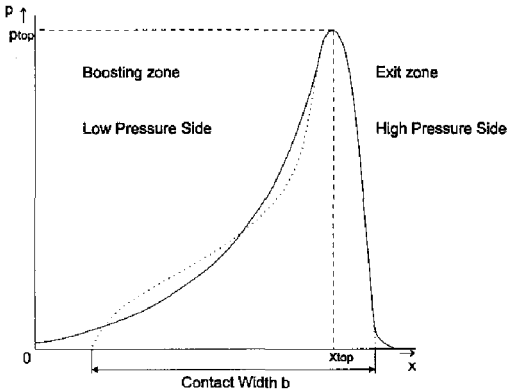


Figure B. 14 Elastohydrodynamic pressure profile with the boosting zone on the low pressure side.

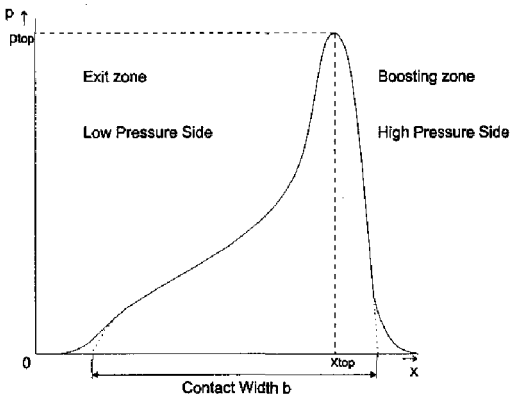


Figure B. 15 Elastohydrodynamic pressure profile with the boosting zone on the high pressure side.

It must be clear that these results do not give any information whatsoever on the validity of the new assumptions. The validation must come from a comparison of the theoretical and experimental leakage and friction of a radial lip seal. On the other hand the proposed assumptions are much better than the ones presented by Kanters [1990] from the point of view that the static CPD will not change much under dynamic conditions.

B.7 Piezo-viscous calculations with SEALCALC

Although it was assumed during the initial stages of the program that the dynamic viscosity, η [Pa.s], is independent of the pressure, SEALCALC also allows for piezo-viscous calculations of the film profile. The pressure-viscosity relationship for a constant temperature is calculated by, Kanters [1990]:

$$\eta(p, T) = \eta_0(p_{atm}, T)e^{\beta(T)(p-p_{atm})} \quad [\text{Pa}\cdot\text{s}] \quad (\text{B.6})$$

The pressure-viscosity coefficient β must be known. For iso-viscous calculations it holds that $\beta = 0$. When β is not known, an approximation for the value of β can be derived from the equation:

$$\beta(T) = (0.6 + 0.965 \cdot \log(\eta_0(p_{atm}, T))) \cdot 10^8 \quad [\text{Pa}^{-1}] \quad (\text{B.7})$$

The value for η_0 must be given in [cP] and can be determined with a viscosity measurement. The difference between a calculation with a piezo-viscous and an iso-viscous viscosity is small. In general, a constant viscosity will be used.

B.8 Dimensionless quantities in SEALCALC

In order to make the program SEALCALC general applicable and in order to prevent numerical problems dimensionless quantities are used. These quantities are defined as:

$$\bar{p} = \frac{p}{p_{max}} \quad \text{Dimensionless pressure} \quad (\text{B.8})$$

$$\bar{x} = \frac{x}{b} \quad \text{Dimensionless axial coordinate} \quad (\text{B.9})$$

$$\bar{h} = \frac{h}{b} \quad \text{Dimensionless film thickness} \quad (\text{B.10})$$

$$\frac{\eta V_{\Sigma}}{p_{max} \cdot b} = \frac{\eta V_{\Sigma}}{p_{max} \cdot b} \quad \text{Dimensionless } \eta V_{\Sigma} \quad (\text{B.11})$$

$$\bar{\tau} = \frac{\tau}{p_{max}} \quad \text{Dimensionless shear stress} \quad (\text{B.12})$$

$$\bar{F}_w = \frac{F_w}{p_{max} \cdot b^2} \quad \text{Dimensionless friction} \quad (\text{B.13})$$

$$\bar{Q}\eta_0 = \frac{Q\eta_0}{p_{top} \cdot b^3} \quad \text{Dimensionless } Q\eta_0 \quad (\text{B.14})$$

These dimensionless quantities are also used to present the results from SEALCALC for the film and pressure profile. To make the results more accessible for the seal designer it is also possible to present the actual values of the film thickness and the fluid pressure in S.I. units.

B.9 Influence of the fluid pressure on the pressure and film profile

In the previous figures the surrounding pressure, p_{sur} , was taken to be equal to zero on both sides of the seal. Normally, radial lip seal are typically pressurized on one side of the seal, the oil side, and there is atmospheric pressure, p_{atm} , on the other side of the seal, the air side. An example of this situation is presented in Figure B. 16.

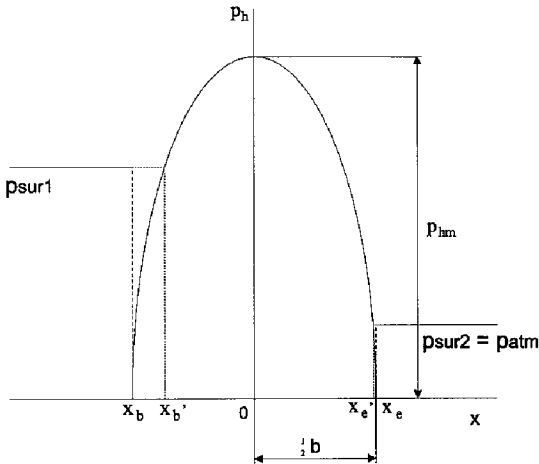


Figure B. 16 Elastohydrodynamic pressure profile with the boosting zone on the high pressure side.

From Figure B. 16 it can be seen that the points x_b and x_e shift towards the center of the CPD. The lubricant penetrates the contact zone until the point where the static contact pressure is equal to the fluid pressure. This fluid penetration results in a change of the static contact pressure profile. In general, it is found that the maximum static contact pressure is much higher than the fluid pressure resulting in only small changes of the CPD and these changes are neglected. For the Hertzian contact the elastohydrodynamic pressure profile, with a non-zero pressure on the oil side is given in Figure B. 16.

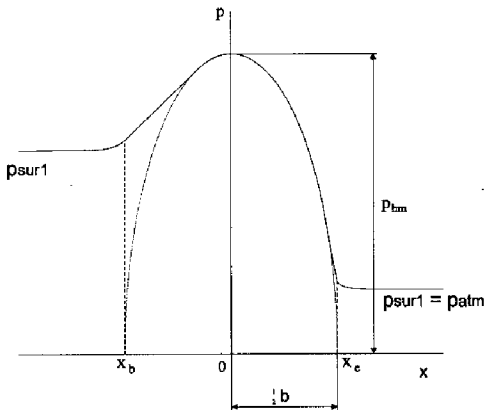


Figure B. 17 Elastohydrodynamic pressure profile for a Hertzian contact.

The method, mentioned above, can not always be applied to the characteristic pressure distribution of radial lip seals. When the surrounding pressure on the low pressure side is relatively high, like in Figure B. 17, two problems occur:

1. The shift from x_b to x_b' is so big that it may no longer be neglected.
2. It has become impossible to achieve a force equilibrium with the assumptions for the film profile of equation B.1.

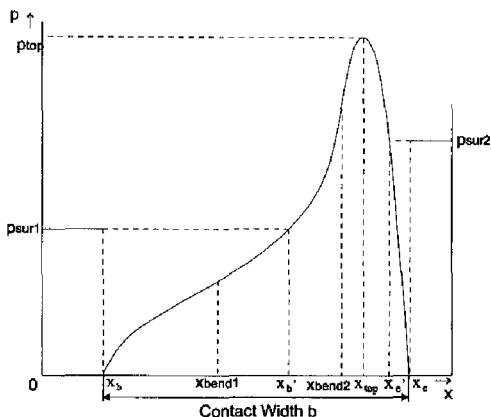


Figure B.18 Contact pressure profile of a lip seal with a high surrounding pressure on the low pressure side.

To be able to use the assumptions of equation B.1 for calculation of the radial lip seal film profile the following complementary demand is necessary. The surrounding pressure on the low pressure side of the seal must be much smaller than the contact pressure in the point x_{bend1} . As it holds that in general the surrounding pressure on the low pressure side of the seal is equal to the atmospheric pressure, this demand is generally met for radial lip seals.

B.10 Quasi-stationary calculations with SEALCALC

As the program SEALCALC is based upon the program PROGRES of Kanters [1990] leakage and friction for a radial lip seal can only be determined for a constant velocity V_{Σ} , and not for the changing velocity profile of a reciprocating shaft. When SEALCALC is used the program calculates the leakage and friction for different constant velocity's between -1 m/s and 1 m/s resulting in a friction and leakage profile over the entire stroke of a reciprocating shaft. However, in the vicinity of the point of zero shaft speed serious discrepancy's between the calculated and experimental values must arise because the squeeze term is not taken into account. The discrete results for shaft speeds between -1 m/s and 1 m/s are used to describe both leakage and friction as a function of the shaft speed, $Q(V_{\Sigma})$ and $F_w(V_{\Sigma})$ (see Figure B. 19 and Figure B. 20). These graphs are only valid when the assumption of a constant V_{Σ} is valid. The area where the sum speed reaches zero and the full film results become questionable are marked in the graphs. The fact that the fluid film in these areas is smaller then the sum of the roughness of the shaft and the seal is taken as the criterion.

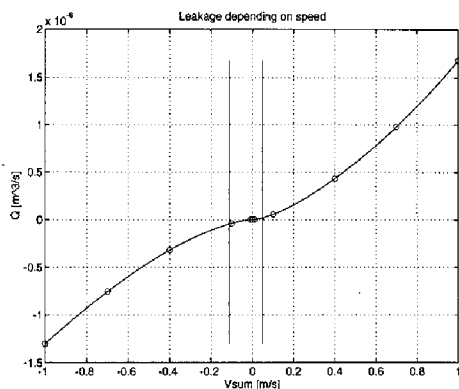


Figure B. 19 Example of the leakage Q as a function of VS calculated and presented by SEALCALC.

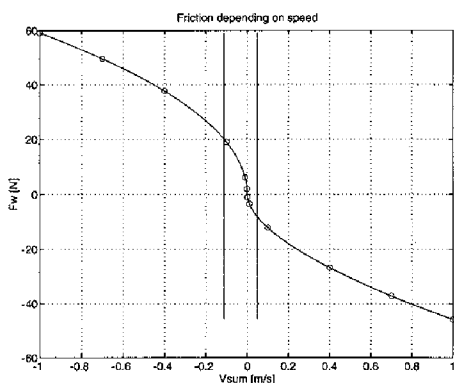


Figure B. 20 Example of the friction F_w as a function of VS as calculated and presented by SEALCALC.

To be able to predict the leakage and the friction of a lip seal over the entire stroke of a reciprocating shaft with changing V_{Σ} , a quasi-stationary approach is used. It is assumed that the influence of inertia- and squeeze effects on the film profile and thus on leakage and friction is small and may thus be neglected. If the quasi-stationary approach is adopted it is possible to determine the leakage, $Q(t)$, and friction profile, $F_w(t)$, for a given shaft velocity profile, $V_{\Sigma}(t)$, as a function of time. Using the sinusoidal shaft velocity profile of Figure B. 21, the leakage and friction profile of Figure B. 22 and Figure B. 23 can be derived.

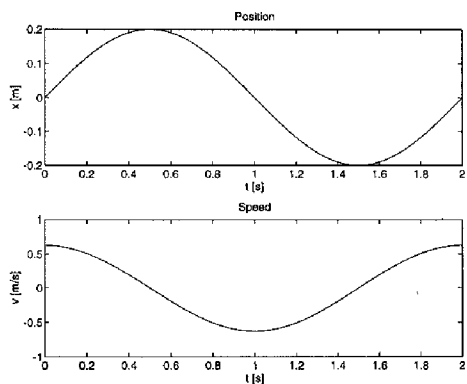


Figure B. 21 Example of VS as a function of t.

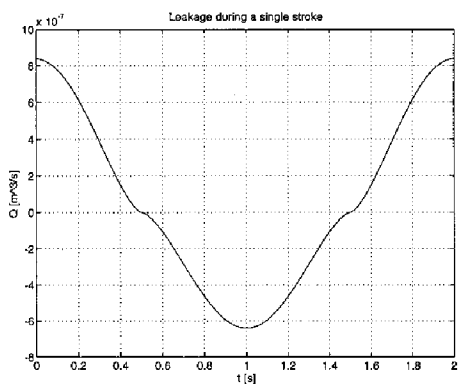


Figure B. 22 Leakage $Q(t)$ for the shaft velocity profile of Figure B. 21 using a quasi-stationary approach.

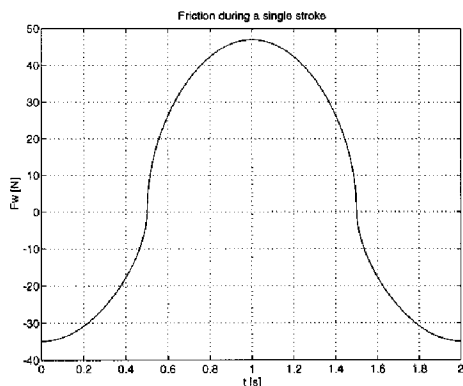


Figure B. 23 Friction $F_w(t)$ for the shaft velocity profile of Figure B. 21 using a quasi-stationary approach.

B.11 Conclusions

Based upon the work of Van Dijnsen [1995] the following conclusions concerning the practical usefulness of the inverse hydrodynamic lubrication approach presented by Kanters [1990] for the design of radial lip seals for reciprocating shafts can be drawn.

A program, SEALCALC, is available which determines for any seal geometry with its numerically determined CPD the theoretical pressure and film thickness profile based upon the IHL theory. Based upon the film profiles for different constant shaft speeds an estimated profile of the seal leakage, Q , and the seal friction, F_w , as a function of the shaft speed is determined.

The assumptions of Kanters [1990] for the boosting and exit zone gives a large difference between the static contact pressures and the dynamic fluid pressures when applied to radial lip seals. Van Dijnsen [1995] presents an alternative set of assumptions which solves the problems encountered with the assumptions of Kanters [1990]. A verification of the new set of assumptions could not be presented due to the large difference between the theoretical and experimental friction values.

Friction measurements for radial lip seals were conducted and, although the available test rig only allowed for a measurement of the difference between instroke and outstroke friction, these measurements were accurate enough to conclude that the measured friction values of radial lip seals for reciprocating shafts were much higher than the theoretical values based upon the IHL theory. Based upon this observation it was concluded that the friction of radial lip seals for reciprocating shafts could not be completely explained by viscous shear stresses in the lubricating film.

Shock absorber seals operate in the mixed/boundary lubrication regime, making the prediction of seal leakage and friction based upon the IHL approach useless for seal design optimization.

A new hypothesis was formulated and in order to investigate seal friction of radial lip seals for reciprocating shafts more thoroughly, the influence of the seal material on seal friction was taken into account.

Appendix C. A hysteresis friction model for elastomeric contact seals

C.1 Introduction

Van Dijnsen [1995] modified and implemented the IHL theory as presented by Kanters [1990] in a MATLAB program SEALCALC. After experimental investigation of the friction of shock absorber seals it was concluded that measured seal friction was much higher than the theoretically predicted friction values. This presented the problem that seal friction could not be determined accurately by a model based on the hydrodynamic lubrication theory, thus only viscous shear of an assumed Newtonian fluid. Kanters [1990] and Van Dijnsen [1995] based their work on the assumption that the fluid film separates the shaft and the seal completely and no interactions between the shaft and the seal surface roughness can take place, see Figure C. 1.

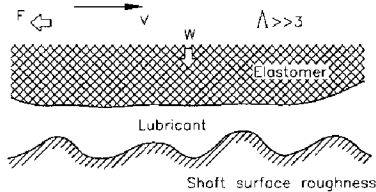


Figure C. 1 Assumed sealing situation in the hydrodynamic lubrication region, Van Klooster [1996].

However, by the work of Van Dijnsen [1995] it seemed that also other mechanisms must be responsible for the seal friction during reciprocating motion of the shaft. It is clear that for thin films and low shaft speeds, "seal-shaft contact phenomena" and thus the surface roughness of the shaft and seal might play an important role in the friction mechanism. In order to investigate and model these phenomena the hysteresis friction hypothesis of Moore [1972] was used and translated into a useful MATLAB model by Van Klooster [1996] to investigate the influence of the surface roughness, visco-elastic seal material properties, and dynamic interaction between moving shaft and seal.

C.2 Mechanisms of elastomeric friction

Moore [1972] stated that there are in general three physical principles to determine the frictional force F_w between an elastomeric material and a rigid counterpart: Adhesion forces F_{adh} ; viscous drag forces F_{visc} and ploughing forces F_{plough} as shown in equation (C.1).

$$F_w = F_{adh} + F_{visc} + F_{plough} \quad (C.1)$$

Viscous effects (assuming Newtonian fluid behavior) have already been investigated by Kanters and Van Dijnsen. It seems that these effects are low or even negligible in the boundary/mixed lubrication region, therefore equation (C.2) can be redefined as a solid-solid contact phenomenon:

$$F_w = F_{adh} + F_{plough} \quad (C.2)$$

According to Moore [1972] the contact area between an elastomer and a rough support surface is characterized by a draping of the elastomer about individual asperities in the rigid base, as shown in Figure C. 2.

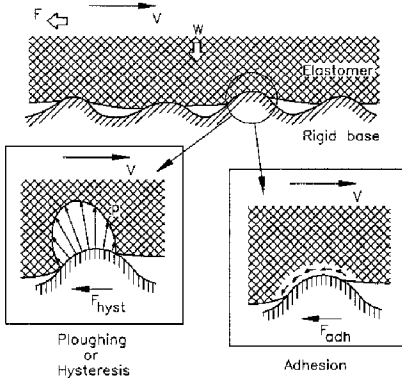


Figure C. 2 Principal components of elastomeric friction, Moore [1972].

Figure C. 2 shows how the total frictional force developed in sliding over a single asperity of the surface roughness may be separated (in absence of a lubricant) into an adhesion and a ploughing term. The ploughing term of friction is caused due to geometrical effects. The adhesion term of friction is caused due to interfacial interaction between two running partners. Moore [1972] stated that: "The adhesion component of the frictional force can be interpreted as a thermally-activated, molecular-kinetic, stick-slip action occurring within a thin surface layer of the elastomer. The exact nature of adhesion is not certain, although it is generally recognized to consist of the making and breaking of junctions on a molecular level. The ploughing term is due to a delayed recovery of the elastomer after indentation by a particular asperity, and gives rise to what is generally called the *hysteresis* component of friction". Therefore it is allowed to write:

$$F_{plough} = F_{hyst} \tag{C.3}$$

The adhesion mechanism can be minimized effectively with an interfacial lubricant film, stated by Moore [1993,1972,1975] and Czichos [1985]. By using a smooth surface roughness the hysteresis mechanism can be minimized, because little elastomeric material will be deformed. Both mechanisms incorporate viscoelastic material behavior and they strongly depend on the used surface roughness.

The situation as displayed in Figure C. 2 shows a great equivalence to the assumed sealing contact situation in the boundary/mixed region. In this particular application it is plausible that the shaft's micro roughness deforms a thin surface layer of the elastomeric seal material.

The assumed sealing situation in the boundary/mixed lubrication region is shown in Figure C. 3. A thin fluid film separates the seal surface from the shaft surface. However, the thickness of this film is smaller than the height of the shaft and seal surface roughness, resulting in an interaction between the seal surface and the moving shaft surface asperities. This interaction opposes the direction of movement and is thus called friction, but it is not certain whether to classify this effect as a hysteresis or/and a adhesion mechanism. The existence of a thin interfacial lubricant film minimizes or even eliminates the influence of adhesion friction to the total frictional force. Though, it should be noted that at slow sliding speeds, squeezing of the lubricant because of the squeeze-film effect reduces the lubricating properties of the remaining film, so the adhesion term could become significant. The shaft surface roughness in Figure C. 3 is assumed to be the most important for hysteresis effects,

while in general the "soft" seal material is draped around the "rigid" shaft surface roughness by the interference fit and the resulting radial load.

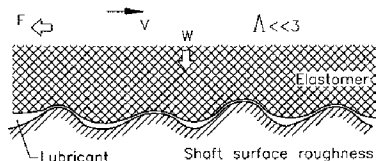


Figure C. 3 Assumed sealing situation in the boundary/mixed lubrication.

Considering Figure C. 3 it is possible that hysteresis or/and adhesion effects could be responsible for a part, maybe a considerable part, of the total frictional force occurring in the boundary/mixed lubrication region. Hysteresis effects induced by a smooth surface roughness might be small, but certainly do exist, because the elastomeric surface layer will be deformed in a direction perpendicular to the shaft surface and thus yields hysteresis effects; all of this besides the possible influence of adhesion effects. In order to quantify the hysteresis effects for small excitations at high frequencies, a model is developed to find out whether or not its influence might be neglected. The hysteresis friction model predicts partially and approximately the friction occurring in the boundary/mixed lubrication region and it can be seen as a contribution to the "complex process of tribological interaction between two running partners and their environment".

Some knowledge of viscoelastic material behavior is necessary because the hysteresis component of friction depends on the viscoelastic properties of the elastomer. In order to characterize the dynamic behavior of the elastomeric material, the one dimensional linear viscoelastic theory is used and therefore be shortly summarized.

C.3 Viscoelastic material behavior

Elastomeric seal materials feature viscoelastic behavior. The mechanical behavior of viscoelastic material can be separated in two different terms: respectively time independent elastic behavior and time dependent viscous behavior. Typical viscoelastic material behavior results in a partly and delayed recovery of the material after indentation, in contrast with elastic material behavior.

C.3.1 Dynamic viscoelastic behavior

Due to periodical deformation of a viscoelastic body, the work will be partly elastically stored and partly dissipated. Hence, hysteresis is associated with internal damping effects within the viscoelastic material.

The main subject of this study is hysteresis friction occurring in the seal contact, therefore it is important to characterize the dynamic seal material behavior. To investigate the dynamic viscoelastic behavior of the seal material, the *one dimensional linear viscoelastic theory* is used. Therefore three assumptions are made:

- The behavior is one dimensional. Note: in reality the seal deformation due to indentation by a particular asperity of the shaft roughness is not one dimensional, but three dimensional.
- The material behavior is geometrically and physically linear. The dynamic deformations are assumed to be of such an order that linear theory is valid.
- The mechanical properties of the material are time invariant (non-aging).

To characterize the dynamic behavior of linear viscoelastic materials use can be made of harmonic excitations, see appendix A of Van Klooster [1996].

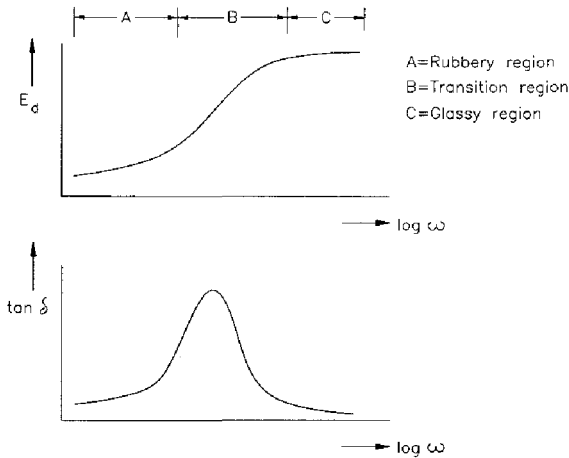


Figure C. 4 Typical master curve of modulus and $\tan \delta$ of viscoelastic materials.

The dynamic modulus versus frequency is referred to the master curve of modulus and characterize the dynamic behavior of linear viscoelastic materials.

The dynamic modulus and $\tan \delta$, schematically shown in Figure C. 4 can be obtained by harmonic excitation of an arbitrary test specimen. This measurement technique is usually referred to as Dynamical Mechanical Analysis (DMA) and a test device¹ is developed within the section “Tribology and power transmissions” of the faculty of Mechanical Engineering at the Eindhoven University of Technology, realized by Jebbink [1995].

According to Figure C. 4: at low frequencies (rubbery region), the dynamic stiffness of the viscoelastic material shows a low value. At high frequencies (glassy region) the dynamic stiffness is much higher e.g. factor 80 for an investigated FPM-compound. Thus, frequency increase causes stiffening. $\tan \delta$ is minimal at low and high frequencies, meaning low energy dissipation, hence the material behavior is nearly elastic. A maximum value of $\tan \delta$ is reached at the transition region. Excitation in this region results in higher energy dissipation.

Furthermore temperature is of great importance. A temperature rise induces a softening effect within the viscoelastic material, meaning a horizontal shift of the total master curve to the right in Figure C. 4.

Temperature effects can be taken into account, because of the exchangeability of frequency and temperature. Williams et al. [1955] investigated this effect and introduced the well known Williams-Landell-Ferry or WLF-equation:

$$\log(a_T(T)) = \frac{-c_1(T-T_0)}{c_2 + T - T_0} \tag{C.4}$$

Where $a_T(T)$ denotes the shift factor necessary to shift the total master curve. T_0 denotes the reference temperature and T denotes the actual temperature. c_1 and c_2 are material parameters of the specific viscoelastic material.

¹ based on compression instead of tension or bending.

C.3.2 Dynamic mechanical thermal analysis of the elastomer pin materials

In order to be able to estimate the contribution of hysteresis friction, determined by the model presented in the next sections, to the measured total frictional force, it is necessary to characterize the dynamic seal material behavior.

A dynamic mechanical thermal analysis (DMTA) of the four elastomeric seal materials was conducted to characterize their one dimensional dynamic linear viscoelastic material behavior. Van Klooster [1996] presents measurements and fitted results for both dynamic modulus and the loss modulus, $\tan \delta$, for the four seal compounds. The moduli of elasticity, the relaxation times and the WLF constants describing the seal materials are listed also by Van Klooster [1996]. A Maxwell fit of the DMTA results for the four seal materials is made. The Maxwell fits are only valid within the frequency range of the test data, thus a frequency range between approximately 1×10^{-1} and 1×10^{10} Hz.

C.4 Multi-mode Maxwell model

In early development of viscoelasticity theory much use was made of the modeling of elastomeric materials by networks made up of simple elastic and viscous elements. The elastic element, a spring, reacts purely elastic and therefore returns all energy that is put in through deformation. The viscous element, a damper, reacts purely viscous.

Multi-mode Maxwell models are useful tools to describe linear viscoelastic behavior. The multi-mode Maxwell model is formed by connecting series of Maxwell elements parallel to each other and a single spring E_∞ parallel, see Figure C. 4.

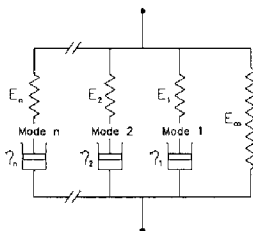


Figure C. 5 A Multi-mode Maxwell model with spring parallel E_∞ .

Here E_n denotes the modulus of elasticity and η_n denotes the viscosity of a n^{th} -mode Maxwell element. E_∞ denotes the “equilibrium modulus”, meaning that for low frequencies, thus nearly static, a negligible influence of dampers occurs. Therefore only spring E_∞ is active:

$$\sigma_{\text{low freq}} = E_\infty \epsilon \quad (\text{C.5})$$

Here ϵ denotes strain occurring and $\sigma_{\text{low freq}}$ denotes stress occurring at low frequencies. Dampers act infinite stiff at high frequencies, hence:

$$\sigma_{\text{high freq}} = \sum_1^n E_n \epsilon + E_\infty \epsilon \quad (\text{C.6})$$

Here ϵ denotes strain occurring and $\sigma_{\text{high freq}}$ denotes stress occurring at high frequencies.

Storage modulus H' , loss modulus H'' and dynamic modulus H_d for a multi-mode Maxwell model can be written as (Moore [1972] and Tervoort [1990]):

$$H'(\omega) = \sum_1^n E_n \frac{\tau_n^2 \omega^2}{\tau_n^2 \omega^2 + 1} + E_\infty \quad (C.7)$$

$$H''(\omega) = \sum_1^n E_n \frac{\tau_n \omega}{\tau_n^2 \omega^2 + 1} \quad (C.8)$$

where $\tau_n = \frac{\eta_n}{E_n}$.

$$H_d = \sqrt{H'^2 + H''^2} \quad (C.9)$$

Here τ_n denotes the relaxation times, n denotes the number of modes used in the multi-mode Maxwell model. Substituting equation (C.7) and (C.8) into equation (C.9) it is possible to fit test data, as schematically shown in Figure C. 4, on a multi-mode Maxwell model. For this purpose a MATLAB program was written (Jebbink [1995]). Input to this program is the master curve, output is generated in forms of E_n and τ_n . The number of modes is variable, though it should at least be chosen equal to the number of decades of the master curve's frequency range.

C.5 Hysteresis friction model

C.5.1 Introduction

In theory hysteresis friction is commonly associated with rolling resistance (Yamaguchi [1990] and Moore [1972, 1975, 1993]). The rolling resistance theory is based on the idea that when a body rolls over a viscoelastic surface, such as rubbers or plastics, a hysteresis loss occurs resulting from the deformation of the surface and its subsequent recovery after unloading.

Before deriving the hysteresis friction model it is necessary to once more consider the assumed sealing situation in the boundary/mixed lubrication regime. The elastomeric seal material is statically pressed against the shaft surface roughness, resulting in a non-linear static stress component. Next the shaft makes a reciprocating motion relative to the elastomeric seal material. The shaft motion results in a small excitation, thus deformation, of the surface of the seal by means of the shaft surface roughness, resulting in a dynamic stress component and hysteresis effects.

Morman and Nagtegaal [1981] developed a finite element method for the dynamic analysis of viscoelastic incompressible materials and showed that a static deformation component x_s due to a large static pre-deformation may be superposed on a small-amplitude sinusoidal deformation component x_d (stated here without proof). The static deformation x_s results in a static stress component and the dynamic deformation x_d results in a dynamic stress component. The static stress component σ_s may also be superposed on the dynamic stress component $\sigma_d(t)$, although the static stress component is a result of a non-linear analysis. See equation (C.10)

$$\sigma(t) = \sigma_s + \sigma_d(t) \quad (C.10)$$

It is therefore allowed to investigate the dynamic component independently of the static component.

In the hysteresis friction model, it is assumed that the applied load W (in Figure C. 3) during relative motion must be in equilibrium with the total vertical deformation force occurring after indentation by a range of asperities of the shaft surface roughness.

The hysteresis component of friction can be visualized by Figure C. 6, which shows the pressure distribution about a single asperity of the shaft surface roughness (a) when no relative motion exists, and (b) in presence of relative sliding. The absence of relative motion produces a symmetrical draping of the elastomer about the asperity. The total symmetrical pressure distribution can be separated into horizontal and vertical components, it can be seen that the summation of vertical pressures must be in equilibrium with the load W_i and the summation of the horizontal components is zero. However, if the shaft surface roughness is moving with a finite velocity v relative to the elastomeric material, it tends to accumulate at the leading edge of the asperity and to break at a higher point on the downward slope. Thus the contact arc moves forward compared with the static case, and this effect creates an asymmetrical pressure distribution where the horizontal pressure components give rise to the net hysteresis force (deformation force) F_{hyst} which opposes the sliding motion.

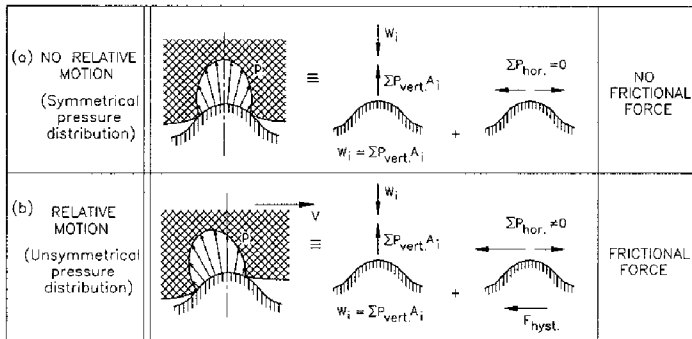


Figure C. 6 Physical interpretation of the hysteresis component of friction (Moore [1972]).

The analytical hysteresis friction model is developed in order to determine the hysteresis friction effects, and is implemented in a MATLAB 4.0 computer program. For this goal an analytical model is preferred instead of a finite element model (FEM). Using an analytical model it is possible to investigate in a fast way the influence of the different design parameters such as: shaft roughness, dimensions of the seal, temperature, shaft speed, etc. A disadvantage of an analytical model is the difficulty to describe the deformed seal- and shaft roughness geometry accurately. Therefore simplifications are necessary, though it should be noted that a finite element model is certainly not a solution to this problem. Modeling the measured shaft surface roughness geometry in FEM is a time consuming task and could lead to possible numerical contact problems and a long CPU time.

C.5.2 Shaft surface roughness model

In this study the seal surface roughness is assumed to be negligible. To determine the hysteresis component of elastomeric friction it is obvious that the shaft surface roughness plays an important role, for the good reason that the one can be regarded as the cause and the other the effect in a practical application.

A large number of different parameters, primarily according to the DIN 4762 standard, exists to characterize a measured shaft roughness profile.

Because the difficulty of mathematically specifying of a random surface roughness, the measured shaft surface roughness geometry must be translated into a simplified shaft surface roughness model in order

to be able to determine its influence upon the hysteresis component of friction. According to Moore [1972], the three basic shapes of an ideal asperity shape are cubes, cones and spheres. Sawtooth and sinusoidal asperity models have also been commonly used because of their mathematical simplicity.

In this study interest is going out to a method and a model to make an estimation of hysteresis frictional effects occurring in the contact area between an elastomeric seal and a shaft. "Small" asperities contribute little to the total hysteresis frictional force and are therefore of less importance. The "small" asperities can be interpreted as being superposed upon a "large" asperity in an actual surface roughness profile, see Figure C. 7.

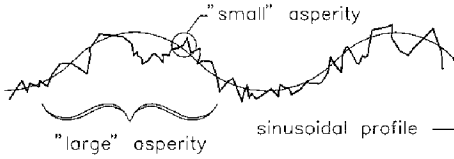


Figure C. 7 Schematically representation of an actual and the model sinusoidal roughness profile.

It is important to take the "larger" asperities into account because they are primarily responsible for the occurring hysteresis friction. Besides the mathematical simplicity, three dimensional sinusoidal roughness profiles could be useful in modeling the measured "larger" asperities of a random surface roughness. Hence, the shaft surface roughness is modeled by a three dimensional sinusoidal profile, see Figure C. 8.

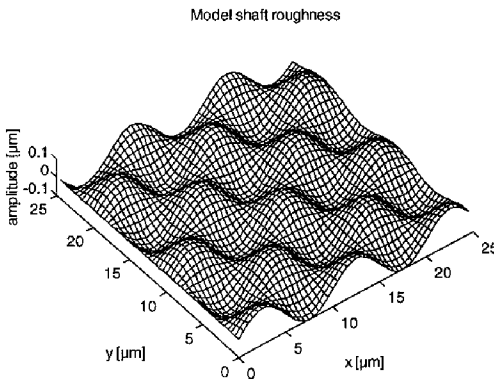


Figure C. 8 Model shaft surface roughness defined as a three dimensional sinusoidal profile.

It can still be presumed that the idealized model shaft surface roughness of Figure C. 8 bears little resemblance to the actual surface roughness. To a certain extend this is true, but the idealized model surface roughness is useful to approximate the influence of the actual surface roughness and by this investigate its influence upon the hysteresis component of friction.

Characteristic for the three dimensional sinusoidal rigid profile are the wavelength λ and the amplitude r . The characteristic mean amplitude and mean wavelength to describe the actual shaft surface roughness are determined based upon data from the scanning atomic force microscope (AFM).

C.5.3 Analytical hysteresis friction model

As a result of an applied load W , the elastomeric seal material drapes around the shaft surface roughness, thus the sinusoidal roughness profile which is defined earlier. In order to minimize or even

eliminate the adhesion component of friction, the existence of a thin interfacial lubricant film is assumed in the hysteresis friction model, see Figure C. 9.

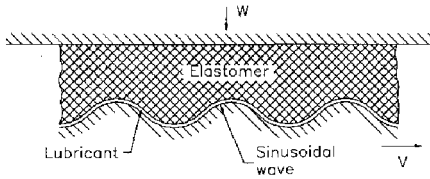


Figure C. 9 Seal contact model: elastomer and model shaft surface roughness.

It was shown that a twelve-mode up to a twenty four-mode Maxwell model fitted on experimental data simulates the one dimensional linear dynamic viscoelastic material behavior over a large frequency range. Therefore we represent the elastomeric seal material, as shown in Figure C. 9, as a multi-mode Maxwell model, see Figure C. 10.

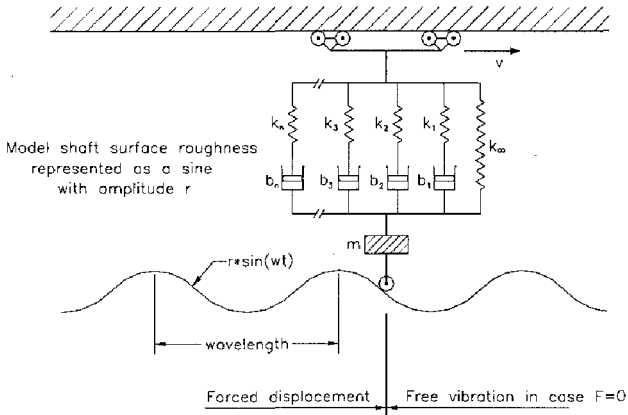


Figure C. 10 The hysteresis friction model.

In the hysteresis friction model a mass m is included in order to take inertial effects into account, as shown in Figure C. 10. The total dynamic behavior can be split into two terms: (1) a forced displacement and (2) a free vibration, when the elastomeric seal material separates, thus the contact load equals zero. The mass-spring-damper system includes many degrees of freedom, therefore the method of *Lagrange* is used to derive a system of differential equations (C.11).

$$\left\{ \begin{array}{l} m\ddot{x} + \sum_1^n b_n \dot{x} - b_1 \dot{x}_1 - b_2 \dot{x}_2 - \dots - b_n \dot{x}_n + k_\infty x = F \\ -b_1 \dot{x} + b_1 \dot{x}_1 + k_1 x_1 = 0 \\ -b_2 \dot{x} + b_2 \dot{x}_2 + k_2 x_2 = 0 \\ \vdots \\ -b_n \dot{x} + b_n \dot{x}_n + k_n x_n = 0 \end{array} \right. \quad (C.11)$$

We are mainly interested in the hysteresis force, thus a force-displacement relation rather than a stress-strain relation. It is therefore necessary to find an expression for the contact stiffness occurring due to indentation by a particular asperity. The Hertzian theory is a commonly used method to solve

contact problems between two elastic bodies under certain conditions, though in literature there are several investigators (Moore [1972, 1975, 1993], Yamaguchi [1990] and Czichos [1985]) who implemented the Hertzian theory in order to solve contact problems between a viscoelastic body and a counterpart. For example, Czichos [1985] implemented the Hertzian theory in an analytical four parameter or Burger model in order to investigate the contact deformation of a polymer ball on a disc configuration. He found a general agreement between the experimentally and theoretically determined values.

Johnson [1985] showed that at low *static* pressures the contact area at a crest of a sinusoidal roughness profile will be given by Hertz' theory. A higher pressure results in an increasing real contact area. Johnson showed that the Hertzian theory deviates more or less at higher pressures. He presented an analytical model in order to find a solution to this problem.

Viscoelastic materials responds almost purely elastic during excitation in the rubbery and glassy region of the master curve. This in combination with the assumption that a specific viscoelastic material is not fully squeezed around the sinusoidal roughness profile, results in an acceptable validation of the Hertzian theory. However, excitation in the transition region of the master curve results in an asymmetrical pressure distribution about a single asperity. Furthermore, it is possible that due to a high applied load, the specific viscoelastic material indeed fully drapes around the sinusoidal model roughness profile. A result of these two particular situations is that the validation of the Hertzian theory is partially discussible and that Johnson's model, as mentioned above, could lead to a probably more accurate calculation of the contact stiffness. Though, it must be understood that as a first approximation the linear Hertzian theory is assumed to be valid in all of the above mentioned situations. Use of this theory enables determination of the contact stiffness due to indentation by a particular asperity.

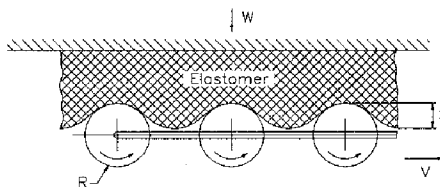


Figure C. 11 Seal contact model: sinusoidal roughness profile replaced by an array of spheres.

The sinusoidal roughness profile, as shown in Figure C. 8, can be approximately replaced by an array of spheres, see Figure C. 11.

A Hertzian circle contact is taken into account to determine the contact stiffness due to a single asperity which is impressing the elastomeric material. For a Hertzian circle contact we write (van Leeuwen et al. [1993]):

$$z = \sqrt[3]{\frac{9F_v^2}{4RE_r^2}} \quad (\text{C. 12})$$

$$\text{where } \frac{1}{E_r} = \frac{1}{2} \left\{ \frac{1-\nu_1^2}{E_1} + \frac{1-\nu_2^2}{E_2} \right\}$$

Here z denotes the approach of the sphere, F_v denotes the applied force acting on a single sphere, R denotes the sphere radius which can be found out of the sinusoidal roughness profile, E_r denotes the reduced modulus of elasticity, ν_1 denotes the Poisson ratio of the elastomer, E_1 denotes the modulus of elasticity of the elastomer, ν_2 denotes the Poisson ratio of the sphere material (e.g. steel), E_2 denotes the Young's modulus of the sphere material.

Resolving the system of differential equations (C.11) and implementing the Hertzian circle contact equation (C.12) leads to the final solution, thus an algorithm to calculate hysteresis forces and an algorithm to calculate the delayed recovery of the elastomeric seal material after indentation by a sinusoidal roughness profile. Other features which are implemented in the hysteresis friction model are: temperature effects using WLF equation and a prediction of the mean contact stress occurring on a single asperity due to deformation.

C.6 Summary

With the developed analytical hysteresis friction model and numerical tools it is possible to predict approximately:

- the hysteresis frictional force,
- the delayed recovery of the seal material and the real contact area,
- the mean contact stress acting on a model roughness asperity.

All of these parameters are determined under dynamic conditions and as a function of several design parameters, like shaft surface roughness, applied load, nominal load, and type of elastomeric seal material.

Although, the initial results of the hysteresis friction model were not in very good agreement with experimental results the model seems capable of predicting the influence of the viscoelastic seal material properties on friction qualitatively.

References

- 1886 **Reynolds, O.**, "On the Theory of Lubrication and its application to Mr. Beauchamps Tower's Experiments Including an Experimental Determination of the Viscosity of Olive Oil," *Phil. Trans., Roy. Soc. London*, Vol. 177, pp. 157-234
- 1955 **Williams, M.L., Landell, R.F., and Ferry, J.D.**, "The Temperature Dependence of Relaxation Mechanisms in Amorphous Polymers and other Glass-Forming Liquids," *Journal Amer. Chem. Soc.*, No.77
- 1963 **Blok, H.**, "Inverse Problems in Hydrodynamic Lubrication and Design Directives for Lubricated, Flexible Surfaces," *Proc. Int. Symp. Lubr. and Wear*, Eds. Muster, Houston USA, pp. 9-151
- 1972 **Hooke, C.J., and O'Donoghue, J.P.**, "Elastohydrodynamic Lubrication of Soft, Highly Deformed Contacts under Non-Uniform Motion," *Journal of Mech. Eng. Science*, 14, 1, pp. 34-48
- 1972 **Moore, D.F.**, The friction and Lubrication of Elastomers, Pergamon Press Ltd., Oxford
- 1975 **Moore, D.F.**, Principles and Applications of Tribology, Pergamon Press, Oxford, ISBN 0-08-017902-9
- 1977 **Gawlinski, M.J.**, "Afdichtingen," *Dict. No. 4.470*, (in Dutch), Eindhoven University of Technology
- 1981 **Morman, K.N., Nagtegaal, J.C.**, "Finite Element Analysis of Sinusoidal Small-Amplitude Vibrations in Deformed Viscoelastic Solids-part1, Theoretical Development," *report*, Ford Motor Co. and MARC Analysis Research Corp.
- 1985 **Czichos, H.**, "Contact Deformation and Static Friction of Polymers, Influences of Viscoelasticity and Adhesion," *American Chemical Soc. Symp. Series*, vol. 287, Washington
- 1985 **Johnson, K.L.**, Contact Mechanics, Cambridge University Press
- 1985 **Kackar, R.N., Raghu,** "Off-Line Quality Control, Parameter Design, and the Taguchi Method," *Journal of Quality Technology*, Vol.17, No.4, pp. 176-188.
- 1987 **Gunter, B.**, "A Perspective on the Taguchi Methods," *Quality Progress*, June, pp. 44-52.
- 1987 **Luijten, R.**, "Bepaling van de radiaalcracht, contactbreedte, en contactdrukverdeling van radiale lipafdichtingen," *Msc Thesis*, (in Dutch), Eindhoven University of Technology
- 1987 **Ten Hagen, E.A.M.**, "Computer Calculations of the Contact Pressure Distribution and the Contact Width in the Shaft-to-Seal Contact Area," *Report*, (in Dutch), Eindhoven University of Technology, Weinheim, Germany
- 1988 **Gohar, R.**, Elastohydrodynamics, Ellis Horwood Limited, ISBN 0-85312-820-0
- 1988 **Stakenborg, M.J.L.**, "On the Sealing and Lubrication Mechanism of Radial Lip Seals," *Ph.D. Thesis*, Eindhoven University of Technology
- 1988 **Ten Hagen, E.A.M.**, "Mechanical Characterisation of Synthetic Rubber," *Msc Thesis*, (in Dutch), Eindhoven University of Technology
- 1989 **Phadke, M. S.**, Quality Engineering Using Robust Design, Prentice Hall, Englewood Cliffs NJ.
- 1989 **Reimpell, J., Stoll, H.**, Fahrwerktechnik: Stoß- und Schwingungsdämpfer, Vogel Buchverlag, ISBN 3-8023-0202-8
- 1990 **Kanters, A.F.C.**, "On the Calculation of Leakage and Friction of Reciprocating Elastomeric Contact Seals," *Ph.D. Thesis*, Eindhoven University of Technology
- 1990 **Müller, H.K.**, Abdichtung bewegeter Maschinenteile, Medienverlag - Ursula Müller, (in German), ISBN 3-920484-00-2, Waiblingen
- 1990 **Tervoort, T.A., Govaert, L.E.**, "Visco-elasticiteit module 3," *lecture notes*, (in

- Dutch), Eindhoven University of Technology
- 1990 Yamaguchi, Y., Tribology of Plastic Materials, Elsevier Science Publishers b.v.
- 1991 Kuiken, J., "Optimisation Tools for Stern Tube Seals," *MSc Thesis*, Eindhoven University of Technology
- 1992 Gabelli, A., Ponson, F., Poll, G., "Computation and Measurement of the Sealing Contact Stress and its Role in Rotary Lip Seal Design," *Fluid Sealing: Proc. of the 13th Int. Conf. On Fluid Sealing*, Kluwer Academic Press, Bruges, ISBN 0-7923-1669-X
- 1993 Brink, R.V., Czernik, D.E., Horve, L.A., Handbook of Fluid Sealing, McGraw-Hill, ISBN 0-07-007827-0
- 1993 Kuiken, J., "Geometrical Optimization of Radial Lip Seals," *IVO Report*, ISBN 90-5282-242-5, Eindhoven University of Technology
- 1993 Meesters, C.J.M., "Practicumhandleiding," *lecture notes*, (in Dutch), Eindhoven University of Technology
- 1993 Moore, D.F., Viscoelastic Machine Elements, Butterworth-Heinemann, ISBN 0-7506-1305-X, Oxford
- 1993 Moore, D.F., Viscoelastic Machine Elements: Elastomers and Lubricants in Machine Systems, Butterworth-Heinemann Ltd.
- 1993 Van de Vrede, C.W., "Het VEHD smeringsconcept voor radiale lipafdichtingen," *Msc Thesis*, (in Dutch), Eindhoven University of Technology
- 1993 Van Leeuwen, H.J., Landheer, D., "Tribotechniek," *lecture notes part 1 & 2a*, (in Dutch), Eindhoven University of Technology
- 1995 Dijusen, G.P.M. van, "Modellering van de smering van een lipafdichting voor een translerende as," *MSc Thesis*, (in Dutch), Eindhoven University of Technology
- 1995 Jebbink, A.J., "Development of a Dynamic Mechanical Analyser for Elastomeric Materials: Dynamic Characterisation of Viscoelastic Seal Materials," *IVO Report*, ISBN 90-5282-446-0, Eindhoven University of Technology
- 1995 Kaas, E.A., "Op weg naar Optimaal Ontwerpen," *Ph.D. Thesis*, Eindhoven University of Technology
- 1995 Salant, R.F., "Elastohydrodynamic Model of the rotary Lip Seal," *ASME Journal of Tribology*, Vol. 118, pp. 292-296
- 1995 Sobeta, Kenji, "Issues on International Competitive Strength of the Automotive Industry," *Japanese Development Bank Research Report*, no. 47, Tokyo, Japan
- 1995 Van Bavel, P.G.M., Ruijl, T.A.M., Van Leeuwen, H.J., and Muijderman, E.A., "Upstream Pumping of Radial Lip Seals by Tangentially Deforming, Rough Seal Surfaces," *ASME Journal of Tribology*, Vol. 118, pp. 265-275
- 1996 Fansson, A., "Evaluation of Nonlinear FEM Calculations with COSMOS/M and ANSYS/ED," *report no. 51/028-1*, CTT BV, Helmond, The Netherlands
- 1996 Klooster, J.M. van, "Determination of Hysteresis Friction for Elastomeric Contact Seals," *MSc Thesis*, Eindhoven University of Technology
- 1996 Maes-Janssen, A.M.W., "Het Ontwerpen van een Schokdemperafdichting," (in Dutch) *Internal Report*, PL Automotive, Kerkrade, the Netherlands

Nawoord

Na het uitvoeren van mijn tweejarige AIO-opleiding, ben ik begonnen aan dit promotieonderzoek in samenwerking met PL Automotive. Het bleek dat de gekozen vorm van nauwe samenwerking tussen de universiteit en de industrie een nieuwe vorm van promotie was, die door het IVO in de toekomst vaker zal worden toegepast om een betere uitwisseling van kennis tussen de universiteit en de industrie te bewerkstelligen. In overleg met het IVO werd besloten om dit project als een promotie op proefontwerp uit te voeren. Het proefontwerp zou niet tot stand zijn gekomen zonder het enthousiaste, de steun en de motivatie van mijn directe werkomgeving gedurende dit project.

Ten eerste wil ik PL Automotive bedanken voor de mogelijkheid om binnen een middelgroot bedrijf mijn promotie op proefontwerp uit te voeren. Naast concrete werkervaring in een multi-disciplinaire productontwikkelingsgroep werd mij door het bedrijf de mogelijkheid geboden om mijn kennis op het gebied van elastomere contactafdichtingen uit te bouwen en over te dragen. Verder wil ik een aantal mensen persoonlijk bedanken, waarmee ik binnen PL Automotive nauw heb samengewerkt tijdens deze periode. Met name met Ruud Keulen, Anita Maes, Rene Bollen en Rob Peters heb ik met veel plezier in het Product Development Team van PL samengewerkt.

Ten tweede wil ik mijn afstudeerders, Gerard van Dijnsen en Jeroen van Klooster, bedanken voor hun geweldige inzet, goede werk, en natuurlijk hun kritische vragen, die richting hebben gegeven aan het verloop van dit promotieonderzoek. Verder wil ik Arjen Jebbink bedanken voor zijn bijdrage om het visco-elastische gedrag van afdichtingsmaterialen met behulp van een eenvoudige opstelling te karakteriseren.

Ten derde wil ik de groep van mensen noemen, waarmee ik in nauwe samenwerking en vriendschap mijn studietijd aan de Technische Universiteit van Eindhoven heb doorgebracht. Door het nauwe contact met Erik van Kemenade, Frank Habraken, en Wil Sampers, bleef ik naast het werkgebied van de elastomere contactafdichtingen op de hoogte van ontwikkelingen in de energietechniek en de materiaalkunde.

Curriculum Vitae

- 01-09-1967 geboren te Emmeloord
- 1979-1985 Atheneum β , Christelijke Scholen Gemeenschap, CSG te Emmeloord
- 1985-1991 Werktuigbouwkunde aan de Technische Universiteit Eindhoven, afgestudeerd bij de sectie Werktuigbouwkundige Onderdelen en Constructies
- 1991-1993 AIO-2 opleiding Computational Mechanics aan de Technische Universiteit Eindhoven in opdracht van Lips BV, Drunen
- 1993-1996 Promotie op proefontwerp 'A New Radial Lip Seal Design Approach' aan de Technische Universiteit Eindhoven in dienst van PL Automotive, Kerkrade

Stellingen

behorende bij het proefschrift

A New Radial Lip Seal Design Approach

- 1 De meeste afdichtingen voor translerende stangen werken in het gemengde of grenssmeringsgebied. Hierdoor is de voorspelling van lekkage en wrijving op grond van de volle smeerfilm theorie niet bruikbaar als beoordelingscriterium voor het ontwerpen van afdichtingen.
- 2 De wrijvingsloze statische contactdrukverdeling kan worden gebruikt als het beoordelings-criterium voor het ontwerpen en optimaliseren van afdichtingen.
- 3 Tijdens het systematisch ontwerpen van afdichtingen vormt de nauwkeurigheid, waarmee de omgevingsomstandigheden kunnen worden vastgelegd, een grote onzekerheid.
- 4 Alle hydraulische werktuigen zullen verdwijnen als de leveranciers er niet in slagen installaties te bouwen, waarbij lekverliezen niet vrijuit in het milieu terecht kunnen komen.
- 5 Het gemak waarmee de term "garter spring" in het Nederlands wordt gebruikt, bewijst dat de letterlijke vertaling "kouseband" niet direct met afdichtingen wordt geassocieerd.
- 6 Door de ontwikkeling van actieve dempingssystemen zullen de fabrikanten van schokdemperafdichtingen zich in de toekomst meer bezig moeten houden met het voorkomen van vervuiling van de ruimte in, dan lekkage van olie uit de schokdemper.
- 7 De toegevoegde waarde van een weldoordacht ontwerpproces wordt groter naarmate een vaste time-to-market van meer belang is voor een product.
- 8 Een praktisch bruikbaar ontwerpproces is niet statisch, maar onderhevig aan de dynamiek van de markt en de onderneming.
- 9 De kwaliteit van een produkt wordt hoofdzakelijk bepaald door het vertrouwen en de tevredenheid van de klant.
- 10 Het begrip optimaal bestaat alleen bij de gratie van een goede afbakening van de grenzen.
- 11 Als Mc Donalds zou worden verplicht om iedere reclamezuil te combineren met een windmolen zou een groot deel van Nederland binnen korte tijd van duurzame energie kunnen worden voorzien.
- 12 De dubbele betekenis van het woord "seal" levert bij het automatisch zoeken van literatuur verrassende resultaten op.